

In addition to a change in the title, there are 9 major changes in response to author comments. The 10th change is in response to a bug in the analysis which we discovered in the process of revisions. Additional changes are made to language for the purpose of clarity throughout (especially the abstract) and several additional references have been included in light of developments in the subject area in the last few months.

MAJOR REVISIONS

1) Model Choice.

Comments from Referee #1

My main concern is that the focus of the paper is to evaluate the MAR model in terms of melting, however there appears to be relatively little discussion on the impact of the chosen model options, such as the horizontal and vertical resolution, which limits the readers understanding of how efficient MAR is at reproducing melt on the ice shelf, as seen in satellite observations. The potential impact of model choice, and model physics is most clear in the results and discussion of the wind direction, where there is a large discrepancy between the model and observations.

The above comment is also linked to the relatively coarse (for this region and this topic) horizontal resolution used here. Previous föhn studies use much finer resolution (5km, 1.5km) and suggest that this resolution is required for adequate föhn representation. Authors discuss the Van Wessem et al (2015) study which suggests higher resolution than 5.5km. However the authors appear to use the following statement: “where hydro- static assumption is preserved (such as this model run), higher resolutions may inhibit flow in the model. . .” (pg 3, line 35/36) to justify using a lower horizontal resolution. To address this issue, I think a sensitivity study using higher resolution is required. It doesn't have to be for the full-time period, but should capture at least a season of melt to assess whether the spatial resolution could improve the results, and whether the breakdown of the hydrostatic equation does limit air flow. You should also add more to the discussion about this. The spatial resolution is not mentioned at all in the discussion, and as found in other papers (Van Wessem et al 2015, Turton et al 2017, Elvidge et al 2015), higher resolution runs do capture föhn winds.

The abstract states that increased spatial resolution and topographic resolution could improve the output from MAR, but there is no mention of this in the discussion or results. You should not include statements in the abstract which do not reflect the results of the study. Either address whether changing the spatial or topographical resolution does impact the modelled melt or near-surface conditions, or remove this from the abstract.

The vertical resolution of MAR's atmosphere is very coarse, especially to have the lowest model level at 2m above the surface (pg 5, lines 10 and pg7 line 29/30). What is the vertical discretisation of your levels? The WRF model for instance has difficulties if there is over 1km between model levels, or if the stretching factor is greater than 20%. Similar to the first major comment, a sensitivity study is required to assess the impact of this vertical resolution on the representation of the near-surface conditions and the wind. This is much coarser than many

studies of this kind and studies using MAR (see for example, Gallee et al 2015 or Wyard et al 2016 who both use 60 vertical levels). Again, this doesn't need to be the full period (and shouldn't be as this would be a huge/long undertaking) but a full season should be tested using a number of higher vertical levels.

Author Response:

We now include a comparison between higher-resolution runs of a newer version MAR over the 2004-2005 melt season. The comparison includes 3 versions of MAR: (a) at 10km (b) where the horizontal resolution is increased from 10km to 5km and (c) where the vertical discretization is increased from 23 to 32 sigma layers. The variables examined are meltwater production, melt occurrence (over the domain) and wind speed/direction at the Larsen Ice Shelf AWS location. We find that an increase in resolution limits melt over the Larsen C ice shelf and increases southeasterly flow, suggesting that while the hydrostatic assumption is kept, the effect of increased resolution will lead to reduced melt overall, but potentially enhance the accuracy of melt just east of the AP due to better-resolved topography. This is specifically presented in the Abstract, discussed in detail in the Introduction and presented in the Discussion and Conclusions.

Author's Changes in the Manuscript

Abstract: P1, L29-31

Introduction: P3, L 4-12, 26-36

Data and Methods: P5, L 30-37

Discussion and Conclusion: P17, L30 – P18, L9

Supplement Fig. S12, S13

2) The hydrostatic assumption

Comments from Referee #1

The hydrostatic assumption and horizontal resolution of MAR. In the abstract, authors state that “melting in the East AP can be initiated by both sporadic westerly föhn flow over the AP and by northerly winds advecting warm air from lower latitudes. To assess MAR's ability to simulate these physical processes, this study. . .” (line Pg 1, 24- 27). Then later in the discussion you state that MAR can't accurately represent the wind direction and föhn processes due to the model's hydrostatic assumption, and state that a non-hydrostatic model would do better (pg 15 line 23-27). Models which have previously, successfully captured the föhn characteristics (WRF and UM) are nonhydrostatic, and this appears to be known to the authors prior to the study as in the introduction (Pg3, line 33), they discuss the (non-hydrostatic) RACMO study, and justify their use of a coarser resolution due to the hydrostatic assumption. If a large part of the study is to assess the impact of wind on the melting, why chose a model which can't represent the dominant westerly flow (and subsequent downward föhn flow) over the AP? If an objective of this study was to attempt to model this type of flow using a model with hydrostatic assumption, then this should be made clearer, and authors should note any previous studies of this kind.

Comments from Referee #2:

It would be interesting to discuss presented results (e.g. the underestimation in melting in the center and east of the Larsen C ice shelf) in greater detail to other studies e.g. to

other regional climate model studies over the Antarctic region or in general in terms of e.g. issues in snow melting (e.g. onset and ending) in other regions. Also GCMs might have similar issues that would be of interest to consider

Author Response:

We have altered the text to emphasize the relative advantages/disadvantages of hydrostatic vs. non-hydrostatic versions of the model, i.e. the accuracy of winds (in non-hydrostatic models such as WRF) vs. the long run periods and sophistication of the snowpack (in hydrostatic models such as MAR or RACMO2.3p2).

We now include a more thorough review of recent non-hydrostatic modeling studies (King et al., 2017; Turton et al., 2018; Bozkurt et al., 2018) noting that factors other than föhn melt are important over the Larsen C ice shelf as well as recent work showing that even a high-resolution non-hydrostatic model was not fully able to resolve föhn characteristics.

We have corrected a typo mis-stating that RACMO2.3p2 is a non-hydrostatic model, added greater detail about recent publications with RACMO2.3p2 over the AP, and included a direct comparison of melt occurrence/meltwater production between RACMO and MAR. References to recent work on RACMO3.2p2 over the AP are included (Van Wessem et al., 2018; Weisenekker et al., 2018)

Author's Changes in the Manuscript

Re: non-hydrostatic models:

Introduction: P3, L 2-12

Discussion and Conclusion: P18, L10-29

Re: hydrostatic models (RACMO2.3p2):

Introduction: P3, 26-36, P4, 7-9

Data and Methods: P 6, 19-23

Results: P10, L 3-19; P11, L18-21

Fig. 3, Fig. 5c

3) Overemphasis föhn winds

Comments from Referee #1:

In the abstract and introduction, a fair amount of emphasis is put on the role of föhn winds and northwesterly winds e.g (Pg 1, line 25, 32, 33, 35, Pg 3, line 5-21, 34-37, Pg 4, line 1, 20). However, in the results and discussion, this is not discussed thoroughly, either in the context of other studies, or how well MAR can model these features. More discussion of the föhn characteristics and melt related effects needs to be included in your discussion to have such a prevalence in the earlier sections.

Author Response:

The original discussion about föhn winds has been substantially limited to where the main emphasis is placed on previous studies with a non-hydrostatic model. More emphasis is placed

here on the distinction between the initial intrusion of föhn flow (which high-resolution hydrostatic models may capture) vs. the eastward propagation towards the edge of the Larsen C ice shelf (where the comparison with AWS stations are conducted). However, a section on northwesterly flow biases is specifically included to address the effects of probably föhn flow

Author's Changes in the Manuscript

Introduction: P3, L 1-12

Results: P16, L7-20

Discussion and Conclusions: P18, L 18-20

4) Length of the model run

Comments from Referee #1:

An additional novel aspect which this paper does not mention is the length of this modelling study. Output for the model are for 15 years, which is a long study period over this region. Previous melt-föhn studies have largely focused on case studies, or shorter time periods (e.g Elvidge et al 2015, Grosvenor et al (2014), King et al 2017). More emphasis could be put on the length of study, as this is of importance.

Author Response:

The length of the study has been emphasized in several places.

Author's Changes in the Manuscript

Abstract: P1, L18-20

Introduction: P4, 1-2

Discussion and Conclusions: P19,L1-5

5) Driving Reanalysis

Comments from Referee #2:

What about the impact of ERA-Interim as driving reanalysis data? Would it be possible to add it in the evaluation? Could the mentioned aspects of wind biases and thus resulting biases of melt occurrence have also their origin in the obtained large-scale atmospheric information given by the boundary condition?

Author Response:

To understand the impact of forcing on the representation of wind dynamics in MAR, we have included a comparison of ERA-Interim wind fields and discussed possible reasons for the differences.

Author's Changes in the Manuscript

Fig. 8 d,k

Data and Methods: P5, L 26-28

Results: P14, L35 – P15 7

6) Explicit comparison of satellite-based, model-based and AWS temperature-based melt occurrence

Comments from Referee #2:

What about observational uncertainty of satellite data or uncertainties introduced by the postprocessing of satellite data? Would it be possible to include a specific errorestimate to better evaluate the model results and to take into account the observational uncertainty?

Author Response

In addition to more focus in the introduction, greater attention is given to the discussion of the spatial resolution of satellite sources, although the errors associated with the postprocessing of satellite data were difficult to quantify here. Additionally, we add a comparison of melt occurrence from all satellite measures with AWS temperature based criteria (and associated temperature biases) in order to assess the sensitivity of melt occurrence criteria independently, before addressing the additional impact of wind direction.

Author's Changes in the Manuscript

Fig. 4: This is a new figure. Fig. 4a uses a meltwater production threshold of 0.4 mm w.e. to detect melt in MAR. A similar figure in Supplemental Fig. S2 (described in #3) Section 3.2 (P10, L21-33) discussed Fig. 4

7) Justification for the use of the MAR meltwater production threshold of 0.4 mm w.e. for melt occurrence

Comments from Referee #2:

What about observational uncertainty of satellite data or uncertainties introduced by the postprocessing of satellite data? Would it be possible to include a specific errorestimate to better evaluate the model results and to take into account the observational uncertainty?

Author Response

The decision to use a threshold of meltwater production exceeding 0.4 mm w.e as a criteria for meltwater occurrence is more thoroughly justified in the context of previous literature as well as via a comparison of melt occurrence estimates both domain-wide and at one AWS station (using satellite-based, model-based and AWS temperature-based estimates for melt occurrence) where multiple MAR thresholds are employed (0.1 mm w.e. – 4 mm w.e.).

Author's Changes in the Manuscript

Data and Methods: P6, L 8-18

Supplemental Fig. S2

Fig. 4

8) Additional model deficiencies

Comments from Reviewer #2:

Could the mentioned cold bias in MAR (when maximum temperature and average daily temperature exceed 0 degree Celsius) origin from other model deficiencies as well? So far only wind is considered.

Author Response

Other potential causes for melt are highlighted in greater detail in the results

The potential effects of horizontal and vertical resolution are also expanded upon (although these do relate to wind flow). This is discussed in Revision #1.

Author's Changes in the Manuscript:

P15 L9-17

9) Excessive Abbreviations

Comments from Reviewer #2:

In Section 4.2 and 4.2.1 there are many abbreviations introduced which makes it a bit difficult to read. Would it be possible to already introduce those in the methods part and provide a table as overview? Or maybe it is possible to reduce the amount of abbreviations used in the text.

Author's Changes in the Manuscript

This now includes an overview table as Table 1

10) Computation of Wind Direction

In the process of addressing the major revisions, we discovered a bug with the computation of wind direction in MAR. The now-corrected computation of wind direction substantially reduced the wind direction biases, although we address the biases that are present in light of how the absence of westerly flow affects melt on the eastern Larsen C ice shelf (where the AWSs are located).

Author's Changes in the Manuscript

Fig. 9: now focuses on the generalized absence of northerly and westerly flow rather than the two cases presented previously.

Fig. S10: now shows corrected wind directions, with Section 5 altered to account for these changes (wind directions are now in better agreement)

Table 2: Previously, wind directions were divided into N/S/E/W categories. This now examines flow divided into mutually-exclusive categories NE/SE/SW/NW with updated values

Section 4: Explicit discussion of the bias in MAR for southerly and easterly winds and an extended discussion of northwesterly flow

Response to Minor Comments (Referee #1):

Abstract:

Line 34: Authors state that reducing the underestimation of flow may be obtained by increasing the spatial resolution, but this is not given much discussion later in the paper. Either remove it and focus on hydrostatic assumption, or include changes to the spatial resolution in the discussion- either results from the suggested sensitivity study, or by discussing other studies. **See Response to Major Concerns above, #1**

Line 35: You mention reducing the underestimation of flow may be obtained by using higher-resolution topography, but this is not mentioned anywhere else in the paper. Similarly, you do not state what topography is used in the model, or what resolution it is. **See Response to Major Concerns above, #1
Topography shown in P5, L21-22**

Introduction:

Pg 2 Line 7: remove ‘finally’

corrected, P2, L2

Pg 2 Line 23: ‘suggested’ should be ‘suggest’

corrected, P2, L18

Pg 3 Line 17: Remove ‘during recent warming’ at the end of the sentence.

Paragraph has been removed.

Pg 3 Line 20: Is there a citation for this? ‘East AP is as vulnerable to wind dynamics as it is to temperature change’. Has a study quantified the difference in vulnerability? What vulnerability mean in this context?

Paragraph has been removed.

Pg 3/4 : Some citations are missing which may need including here, such as King et al 2017 and Elvidge et al 2015 which discuss föhn and melting on Larsen C.

Added, P3, L1-12, L29-33

Pg 4 Line 2/3: ‘These last studies taken together’ doesn’t read well. Perhaps change to ‘Both of these studies, along with others by Elvidge et al 2015 and King et al 2017, discuss both the atmospheric. . .’. This would include the previous comment also.

Paragraph has been removed.

Pg 4 Line 10: AWS is not defined yet (but is later defined on line 13/14). –

Corrected, P4, L5

Pg 4 Line 14: Which satellites? Just give their names/abbreviations here.

Corrected, P4, L11-12

Pg 4 Line 15 and 20: Be consistent with use of abbreviations or names. AP for example.

Corrected, “AP” used throughout

Pg 4: Line 24: from what date to 2014?

Corrected; P4, L 20

Data and Methods:

Pg 4 Line 27/28: MAR and AWS have been defined earlier. – **Corrected, P4, L29-30**

Pg 5 Line 5: Which part of Antarctica?

Corrected, Reference to Terra Nova Bay, Antarctica is added P5, L5

Pg 5, section 2.1: Where can readers can get more information about MAR, such as physics set up? Include a citation for this. What is the model top? 23 Sigma layers is very coarse (see major comments). Why was this vertical resolution used? Only 1 domain or is it nested? What is the resolution of the topography, and what dataset is used? BEDMAP2 for instance?

Corrected: Substantially more detail provided about

- Initial snow density
- Reference to previous model setup (P5, L12)
- Resolution and domain, nesting, topography
- P5, L10-37

Pg 5 Line 17: what mask? Land use? Land/sea?

Corrected, P5 L28

Pg 5 Line 20-26: reorder this paragraph to make it clearer what each notation is. For example, line 20-23, both notations are stated, but more emphasis is put on LWC0.4. It could be split into 2 sentences, one for LWC0.4 and one for MF0.4.

Addressed in Page 6, Line 1-11(rewritten)

Pg 5 Line 25: What is the justification for this condition? The same as LWC0.4 (Tedesco et al 2007)?

The meltwater threshold is discussed in Response to Major Concerns #5

Pg 5 Line 30: change ‘microwave sensors are weakly affected. . .’ to ‘microwave sensors are only weakly affected’.

Corrected, P6, L26

Pg 5 line 31: after citation, change ‘where’ to ‘whereas’ . .

Corrected, P6, L28

Pg 6, line 6/7: ‘used extensively’ is stated, but there is only 1 citation. Are there other important citations? The Drinkwater and Liu (2000) reference only looks at Antarctica, not Greenland.

– additional citations added, P7, L 4-5

Pg 6, equation 1: what is T_c ? The new paragraph is rewritten for clarity (P 7, L 32-36)

Pg 6: active and passive microwave: what are the spatial resolutions of the satellites? To allow some comparison with the 10km resolution of MAR.

P6, L 34; P7 L 21

Pg 7, line 2: confused what ‘here’ means in this context. For this location?

The new paragraph is rewritten for clarity (P 7, L 32-36)

Pg 7, line 3: ‘zwa is based on the winter mean threshold’. Threshold of what? Winter mean air temperature?

The new paragraph is rewritten for clarity (P 7, L 32-36)

Pg 7, line 8: pressure observations are not mentioned here but they are in line 27 onwards.

P8 L6,7 explicitly explains that the surface pressure comparison is provided in the supplemental material

Pg 7, line 19: what is meant by ‘expected’? This is also used in terms of wind speed later in the paper, and I don’t understand its use.

I have added an explanation for this in text, I am using the term ”expected value” (derived from the shape and scale parameters in the Weibull fit) interchangeably with the term “predicted mean” or “1st moment” to differentiate it from an arithmetic mean

P7 L17,18

Pg 7, line 27: What is meant by ‘estimating’ pressure from the AWS? Is pressure observed by the AWS or not? Pressure is also not mentioned elsewhere in the paper, so if it is not used, remove it. P8 L6,7 explicitly explains that the surface pressure comparison is provided in the supplemental material. Avoiding the word “estimated” P8, L 25

Pg 7, line 28: remove ‘a’ from ‘also estimated at a approximately. . .’ – corrected, P8, L 26

Pg 7, line 29: your lowest model level is 2m but only 23 sigma levels are used- this is very coarse. See major comments above. Are 2m diagnostics output from MAR?

As you could use these instead of taking it from the lowest model level, if this should

change when you run the sensitivity study for varying the number of vertical levels.

2m values for P were not available in this model version
(but will be in future model runs)

Results:

Pg 8, line 1: 'assess the extent to which each station is representative of larger scale climate variability'. Even though AWS14/Larsen and AWS15 are so close together? Do they have a different extent?

It is not *very* different but there's a slightly greater correlation in AWS15 to southerly regions as well as to the other side of the AP which is enough to be more affected by southwesterly flow

Pg 8, line 13: keep consistent with abbreviations.

- Corrected, P9, L10

Pg 9, line 3/4: you state coordinates/latitudes in the text but there are no coordinates on your Figure 2 plots. Include coordinates on the plots.

-Corrected, now Fig. 5

Pg 9, line 19: 'data sources ad secondarily' should read 'data sources and secondarily'.

Rewritten, P11, L 29

Pg 9, line 19: What are the spatial resolutions of the data sources? You mention this, but then don't go into it any further. However, you mention the depths presumed for melt water content and then discuss it for the next paragraph. Perhaps more information on the spatial resolutions is needed.

Added explanation in text, P11, L26-29

Pg 9, line 28: Give some examples of these 'low' melt occurrence regions. From elevation information in supplement table 1, they aren't on the ice shelf, are they on the main spine of the AP?

-Addressed, P 12, L2-3

Region also coincides with NL region, described: P12, L 34-36

Pg 9, line 28: heterogeneous in what way? Elevation? Surface type?

P12, L1,2

Pg 9, line 37: what is 'N column'?

Corrected, P12, L11

Pg 10, line 17: what is PMWAll-coincident?

Rewritten for clarity. P 12, L 27-30
Table 1 now has abbreviations

Pg 10, line 31: 'early pulse around Dec 15th', do you mean Nov 15th? As there are small pulses of melt here, and December 15th melt looks much larger.

Clarified. P10, L 8-12

Pg 11, line 25: 'during that period'. Which period? Be more specific.

Corrected, P14, L1-2

Pg 12, line 4: remove 'station' after AWS.

Corrected, P14, L16

Pg 12, line 8: remind readers of MAR-R/MAR differences here.

References to MAR-R are removed for clarity because results are unchanged, but the definition for MAR-R is included in Table 1 and kept in the figure

Pg 12, line 15/16: 'demonstrate the consistency of wind biases' and 'how wind biases vary by latitude' are slightly contradictory. Are they consistent or variable?

Rewritten for clarity, P14, L23-27

g 12, line 16: remove 'whereas', as you aren't comparing AWS and MAR, as one is for low wind and the other for high wind speeds. - Rewritten for clarity, P14, L23-27

Pg 12, line 16: 'MAR is dominated by northerly winds'. . Paragraph rewritten

Pg 12, line 27/28: Might be useful to highlight which rows of the table you mean here. When comparing all times and melt times. It isn't immediately clear that 'increased N and W flows' means compared to when there all days are included.

References to table rows added throughout

Pg 12, line 34: citation style.

Corrected, P15, L12

Pg 12, line 36: the abbreviation Ts is used in the table for when temperature is >0degC. However, in the text you say that when 2m-temperatures exceed 0degC. Stick to the T2m abbreviation.

Corrected

Pg 13, line 5: remove extra space before -3.04.

Paragraph rewritten

Pg 13, line 8-12: include reference to figures here.

Paragraph rewritten

Pg 13, section 'observed NE flow and observed SW flow': It needs to be clearer that when MAR has different wind directions to the observations, MAR is wrong. Especially in the case where there are large differences (NE vs NW for instance). And explain what the possible reasons are for this. Is MAR not getting the synoptic scale wind direction right? Or is there not enough blocking on the west of the AP to prevent flow over the AP when there shouldn't be? This section is a good idea to see what impact the wind direction is having in MAR, but it should also be stated that if MAR is getting something like large scale flow wrong, it might be getting other processes wrong due to this.

Paragraph rewritten due to recomputation in wind fields

Pg 14, line 1-6: In this section, it might be good to remind the reader, that in case 2, MAR is getting the wind direction wrong when compared to AWS. So that the reader can put these results into context.

Paragraph rewritten due to recomputation in wind fields

Pg 14, line 7: Using Ts abbreviation but you have only talked about air temperature and used T2m previously.

Paragraph rewritten due to recomputation in wind fields

Pg 14, line 11-13: confusing sentence. What is meant by expected?

Paragraph rewritten due to recomputation in wind fields

Pg 14, line 13: I don't think figure 6 e-h are necessary. They are not discussed as much in the text, and the information is given by the 6a-d. Similarly, figure 7 could be included into figure 6 in place of 6e-6h.

Fig. 9 now shows more general wind biases in response to the recomputation of wind fields and figures have been combined

Discussion:

Pg 14, line 30: remove 'in the aggregate'.

Corrected, P.16, L22

Pg 15, line 4: where should be when.

Discussion has been rewritten for clarity

Discussion has been rewritten for clarity

Pg 15, line 6/7: Any suggestions for why there are less westerly winds in MAR?

See: Response to Major Concerns #1

Pg 15, line 17-21: considering the impact of föhn winds is prominent in the abstract and introduction, this seems like a short discussion of them. See major comments.

See: Response to Major Concerns #3

Pg 15, line 19-21: wind speed may not be the biggest issue here if MAR is unable to get wind direction right.

The corrected calculation for wind direction has altered these results considerably, and we have emphasized that wind biases account for a relatively small proportion of melt occurrence captured by satellites, but not by MAR

Pg 15, line 23-25: include references to and discussion of non-hydrostatic models that have captured föhn flow- e.g Elvidge et al, 2015 (Met UM model), Turton et al 2017 (WRF model).

See: Response to Major Concerns #3

Pg 15, general: The abstract suggests that increasing the spatial resolution of MAR or the topography in the model may improve output, but this isn't discussed in your discussion. See major comment.

See: Response to Major Concerns #1

Pg 16, line 7: Figure 8 should come earlier in the text. This is a good summary figure and could be included in page 11 where interannual variability is mentioned.

This has now been moved to Fig. 2 and Sect. 3.1 (along with a comparison with RACMO in Fig. 3)

Pg 16, line 19/20: 'melt in the NL region is particularly sensitive to föhn induced melt'. You need to support this with other studies (e.g Elvidge, et al 2015, Cape et al 2015), as your study only mentions föhn jets on the SW of the ice shelf in earlier discussion.

See: Response to Major Concerns #3

Pg 16, line 22/23: is this future work? As this study doesn't talk about large-scale atmospheric drivers at all. Or you need to support this with studies which look at largescale atmospheric patterns and their related wind patterns in this region (such as Cape et al 2015).

I've eliminated this section to discuss a paper more specifically which is currently in progress.
P19, L1-5

Figures:

Figure 1: include in the caption that Larsen IS and AWS14 have the same MAR grid cell, which is why they are on the same marker. – addressed

Figure 1: Where is the topography data from? - addressed

Figure 1: include coordinates. - addressed

Figure 2: include coordinates. - addressed

Figure 3/4: make insert bigger, or include it in figure 1. - Inserted in Fig. 2

Figure 6: make a heading over a/b 'Case 1' and over c/d 'Case 2'. I don't think anything else is gained from e-h, as they are mentioned only briefly in the text. – Addressed. Figure is combined into Fig. 8, although the recomputation of wind directions means that different (more generalized) biases are discussed

Figure 6: g and h are not described in the caption. – Now removed

Figure 6/7: 'yellow as only shown for g,h'. Not sure what this means, as yellow markers are used in every subplot, not just g and h. - addressed (with a legend included)

Figure 7: could be combined with Figure 6. - addressed

Figure 8: if this goes earlier in the text, then the size of the insert is sufficient for the other figures which require it. – This is now Fig. 2

Supplementary Figure 6: lettering is not right. There is no a-c as in the figure, and g-m are not in the caption. There are only 6 subplots, so I assume a-f is correct.

- corrected

Table:

Table 1: Ts should be T2m, unless actual surface temperature data is being used, but is not mentioned elsewhere in the paper.

- Corrected (now table 2)

Typos:

Pg 1, Line 29: satellites should be satellite

Abstract has been changed considerably

Pg 2, line 21: comma after citation

Corrected, P2, L16

Pg 2, line 27: comma after citation

Corrected, P2, L23

Pg 4, line 20: umlaut missing over o in föhn

Final paragraph of Intro changed

Pg 5, line 31: comma after citation

Corrected, P6, L28

Pg 6, line 6: remove full stop after algorithm, there is one after the citation. Corrected, P7, L3

Response to Minor Comments Referee #2:

Page 3 l. 29 + l. 33: use same space before unit

– corrected, P3, L23

Page 4 l. 20: change to föhn

Paragraph reordered

Page 5 in section 2.1: Please mention the size of the model domain

Lat/lon boundaries added in P 5 L25

Page 5 l. 2: explain abbreviation RCM

Term now fully introduced in Introduction P3, L14,15

Page 7 l. 6: add space after where

Paragraph reorganized for clarity

Page 7 l.35: remove space before Wilks

- corrected, P8, L33

Page 12 l. 34: citation with 2 brackets

- corrected, P15, L12

Page 34 l. 34: remove second brackets (assuming related to the previous comment)

Page 18 l. 8: remove slash in Royal

- corrected, P21, L19

Page 24 l. 5: add space before Greenland

- corrected

Figures:

Fig. 1: Please add coordinates to the axes

– added

Fig. 2: Please add coordinates to the axes

– added, Now Fig. 5

Fig. 3: Please have a consistent labeling of axes throughout all the figures 1-8; variable [unit]

- corrected

Fig: 4: Same as Fig. 4

- corrected

Fig. 7: ended with a comma] – corrected, Figure now combined with previous figure.

Melting over the Northeast Antarctic Peninsula (1999-2009): evaluation of a high-resolution regional climate model

Rajashree T. Datta¹, Marco Tedesco², Cecile Agosta³, Xavier Fettweis³, Peter Kuipers Munneke⁴, Michiel R. van den Broeke⁴

¹The Graduate Center, City University of New York, NY 10016, USA

²Lamont-Doherty Earth Observatory of Columbia University, Palisades, New York, New York 10964, USA

³Department of Geography, Université de Liège, Liège, Belgium

⁴Institute for Marine and Atmospheric Research, Utrecht University, Utrecht, The Netherlands

Correspondence to: Rajashree Tri Datta (Tri.Datta@gmail.com)

Abstract. Surface melting over the Antarctic Peninsula (AP) may impact the stability of ice shelves and therefore the rate at which grounded ice is discharged into the ocean. Energy and mass balance models are needed to understand how climatic change and atmospheric circulation variability drive current and future melting. In this study, we evaluate the regional climate model MAR over the AP at a 10 km spatial resolution between 1999 and 2009, a period when active microwave data from the QuikSCAT mission is available. This is the first time that this model, which has been validated extensively over Greenland, has been applied to the AP at a high resolution and for a relatively long time period (full outputs are available to 2014). We find that melting in the northeastern AP, the focus area of this study, can be initiated both by sporadic westerly föhn flow over the AP mountains, and by northerly winds advecting warm air from lower latitudes. A comparison of MAR with satellite and automatic weather station (AWS) data reveals that satellite estimates show greater melt frequency, a larger melt extent, and a quicker expansion to peak melt extent than MAR in the center and east of the Larsen C ice shelf. These differences are reduced in the north and west of the ice shelf, where the comparison with satellite data suggests that MAR is accurately capturing melt produced by warm westerly winds. MAR shows an overall warm bias and a cool bias at temperatures above 0°C as well as fewer warm, strong westerly winds than reported by AWS stations located on the eastern edge of the Larsen C ice shelf, suggesting that the underestimation of melt in this region may be the product of limited eastward flow. At higher resolutions (5km), MAR shows a further increase in wind biases and a decrease in meltwater production. We conclude that non-hydrostatic models at spatial resolutions better than 5km are needed to better-resolve the effects of föhn winds on the eastern edges of the Larsen C ice shelf.

1 Introduction

Increased meltwater production over the Antarctic Peninsula (AP) in the latter half of the 20th century has been linked to a warming atmosphere, with potential implications for future sea-level rise (Barrand et al., 2013; Turner et al., 2005; Vaughan, 2006). Surface melting has been implicated in the weakening and eventual collapse of ice shelves as well as the subsequent acceleration of contributing glaciers, with the Larsen A (1995) and Larsen B (2002) on the eastern

Deleted: East

Deleted:) plays a crucial role for

Deleted: dynamics of

Deleted:

Deleted: , hence modulating the mass balance in a region of the world which is particularly sensitive to increasing surface temperatures. Understanding the processes that drive melting using surface energy and mass balance models is fundamental to improving estimates of current and future surface melting and associated sea level rise through ice-shelf collapse. This is even more important in view of the specific challenges presented by how circulation patterns over the topographically-complex Antarctic Peninsula, especially föhn winds, impact surface melt.

Deleted: Modèle Atmosphérique Régionale (MAR)

Deleted: Antarctic Peninsula (AP)

Deleted: horizontal

Deleted: which coincides with the availability of

Deleted: Antarctic Peninsula

Deleted: Our primary regional focus is the

Deleted: ern East

Deleted: Antarctic Peninsula

Deleted: (East AP)

Deleted: where we define smaller sub-regions according to divergent melt occurrence biases. Melting in the East AP

Deleted: To assess MAR's ability to simulate these physical processes, this study takes a unique approach, examining model biases for melt occurrence on the Larsen Ice Shelf, as evaluated by satellite estimates from passive and active microwave data, with concurrent temperature biases associated with wind direction biases as evaluated by three automatic weather stations (AWS). Our results indicate

Deleted: s

Deleted: The difference between the remote sensing and modeled estimates reduces in the north and west of the East AP. Our results indicate that although

Deleted: , it also shows

Deleted: which may lead to an underestimation of melt

Deleted: eastward flow and

Deleted: The underestimation of föhn flow in the east of the Larsen C may potentially be resolved by removing the hydrostatic assumption in MAR or increasing spatial resolution. The underestimation of southwesterly flow in particular may be reduced by using higher-resolution topography. (... [1])

Deleted: East

1 AP as the most notable examples (Vaughan et al, 1996; Rott et al, 1998; Scambos, 2004). In July 2017, a rift on the
2 Larsen C Ice Shelf, which had been expanding for several years, resulted in the calving of the 5800 km² iceberg A68
3 (Hogg and Godmundsson, 2017).

Deleted: finally

Deleted: .

4 Surface melting influences ice shelf stability through the stress produced by meltwater ponding as well as
5 meltwater percolation through firn. One proposed mechanism for the disintegration of ice shelves hypothesizes that
6 surface meltwater infills and deepens pre-existing crevasses, through a process called hydrofracture (Scambos et al.,
7 2000; Weertman, 1973; van der Veen et al., 1997). In addition, a complementary mechanism proposes that when
8 supraglacial lakes drain (becoming dolines), an upward flexure is induced which can weaken an ice shelf, both at the
9 surface and at the base (MacAyeal and Sergienko, 2013). Large open-rift systems were observed over the Larsen B
10 ice shelf in the summer of 2002 which are consistent with substantial melt initiating both mechanisms and leading to
11 ice shelf disintegration (Glasser et al., 2008; MacAyeal and Sergienko, 2013). Alternatively, meltwater can affect ice
12 shelf dynamics by percolating into firn and increasing its density until no pore space remains. In the absence of pore
13 space, meltwater moves through the underlying ice sheet or collects on the surface in melt ponds. This process,
14 operating over decades, can pre-condition the ice shelf for both hydrofracture and post-drainage flexure stress during
15 high-melt seasons (Kuipers Munneke et al., 2014). Meltwater can also form below the surface in blue ice areas, due
16 to the smaller extinction coefficients and lowered albedo of ice (Brandt and Warren, 1993), as well as under low-
17 density snow on clear days, when temperatures are slightly below freezing (Koh and Jordan, 1995). Modeling studies
18 suggest that the different sensitivities of subsurface blue-ice vs subsurface snow melt is a product of the radiative and
19 heat transfer interactions, resulting from their differing albedo, grain size and density (Liston et al., 1999a; Liston et
20 al. 1999b). Meltwater forming over blue ice and flowing downstream to collect in subsurface layers (the ice-albedo
21 feedback) has recently been shown to be substantial in parts of East Antarctica (Lenaerts et al., 2016). Recent work
22 has also shown the lateral flow of meltwater (supraglacial runoff) on the Larsen A Ice Shelf in 1979 (Kingslake et al.,
23 2017), which imply prolonged periods of lowered albedo. These surface rivers could become much more prevalent
24 across Antarctica in future warming scenarios than previously expected, and may provide a means of stabilizing ice
25 shelves by routing meltwater away (Bell et al., 2017).

Deleted: ent

Deleted: air

Deleted: therefore

Deleted: sheet

Deleted: under

Deleted: surfaces

Deleted: likely

Deleted:

Deleted: ed

Deleted:

Deleted: The net effects of melt

Deleted: rface rivers

26 Since the collapse of Larsen A and Larsen B ice shelves, ice velocities of several of their feeding glaciers
27 have increased, and seasonal variations in flow have suggested that both summer meltwater percolation (Zwally, 2002)
28 and the removal of backstress played a role in the acceleration (Scambos, 2004; Rott et al., 2002). The remaining
29 Larsen C ice shelf to the south could prove to be similarly vulnerable to collapse due to atmospheric warming (Morris
30 and Vaughan, 2013). Radar analysis over a 15-year period has shown that the surface of Larsen C has been lowering
31 from both firn air depletion (due to either limited accumulation or high surface melt) and basal ice loss, although the
32 latter term is thought to be more substantial (Holland, 2015). While most regional climate models (RCMs) do not
33 account for englacial flow or surface rivers, accurate modelling of surface meltwater production is a crucial step in
34 assessing the potential effects on the ice sheet, especially in the case of the Larsen C ice shelf.

Deleted:

Deleted: g

Deleted: such as MAR

Deleted: models

Deleted: are

Deleted:

Deleted: .

Formatted: Indent: First line: 0.5"

Deleted: East

Deleted: I

Deleted: West

35 The eastern AP, where the Larsen C ice shelf is located, is on average 3-5°C cooler than the western AP at
36 the same latitude (Morris and Vaughan, 2013). When strong westerly winds force air across the bisecting mountain
37 range of the AP (Fig. 1), the resulting föhn winds can produce pulses of warming on the eastern AP ice shelves

(Marshall, 2007). Föhn is a warm, dry air flow on the lee slopes of a mountain range (Beran 1967) that can contribute to melt and sublimation. Multiple studies have focused on the use of high-resolution non-hydrostatic models over the eastern AP to determine the frequency of föhn occurrence over relatively short periods (Elvidge et al., 2015; Grosvenor et al., 2014; Elvidge et al., 2016; King et al., 2017). King et al. (2017) found that over a single season, föhn flow occurred 20% of the time. This study showed substantial melt occurrence observed by satellites without föhn flow, suggesting that surface melt was influenced by other factors as well. A recent study by Turton et al., (2017), using a non-hydrostatic model, compared modelled flow characteristics during two föhn events and found that a 1.5 km version of the model was able to capture the eastward propagation of melt-inducing winds, whereas a 5km version could not, according to a comparison with AWS stations. However, Bozkurt et al. (2018) demonstrate that a 2km version of the same model was still unable to resolve high temperatures associated with the initiation of föhn flow during a short period. We note that because these modelling studies use a non-hydrostatic model, they are limited to short periods due to the prohibitive computational cost.

Models are limited by the parameterization of physics and our incomplete understanding of the physical processes driving the observed changes. Regional climate models (RCMs) such as the Modèle Atmosphérique Régionale (MAR), evaluated here, can be used for simulating the coupled atmosphere/surface system at a continental and decadal scale (Gallée and Schayes, 1994). The trade-off, in this case, is that RCMs might not be able to capture physical processes with the required accuracy and must be thoroughly evaluated with in-situ and remotely sensed observations. Several studies have used passive microwave estimates for melt occurrence alongside in-situ temperature data (Liu et al., 2003; Ridley, 1993; Tedesco et al., 2007; Tedesco et al 2009; Tedesco and Monaghan, 2009), reporting an increase of surface melting over the AP over the 1980-1999 period (Torinesi et al., 2003). However, other studies have suggested that the findings may have been impacted by a change in the acquisition hours of the satellite and that changes in melt over the 1979-2010 period were insignificant (Kuipers Munneke et al., 2012). Melt occurrence over the AP has also been investigated using the QuikSCAT satellite product at a ~2.225km resolution (Long and Hicks, 2010) in combination with model outputs from the RCM RACMO2 (Regional Atmospheric Climate Model) and in-situ temperature estimates (Barrand et al., 2013). Raw backscatter values from QuikSCAT have also been used to estimate melt flux over the AP (Trusel et al., 2013; Trusel et al., 2012). A recent study using 5.5km horizontal resolution run of RACMO 2.3 over the AP, suggested that a further increase in resolution would be required to properly resolve föhn wind propagation, which would imply the removal of the hydrostatic assumption (Van Wessem et al., 2015a; Van Wessem et al., 2015b). However, Wiesenekker et al. (2018) show that föhn events observed by an AWS close to the AP mountain range were well captured by a later version of the same RCM, enabling a reconstruction back to 1979. Where the hydrostatic assumption is preserved (such as with MAR), higher resolutions may inhibit flow in the model, resulting in limited eastward föhn flow in the eastern AP (Hubert Gallée, personal communication). Despite these drawbacks, the current class of hydrostatic RCMs which include relatively complete representations of the snow physics are useful tools to simulate the effect of surface melt on the snowpack over long timescales. Additionally, these high-resolution runs can easily be compared to, and potentially nested into, continental-scale runs of the same model.

Moved (insertion) [1]

Deleted: Observation-based studies on the formation of melt ponds in the Cabinet Inlet portion of the Larsen C Ice Shelf have focused on the response to föhn winds (Luckman et al., 2014) and the formation of subsurface ice (Hubbard et al., 2016). These last studies taken together discuss both the atmospheric drivers for melt as well as the effects on the ice shelf within our region of interest, but are necessarily limited to a small region where observations are available. By contrast, spaceborne satellites allow us to estimate surface melt occurrence and meltwater production over the entire AP, complementing in-situ data. The combination of satellite-based and in situ data provide an excellent toolset for model validation.

Deleted: ; Wiesenekker et al., 2018

Formatted: Font color: Text 1

Formatted: Font color: Text 1

Deleted: This is primarily caused by more exposure to open water in combination with prevailing westerly winds on the west AP and southerly winds on the east AP. Moreover, when strong westerly winds cross the bisecting mountain range of the AP (Fig. 1), the resulting föhn winds can produce pulses of warming on the East Antarctic Peninsula's ice shelves (Marshall, 2007). Föhn winds are warm, dry air flow on the lee slopes of a mountain range (Beran 1967). This resultant warming can be produced by four main mechanisms. Elvidge (2016) uses a modeling approach to trace four physical processes that occur during föhn flow in the East AP, namely *isentropic drawdown* (sourcing of föhn air from higher altitudes), *latent heating and precipitation* (where cooling during uplift on the windward side promotes precipitation), *mechanical mixing* (turbulent sensible heating and drying of low-level flow) and *radiative heating* (where cloudless conditions on the lee side increase the availability of shortwave radiation for heating). The relative importance of each of these mechanisms for surface melt has been shown to be related to the source of föhn flow in the East AP (Elvidge et al., 2015; Grosvenor et al., 2014). For example, southwesterly föhn jets descending from gap flow (from lower-elevation passages in the mountain range) have been shown to be cooler and moister than surrounding föhn flow descending from higher elevations (Elvidge et al., 2015). Recent warming in the East AP has been linked to an increase in föhn winds during recent ... [2]

Formatted: Font color: Auto

Deleted: RCMs

Deleted: alongside

Formatted: Font:Italic

Moved (insertion) [3]

Deleted:

Deleted: ;

Moved up [3]: Liu et al., 2003; Ridley, 1993; Tedesco et al., 2007; Tedesco et al 2009; Tedesco and Monaghan, 2009

Deleted:

Deleted: and focusing on overall surface mass balance (SMB

Deleted:)

Deleted: s

Deleted: We note, however, that where

Deleted: as with this model run

Deleted: East

Deleted:

Moved up [1]: Observation-based studies on the formation of melt ponds in the Cabinet Inlet portion of the Larsen C Ice Shf ... [3]

1 Here, we assess the MAR model at a 10 km horizontal spatial resolution over the AP, where outputs are
 2 available over a relatively long time period (1999-2014, i.e. 15 years), using both satellite and *in-situ* data, aggregating
 3 meltwater production to drainage systems (basins) as described by Zwally (2002). While previous studies have
 4 evaluated how surface melt is modelled using satellite data, or evaluated the representation of the near-surface
 5 atmosphere with automatic weather station (AWS) data, we use both sources in conjunction to understand MAR's
 6 ability to simulate specific physical processes, i.e. to assess melt and temperature biases by wind direction. We first
 7 report total meltwater production from MAR at the basin scale and compare mean annual meltwater production with
 8 outputs from RACMO2.3p2 (Van Wessem et al.m 2018), another hydrostatic RCM run at a 5.5km resolution (Sect.
 9 3.1). We evaluate surface melt occurrence from MAR at the sub-basin scale using satellite estimates and link melt
 10 occurrence biases to temperature and wind biases at a point scale using AWS data. We compare meltwater occurrence
 11 derived from two satellite sources, passive microwave "PMW" and QuikSCAT active microwave, with MAR outputs
 12 over the AP (Section 3.2). We focus primarily on the NE basin in the East AP as it contains the former Larsen A,
 13 Larsen B and current Larsen C Ice Shelf, where we define sub-regions based on high and low melt occurrence
 14 estimated by PMW algorithms (Tedesco, 2009). We then compare climatologies of melt extent, as well as inter-annual
 15 trends, from both passive and active microwave data with those computed from MAR outputs (Section 3.3). Because
 16 melt on the Larsen C Ice Shelf can potentially be initiated by northwesterly föhn flow sourced from over the AP or
 17 southwesterly flow through gaps in the mountain range (even at sub-zero temperatures), we compare melt occurrence
 18 reported by satellite estimates vs MAR (coinciding with the 2000-2009 QuikSCAT period) partitioned by temperature
 19 differences and wind direction at the location of the Larsen Ice Shelf AWS. Two additional stations (AWS14 and
 20 AWS15 are used to examine the persistence and spatial distribution of wind biases from 2009 to 2014. (Section 4).
 21 Because all three stations are located on the eastern side of the Larsen C Ice Shelf, this comparison can assess the
 22 impact of limited eastward flow on temperature and melt occurrence. In light of the model biases found in this analysis
 23 and the potential to correct them with an enhanced resolution model in the future, the discussion (Section 5) includes
 24 a sensitivity test with MAR at multiple resolutions. This is performed to specifically assess the effects of increased
 25 resolution on eastward flow and resultant surface melt. Table 1 lists abbreviations used throughout the text along with
 26 sections in which the terms are introduced.

Deleted: Antarctic Peninsula

Deleted: (and co-temporally)

Deleted: automatic weather station (

Deleted:)

Deleted: first

Deleted:

Deleted: ,

Deleted: Antarctic Peninsula

Deleted: 1

Deleted: 1

Deleted: S

Deleted: three AWS stations are located. In this basin, we

Deleted: three different passive microwave (PMW)

Deleted: 2

Deleted: 1

Deleted: S

Formatted: No underline

Deleted: fo

Deleted: Two additional stations (AWS14 and AWS15) are used to examine the persistence of these wind bias trends to 2014 (Sect. 4). Discussion and conclusions follow in Sect. 5.

Formatted: Font color: Text 1

27 2. Data and Methods

28 This study takes a combined observational and modelling approach. The primary tool used to understand the coupled
 29 atmosphere and snowpack is the MAR RCM. We employ *in-situ* data collected from 3 AWS stations to evaluate the
 30 near-surface atmosphere biases in MAR as well as to assess inter-annual trends. While in-situ observations of 2m air
 31 temperature are frequently treated as a proxy for melt (Braithwaite 1981), this method is most effective when the
 32 energy budget is dominated by the turbulent sensible heat flux and incoming longwave radiation and does not capture
 33 melt which can occur due to shortwave radiative forcing when air temperatures are below 0°C (Hock, 2005; Kuipers
 34 Munneke et al., 2012). We also use observations from the QuikSCAT (QS) and SM/MR (Scanning Microwave
 35 Multichannel Radiometer, 1978-1987) / SSM/I (Special Sensor Microwave/Imager, 1987 - to date) satellites to
 36 evaluate both melt occurrence and intensity in MAR.

Deleted: , using both model results and observations

Deleted: Modèle Atmosphérique Régionale (MAR)

Deleted: automatic weather stations (AWS)

Deleted: Accordingly, we

Deleted: S

1 **2.1 Regional climate model outputs**

2 The MAR RCM is a modular atmospheric model coupled to the Soil Ice Snow Vegetation Atmosphere Transfer
3 scheme (SISVAT) surface model (De Ridder and Gallée, 1998), which includes the multi-layer snow model Crocus
4 (Brun et al., 1999). MAR was originally implemented to simulate energy and mass balance processes over Terra Nova
5 Bay, Antarctica (Gallée and Schayes, 1994). Within SISVAT, meltwater is calculated at the surface when the surface
6 reaches the melting point in combination with a surplus of energy (a deficit results in refreezing). The presence of
7 meltwater alters the snow characteristics (for example, the type and size of snowgrains) and percolation through the
8 snowpack is determined through a tipping bucket method based on snow density. A diagram and description of the
9 sequence of these specific processes in MAR is provided in Figure S1.

10 The model configuration primarily used in this study is MAR version 3.5.2, with 23 sigma layers from 200
11 hPa to the surface. This version has been used in multiple studies over Greenland; the specific updates to the physics
12 from the original version of MAR as well as multiple uses of this model are described in detail in Fettweis et al. (2016).
13 The fresh snow density scheme used here is a new MAR implementation specific to Antarctica which has been tested
14 with *in-situ* observations (Agosta et al., 2018, in review) and discussed further in that study. Here, fresh snow density
15 (ρ) is computed as a function of 10m wind speed (WS, $m s^{-1}$) and surface temperature (T_s , K) such that:

16
$$\rho = 149.2 + 6.84 WS + 0.48 Ts \tag{1}$$

17 with a lower boundary of $200 kg m^{-3}$ and an upper boundary of $400 kg m^{-3}$. This parameterization was tuned such that
18 the density of the first 50cm of snow fits observations collected over the Antarctic ice sheet, although we note that no
19 reliable measurements were available over the AP. The subsequent compaction of snow layers uses the formulation
20 from Brun (1989). There are 30 snow/ice layers of variable thickness from the surface to a 20 m depth (below which
21 ice is assumed present). Topography is interpolated from 1 km Bedmap2 (Fretwell et al., 2013 ; Green et al., 2016) to
22 the MAR grid. The snowpack is initialized at $300 kg m^{-3}$ at the surface and $600 kg m^{-3}$ at depth. Following 2 years of
23 spinup, MAR results are independent of the initial conditions ; for these results, 5 years of spinup were run.

24 MAR outputs are generated at a horizontal spatial resolution of 10 km for the years between 1999 and 2014.
25 The model domain includes the AP region between -79.5° and -56.9° latitude and -94.9° and -39.7° longitude. Lateral
26 boundary conditions are specified from the European Centre for Medium-Range Weather Forecasts (ECMWF), using
27 the ERA-Interim reanalysis (Dee et al., 2011), which is also used for a direct comparison with AWS wind
28 speed/direction. This is a single model domain with no nesting. We note that the ice (vs sea) mask used does not
29 include the Larsen A or Larsen B Ice Shelf in order to preserve consistency for comparison between years (most of
30 which post-date the collapse of these ice shelves). For the analysis of the effects of resolution on surface melt estimates
31 presented in Section 5, we use three version of MAR v. 3.9. Relative to version 3.5.2, which is primarily used in this
32 study as well as in Fettweis et al. (2017), the computational efficiency of MAR v3.9 has been improved such that
33 increased resolution runs are potentially viable. The improvements in the physics include an increase in the lifetime
34 of clouds, partly correcting for the underestimation of downward longwave radiation and the overestimation of inland
35 precipitation found in Fettweis et al. (2017). MAR v3.9 setups include a version at a 10km horizontal resolution similar
36 to the model used for the main analysis, one where the horizontal resolution is reduced to 5km and one where the
37 vertical discretization is increased to 32 sigma layers (at a 10km resolution).

- Deleted: The Modèle Atmosphérique Régionale (MAR) regional climate model
- Deleted: The Modèle Atmosphérique Régionale (MAR) RCM
- Deleted: over
- Deleted:
- Deleted: there is a
- Deleted:
- Deleted: e
- Deleted: history
- Deleted: Supplemental

Formatted: Font:Italic

Formatted: Superscript

Deleted: The snowpack is represented by

Deleted:

Deleted: this model run had a

Deleted: spin-up of 5 years for each final model year

Deleted: For the purposes of this study,

Deleted: .

1 We consider two conditions for identifying melting based on previous work comparing MAR outputs
 2 (version 3.2) and satellite microwave melt estimates that found that passive microwave estimates were sensitive to a
 3 meltwater content of 0.4% (or mm w.e.) in the first meter of the snowpack (Tedesco et al., 2007). The first condition
 4 ($LWC_{0.4}$) determines melt occurrence in MAR when the daily-averaged integrated liquid water content (LWC) in the
 5 first meter of the snowpack exceeds 0.4% for at least three consecutive days. The second condition ($MF_{0.4}$) determines
 6 melting when total meltwater production over the day exceeds 0.4 mm w.e., and is intended to capture both sporadic
 7 melt (which may refreeze) and melt which has percolated into the snowpack column below 1m, i.e. equivalent satellite-
 8 based estimates could have potentially shown melt occurrence during some portion of the day. A sensitivity test was
 9 conducted with multiple thresholds, finding that the differences between a threshold of 0.1 and 1 mm w.e. (suggested
 10 by Franco et al., 2013 as a melt threshold for Greenland) was negligible overall, but more substantial on the northern
 11 Larsen C Ice Shelf, where the 4 mm w.e. threshold proved insufficient to capture melt occurrence (Fig. S2). Similarly,
 12 we performed a comparison of melt occurrence computed from 2000-2009 at the Larsen Ice Shelf AWS for all
 13 satellite-based algorithms as well as AWS-based melt-occurrence criteria, i.e. where $MaxT2m > 0^{\circ}C$ and $AvgT2m >$
 14 $0^{\circ}C$ (Fig. S2h). We found that neither total MAR melt occurrence nor the relative agreement with observed sources
 15 varied substantially between thresholds until a threshold of 4 mm w.e. Consequently, we use a meltwater production
 16 threshold of 0.4 mm w.e. to define melt occurrence for the remainder of the study due to its sensitivity at the northern
 17 Larsen C ice shelf. The differences in sensitivity for each satellite-based criteria for melt occurrences, as well as
 18 associated temperature biases, are discussed in detail in Section 3.1.

19 MAR meltwater production is compared to melt outputs from the RCM RACMO2.3p2, a hydrostatic model
 20 which has been run extensively over polar regions and over the AP at a 5.5km resolution at 40 vertical levels.
 21 RACMO2.3p2 is forced at the boundaries by ERA-Interim every six hours, as with MAR in this study. (Van Wessem
 22 et al., 2018). Model results over the AP for RACMO 2.3p2 did not vary substantially from RACMO2.3, which was
 23 evaluated extensively in previous work (Van Wessem et al., 2015a; Van Wessem et al., 2015b).

24 2.2 Microwave satellite estimates of melt extent, duration

25 Spaceborne microwave sensors can detect the presence of liquid water in snow over those regions where poor or no
 26 observations and unlike sensors in the visible range, microwave sensors are only weakly affected by the presence of
 27 clouds. In the case of active measurements (e.g., radar, scatterometer), the presence of wet snow is associated with a
 28 sharp decline in backscatter (σ^0) (Ashcraft and Long, 2000), whereas in the case of passive microwave data the
 29 detection is associated with an increase in brightness temperature (T_b) (Mote et al., 1993; Tedesco et al., 2007). In
 30 either passive or active microwave estimates, even the presence of a relatively small amount of liquid water (i.e. a few
 31 percent) triggers a substantial increase in the imaginary part of the dielectric constant (Ashcraft and Long, 2006; Ulaby
 32 and Stiles, 1980).

33 2.2.1 Active Microwave Data: QuikSCAT

34 We employ a wet snow high-resolution product (~2.225km) described in Steiner and Tedesco (2014) to derive melt
 35 occurrence from active microwave data. Both melt occurrence and raw backscatter values used in this analysis use

Deleted: .
Moved (insertion) [2]
Deleted: from MAR
Deleted:
Deleted:
Deleted: W
Deleted: E
Deleted: ,
Deleted:). Specifically, we assume melting in MAR either
Deleted: (equivalent to 0.4 mmwe in a 1 meter column)
Formatted: Subscript
Deleted: i
Deleted: W
Deleted: Differences between meltwater production thresholds were greater in the northern Larsen C ice shelf, where the 4 mm w.e. threshold proved insufficient to capture melt occurrence (Fig. S2).
Formatted: Font color: Text 1
Formatted: Font color: Text 1
Deleted: thresholds
Formatted: Font color: Text 1
Deleted: except
Formatted: Font color: Text 1
Deleted: for the
Deleted: , which provides sufficient
Formatted: Font color: Text 1
Deleted: between melt occurrence
Formatted: Font color: Text 1
Deleted: algorithms
Formatted: Font color: Text 1
Deleted: non-
Deleted: or when total meltwater production over the day exceeds 0.4 mm w.e. The threshold value in the first condition (denoted as $LWC_{0.4}$) of 0.4% has been selected based on previous work comparing MAR outputs (version 3.2) and microwave melt estimates (Tedesco et al., 2007). The second condition is denoted as $MF_{0.4}$. This less-restrictive condition is intended to capture both sporadic melt and melt which has percolated into the snowpack column below 1m. .
Moved up [2]: based on previous work comparing MAR outputs (version 3.2) and microwave melt estimates (Tedesco et al., 2007).
Deleted: satellites
Deleted: melting
Deleted: exist at high temporal resolution, because unlike sensors in the visible range, microwave sensors are weakly affected by the presence of clouds
Deleted: .

1 normalized backscattering values as measured by the Seawinds sensor onboard the QuikSCAT satellite at Ku band
2 (13.4 GHz), with the enhanced resolution provided by the application of the Scatterometer Image Reconstruction
3 (SIR) algorithm (Long and Hicks, 2010). Both Ku- and C-band scatterometers have been used extensively to detect
4 melt onset and freeze-up in Antarctica and Greenland (Drinkwater and Liu, 2000; Steiner and Tedesco, 2014; Ashcraft
5 and Long, 2006; Kunz and Long, 2006).

Deleted: .
Deleted:
Deleted:

6 Threshold-based approaches with active microwave data, as used in this study, identify the point of melt
7 onset based on the departure in σ^0 from values in dry-snow with various thresholds (Ashcraft and Long, 2000; Ashcraft
8 and Long, 2006; Trusel et al., 2012). The approach used here derives melt occurrence from a threshold-based method
9 (ft3), which identifies melt when backscatter falls 3 dB below the preceding winter mean (Steiner and Tedesco, 2014;
10 Ashcraft and Long, 2006). This method, along with a wavelet approach have been evaluated over the AP with AWS
11 data at 5 locations: melt was assumed to occur at the AWS location, when 2m air temperature exceeded 0°C for more
12 than 6 hours (Steiner and Tedesco, 2014).

Deleted: s estimating melt occurrence from
Deleted: AWS as

13 In addition to the binary detection of melt, several methods have been proposed which relate seasonally-
14 integrated backscatter reduction to measures for melt intensity (Wismann, 2000; Smith, 2003; Trusel et al., 2013). As
15 these methods provide seasonally-cummulative values, we do not employ them in this study, although we do examine
16 raw backscatter values as a proxy for melt flux.

17 2.2.2 Passive Microwave Data

18 We complement the assessment of MAR with estimates of melt extent and duration obtained from passive microwave
19 observations which have been used in the past to assess melt occurrence in Antarctica and Greenland using brightness
20 temperature at 19.35 GHz with a horizontal polarization (Tedesco, 2007). One of the major disadvantages of passive
21 microwave is the relatively coarse horizontal spatial resolution (25 km) with respect to the fine-scale topography
22 characterizing the AP. However, the historical record for passive microwave data extends as far back as 1972.
23 Threshold-based methods for melt detection from passive microwave data range from a combination of multiple
24 frequencies and polarizations (Abdalati and Steffen, 1995) to using a single frequency, single polarization (e.g., Mote
25 et al. 1993, Tedesco 2009), as is used in this study. Three algorithms are used here which are described in detail in
26 (Tedesco, 2009). These include the 240-algorithm where the threshold was determined as the value above which an
27 increase in liquid water content above 1% no longer produces an increase in T_b , based on output of an electromagnetic
28 model. The original threshold of 245K was found to be insufficiently sensitive and reduced to 240K for this study
29 (Tedesco, 2007) (M. Tedesco, personal communication). The second algorithm uses the winter mean threshold-based
30 method ALA:

Deleted: from
Deleted:

$$31 T_c = T_{winter} * \alpha + T_{wet_{snow}} * (1 - \alpha)$$

(2)

Deleted: .
Deleted: 1

32 where snowmelt is assumed to occur when the brightness temperature (T_b) exceeds a threshold brightness temperature
33 (T_c) based on the mean winter (JJA) T_b , the wet snow T_b ($T_{wet_{snow}}$, equal to 273K) and a mixing coefficient (α , equal
34 to 0.47). For the ALA algorithm, Ashcraft and Long (2006) presume a wet layer of 4.7 cm and a Liquid Water Content
35 of 1%. Finally, the third algorithm (zwa), determines melt occurrence when T_b exceeds a threshold value T_c which is

1 based on the on the winter mean threshold (T_{winter}) and a threshold value (ΔT), in this case 30K (Zwally and Fiegles,
2 1994).

$$3 T_c = T_{winter} + \Delta T$$

4 2.3 AWS measurements

5 We evaluate the MAR simulation of the near-surface atmosphere using pressure, temperature and wind speed data
6 collected by three automatic weather stations (AWS) on the AP (Fig 1). The comparison between MAR outputs and
7 AWS data for surface pressure are provided in supplementary data. Data from the Larsen Ice Shelf AWS is obtained
8 from the University of Wisconsin Madison (AMRC, SSEC, UW-Madison) at a 3-hourly temporal resolution. AWS
9 data from two additional sites on the Larsen Ice Shelf (AWS14 and AWS15) are obtained from the Institute for Marine
10 and Atmospheric Research at Utrecht University (IMAU) at an hourly resolution (Kuipers Munneke et al., 2012). We
11 note that the Larsen Ice Shelf AWS (-67.00°S, -61.60°W) and AWS14 (-67.00°S, -61.5°W) fall within the same MAR
12 grid cell.

13 AWS values are temporally averaged to obtain mean daily values for the comparison with MAR outputs.
14 Metrics are computed for December-January-February (DJF, summer). We did not compute a seasonal average when
15 more than 5 consecutive days of data were missing. The five-day period was chosen as an upper limit for the length
16 of a synoptic event, corresponding spatially to approximately 145 MAR grid cells (or half the model domain) of
17 continuous flow in a single direction for an average windspeed of 3.4 m/s, which is the expected value (i.e. the
18 predicted mean based on the Weibull distribution), for Larsen Ice Shelf AWS in DJF from 1999-2014 (Fig. 7c). Near-
19 surface (2m) air temperature values are corrected for a difference between AWS station elevation and the elevation
20 averaged by the corresponding MAR gridcell by calculating the elevation gradient from surrounding MAR gridcells
21 and interpolating the final value for the AWS location's recorded elevation using the Bedmap2 DEM (Fretwell et al.,
22 2013). Differences in elevation values between MAR at 10km resolution and those recorded at AWS stations were as
23 large as 23 m. Maximum daily 2m air temperature (MaxT2m) is calculated as well because this measure may help
24 capture sporadic melt events. MaxT2m values are extracted from available 3-hourly values and are used only when
25 no more than one 3-hour measurement is missing during the day. Pressure values from AWS stations are also observed
26 at approximately 2m above the surface, and compared to MAR values at the first atmospheric layer in MAR. Because
27 the height of this layer is generally between 2 and 3 m above the surface, this is treated as an acceptable proxy for 2m
28 pressure values. Pressure values from MAR are corrected for elevation using the hypsometric equation (Wallace and
29 Hobbs, 1977).

30 2.4 Statistical Methods

31 To evaluate and quantify the differences between MAR outputs and AWS data for temperature and wind speed we
32 use a mean bias. Additional statistical measures shown in supplemental data include the coefficient of determination
33 (R^2), root mean squared error (RMSE) and mean error (ME) (Wilks, 1995). We assess the extent to which each station
34 is representative of larger scale climate variability by constructing correlation (R^2) maps between MAR values co-

Deleted: where T_{winter} is mean winter (JJA) brightness temperature (T_b), $T_{wet, snow}$ is wet snow brightness temperature (equal to 273K) and α is the mixing coefficient (equal to 0.47). Ashcraft and Long (2006) here presume a wet layer of 4.7 cm and a Liquid Water Content of 1%. Finally, the third algorithm (zwa) is based on the winter mean threshold.

Deleted: .

Deleted: 2

Deleted: where ΔT is a threshold value, in this case 30K (Zwally and Fiegles, 1994).

Deleted: assess

Deleted: station

Deleted: . These also include values for the surface energy budget

Deleted: S

Deleted: station

Deleted: the

Deleted: station

Deleted: are co-located to

Deleted: the

Deleted: i.e. the expected value

Deleted: S

Deleted: station

Deleted: 5

Deleted: b

Deleted: the

Deleted: better

Deleted: indicate

Deleted: than values averaged to the daily scale

Deleted: temperatures

Deleted: estimated

Deleted: a

Deleted: .

Deleted: agreement

Deleted: used

Deleted: (

Deleted: Also included in supplemental data, w

1 located with AWS stations vs all other gridpoints in the full MAR domain (Fig. S7). We ignore all R^2 statistics where
2 the p-value exceeds 0.05.
3 To capture wind speed frequency distributions, we fit available data for each season for MAR (for the full
4 2000-2009 period), AWS (when AWS data are available) and MAR-R (MAR values collected only when AWS data
5 is available) with a Weibull distribution (Wilks, 1995). The shape (β) parameter roughly captures the degree of skew,
6 with higher values being closer to a normal distribution. The scale (λ) parameter approximates the peak frequency
7 (we note that this is not equivalent to the arithmetic mean). We report expected values (i.e. first moment or mean) for
8 each windspeed distribution using the best Weibull fit.

9 3. Results: Melt Occurrence and Meltwater Production

10 In this section, we show results concerning total meltwater production in the AP and compare melt occurrence
11 estimated by MAR with estimates from three passive microwave algorithms as well as QuikSCAT ft3. The relative
12 sensitivity of each melt occurrence criteria, as well as their associated temperature biases, are first compared at the
13 location of the Larsen Ice Shelf AWS. We then identify spatial biases for melt occurrence at the domain scale, finding
14 substantial differences in the center of the Larsen C Ice Shelf as well as to the north and west of the NE basin, a region
15 which includes the former Larsen A and B ice shelves as well as the northernmost portions of the Larsen C ice shelf
16 (Section 3.2). These differences could result from either weaknesses in the MAR representation of wind dynamics
17 (discussed in Section 4) or from limitations of the satellite sensor or algorithm. Finally, we compare the climatology
18 and inter-annual variability of melt extent (calculated by multiple algorithms) over the CL and NL region (Section
19 3.3).

20 3.1 Meltwater production over the AP

21 We show MAR meltwater production over the 1999-2009 period (Fig. 2). The total annual meltwater production
22 estimated by MAR shows substantial inter-annual variation with the NE basin accounting for the highest meltwater
23 production, closely followed by the SW basin (in green). The NE basin is divided into three regions: the NL and CL
24 masks (discussed in Section 3.2) and the remainder of the basin. We note that the SW basin does not covary with the
25 NE basin and the subregions of the NE basin do not consistently covary with one another. The meltwater production
26 shown here does not account for refreezing and we note that the effects of refrozen melt on the snowpack will vary
27 regionally depending on local properties. The NL region dominates meltwater production in the NE basin in most
28 years except for 1999-2000, 2002-2003 and 2003-2004. The 2001-2002 melt season shows the second lowest overall
29 melt production during the study period (only the preceding year is lower). Declining aggregate meltwater production
30 across the AP does not necessarily correspond to declining meltwater production in the most vulnerable regions of the
31 northeastern AP (including the Larsen C Ice Shelf). Because melt in the NL region is particularly sensitive to föhn-
32 induced melt, we note that changes in circulation patterns may affect the northwest regions differently than the
33 southern regions. The strong relationship between wind direction and temperature bias points to the need for isolating

Deleted: .

Deleted: (indicating the probability that the underlying R value would exceed the result reported)

Deleted: is

Deleted: n even

Deleted: over the Antarctic Peninsula.

Deleted: first

Deleted: (the "CL" region, where PMW melt occurrence is highest) as well as to the north and west of the NE basin, a region which includes the former Larsens A and B ice shelves as well as the northernmost portions of the Larsen C ice shelf (the "NL" region, where MAR and QuikSCAT ft3 melt occurrence is highest)

Deleted: t

Deleted: 1

Deleted: .

Deleted: Additionally

Deleted: 2

Formatted: Heading 2

1 dominant inter-annual patterns of melt in the Northern Larsen C Ice Shelf and associating them with large-scale
2 atmospheric drivers.

3 A comparison between mean annual meltwater production from 2000-2009 calculated using RACMO2.3p2
4 (5.5 km) vs MAR (10km) is shown in Fig. 3. MAR shows higher meltwater production overall (Fig. 3b vs 3a), with a
5 difference of over 150 mm w.e. on the Larsen C ice shelf north of 67°S latitude. Over the NE basin, MAR meltwater
6 shows enhanced meltwater production near the AP mountains, including towards the southern edges, and declines
7 eastward and southward. By comparison, meltwater production from RACMO2.3p2 melt declines southward, but no
8 similar west-to-east gradient is apparent. Although inter-annual standard deviations over the northern Larsen C ice
9 shelf are generally above 100 mm w.e. in both models, there are major differences in other regions, with MAR
10 meltwater production exceeding RACMO2.3p2 values by 30 mm w.e. on the southern Larsen C ice shelf as well as
11 the George VI ice shelf (Fig. 3d vs 3e). Van Wessem et al. (2015a) suggest that even at 5.5 km resolution, the
12 underestimation of the height and slope of the orographic barrier may result in an underestimation of föhn winds as
13 well as precipitation in RACMO2.3p2. We note that in addition to the difference in horizontal model resolution,
14 RACMO2.3p2 contains 40 atmospheric layers while MAR implements 23 layers. While the differences in total
15 meltwater production from RACMO2.3p2 and MAR could be a product of dissimilar physics, the potential effect of
16 model resolution on meltwater production in MAR is specifically discussed in Section 5. While melt occurrence and
17 meltwater production are not related in any linear fashion, we note that the spatial pattern produced by MAR, i.e. the
18 eastward gradient from the edge of the AP, is also shown in observed melt occurrence estimates, most notably from
19 the PMW zwa and QS algorithms (Fig. 5f,g), as discussed in greater detail in the next section.

20 **3.2. Melt occurrence over the AP**

21 Fig. 4 shows melt occurrence (in days) at the Larsen Ice Shelf AWS location (shown in Fig. 1) as estimated from the
22 satellite-based algorithms QuikSCAT ft3 (Section 2.2.1), three passive microwave algorithms (Section 2.2.2),
23 temperature-based criteria from the AWS station ($\text{MaxT2m} > 0^\circ\text{C}$ and $\text{AvgT2m} > 0^\circ\text{C}$), and the $MF_{0.4}$ metric derived
24 from MAR (Section 2.1). At this location, we find that QuikSCAT ft3 and PMW ZWA show the greatest sensitivity
25 to melt occurrence. Of the AWS-based metrics, M ($\text{MaxT2m} > 0^\circ\text{C}$) shows a sensitivity to melt occurrence comparable
26 to PMW ALA while the T metric ($\text{AvgT2m} > 0^\circ\text{C}$) compares poorly to satellite-based measures (Fig. 4a). We find
27 that at colder temperatures (when $\text{MaxT2m} < 0^\circ\text{C}$), AvgT2m values reported by MAR are substantially higher than
28 those reported by the AWS when only MAR reports melt (Fig. 4b). However, at higher temperatures (where MaxT2m
29 $\geq 0^\circ\text{C}$), the AWS reports higher MaxT2m temperatures than MAR and biases are even stronger when only
30 observation-based metrics report melt (Fig. 4e). We note that the Larsen Ice Shelf AWS is located on the eastern edge
31 of the Larsen C ice shelf and the major discrepancies in melt occurrence at this location will be explored further in
32 Section 4, where we further expand the analysis of melt occurrence and temperature biases to include wind direction
33 biases as well.

34 In Fig. 5, we show melt occurrence over the full domain derived from satellite sources, both metrics derived
35 from MAR (Section 2.1) as well as the $MF_{0.4}$ criteria applied to RACMO2.3p2. QuikSCAT ft3 generally estimates
36 higher average yearly melt occurrence than either of the MAR melt metrics over the full domain. In the NE basin, the

Formatted: Indent: First line: 0.5"

Deleted: values

Deleted: 4

Deleted: e,f

Deleted: 1

Formatted: Font color: Text 1

Deleted: estimates

Formatted: Font color: Text 1

Formatted: Font color: Text 1

Deleted: Fig. 2 shows average annual melt occurrence (in days) over the model domain, estimated from the satellite-based algorithms QuikSCAT ft3 (Sect. 2.2.1) and three passive microwave algorithms (Sect. 2.2.2) as well as two metrics for melt derived from MAR outputs (Sect. 2.1). Because the MAR $MF_{0.4}$ melt metric shows more sensitivity to melt occurrence than the $LWC_{0.4}$ metric, it is used for comparison to QuikSCAT ft3 and PMW zwa (the most sensitive satellite-based algorithms). We use the term "PMWAll" to define the condition when all PMW algorithms report melt occurrence. Our primary focus is on the NE basin in the AP (shown in Fig. 1) .

1 difference is on the order of 25 more days than the MAR $MF_{0.4}$ melt metric (Fig. 5g). Differences between QuikSCAT
 2 ft3 and $MF_{0.4}$ also show a strong latitudinal dependence in the NE basin, shifting from near agreement in the northern
 3 regions of the Larsen C Ice Shelf to QuikSCAT ft3 reporting over 500% of the melt days reported by MAR towards
 4 the southern edge. Melt onset is on the order of 22 days earlier in QuikSCAT ft3 than in $MF_{0.4}$ in the NE basin, except
 5 at the northern edge of the Larsen C ice shelf, where $MF_{0.4}$ reports average yearly melt onset as much as 25 days
 6 earlier than QuikSCAT ft3 (Fig. S3). A comparison between the two MAR melt metrics shows that $MF_{0.4}$ reports as
 7 much as 40 more days of melt than $LWC_{0.4}$ at the northern tip of the Larsen C Ice Shelf (Fig 5b vs Fig 5a). The portion
 8 of the Larsen C ice shelf which experiences an average of 25 days of melt or more extends as far south as 80.0°S on
 9 the eastern side of the Larsen C ice shelf according to the $MF_{0.4}$ metric but extends only to 70.5°S according to $LWC_{0.4}$.
 10 Towards the very south of the Larsen C Ice Shelf, the two MAR metrics show similar values, although $LWC_{0.4}$ reports
 11 melt onset as late as early January (Fig. S3a) while $MF_{0.4}$ reports melt onset in December (Fig S3b). The formulation
 12 for the $MF_{0.4}$ metric, which considers melt at any time of the day for the full depth of the snowpack, suggests that the
 13 early season melt observed only by $MF_{0.4}$ is either sporadic (i.e. can refreeze) and/or percolates below 1m in the
 14 snowpack in the south of the Larsen C Ice Shelf, i.e. below the depth range at which $LWC_{0.4}$ is calculated. Whereas
 15 QuikSCAT ft3 and MAR melt metrics report maximum melt occurrence in the north and west of the Larsen C Ice
 16 Shelf ($MF_{0.4}$ reporting > 60 days, Fig. 5b), PMW algorithms report maximum melt occurrence in the center-east of
 17 the Larsen C Ice Shelf, specifically 43 days (240, Fig. 5c), 57 days (ALA, Fig. 5d) and 69 days (ZWA, Fig. 5e).
 18 RACMO2.3p2 reports substantially higher melt occurrence than MAR at the center of the Larsen C ice shelf as well
 19 as a comparatively limited west to east gradient. Because overall average annual meltwater production in MAR was
 20 shown to be substantially higher, with a stronger west-to-east gradient away from the AP (Fig. 3), we conclude that
 21 in comparison to RACMO2.3p2, MAR produces melt less frequently, but with greater intensity.

22 In summary, a comparison between observed and modeled data sources show two distinct spatial patterns for
 23 maximum melt occurrence. QuikSCAT ft3 as well as both MAR melt metrics show the highest range of melt days in
 24 the northern and western edges of the Larsen C Ice Shelf (including both high and low elevation regions) while PMW
 25 algorithms show the highest number of melt days in the center of the Larsen C Ice Shelf, where elevations are lower
 26 and topography is less complex. We hypothesize that the major difference in spatial patterns between algorithms/melt
 27 metrics is related to the different resolutions of the data sources (~2,225 km for QuikSCAT, 10km for MAR and
 28 25km for PMW), such that QuikSCAT is better able to resolve melt where topography is complex, such as near the
 29 spine of the AP. Secondly, the differences are a product of the depths presumed for the calculation of meltwater
 30 content. This is true for both the MAR metrics and for the three PMW algorithms; the “ALA” algorithm, for example,
 31 presumes a 4.7cm depth and a 1% liquid water content. (see Section 2). To confirm this, we find the maximum depth
 32 to which meltwater percolates (according to MAR) associated with the number of days when melt occurs (according
 33 to PMW algorithms). Histograms for total PMW melt days in Fig. S4 show three peaks (two major inflection points)
 34 for each algorithm which are used to create three classes for meltwater occurrence (“low”, “medium” and “high”). For
 35 these classes, the maximum depth to which meltwater percolates (in MAR) is shown in Fig. S6 and the associated
 36 elevation and MAR meltwater production is shown in Table S1.

Deleted:

Deleted: 2f

Deleted:

Deleted: Supplemental

Deleted: 2

Deleted: 2

Deleted: 2

Deleted: 0

Deleted: Supplemental

Deleted: 2

Deleted: Supplemental

Deleted: 2

Deleted: (considering

Deleted:)

Deleted: , even immediately

Deleted: 2

Deleted: 2

Deleted: zwa

Deleted: 2

Formatted: Font color: Text 1

Deleted: However, we note that

Formatted: Font color: Text 1

Deleted: suggesting

Deleted: that while

Formatted: Font color: Text 1

Deleted: it is generally in greater quantities.

Formatted: Font color: Text 1

Deleted: are primarily

Deleted:

Deleted: ad s

Deleted: to

Deleted: .

Deleted: Supplemental

Deleted: 3

Deleted:

Deleted:

Deleted: Supplemental

Deleted: 5

Deleted: Supplemental

1 Spatial regions defined as having “low” melt occurrence are highly heterogeneous with regard to elevation,
 2 meltwater percolation and the relative sensitivity of PMW algorithms. Low melt occurrence regions largely include
 3 the spine of the AP and regions just east of it. Bedmap2 (Fretwell et al., 2013) reports a large range of elevations while
 4 MAR reports low coincident meltwater production and a relatively shallow meltwater depth. Both the ALA and ZWA
 5 algorithms report melt at higher elevations (above approximately 1300m and 1900m, respectively) than the 240
 6 algorithm, which neither reports any melt occurrence above 1100m in the NE basin nor at lower elevations to the north
 7 and south. (Table S1, rows 1,4,7 and Fig. S6). Where melt occurrence is low, the 240 and ALA algorithms generally
 8 detect melt only where MAR reports a maximum meltwater percolation depth below 0.4 m, (Fig. S6a,b), whereas the
 9 ZWA algorithm can detect melt at a substantially shallower depth of 0.1 m (Fig. S6c). Although generally meltwater
 10 in MAR rarely percolates below 3m, in low melt-occurrence regions, modeled meltwater occasionally percolates
 11 below 10m in the beginning of the melt season (Fig. S6 a,b,c, column “N”, indicating November). We remind the
 12 reader that melt occurrence within the firm layer (as calculated by MAR $MF_{0.4}$) will capture melt that can refreeze
 13 immediately, so this does not necessarily correspond to melt which is retained in the snowpack. Rather, the snowpack
 14 layer depth represents the deepest layer which is affected by the melt process according to MAR.

15 By contrast, where PMW reports high melt occurrence in the NE basin, MAR consistently reports high
 16 coincident meltwater production, low elevations and the deepest average meltwater percolation in the region. In the
 17 month of January, we find that where PMW algorithms report melt, coincident MAR meltwater percolates to 2 m into
 18 the snowpack for 35-47% of the total day-pixels in the NE basin which report any melt, and as deep as 3 meters for
 19 more than 30% of total day-pixels (Table S1, 240-H, ALA-H, ZWA-H, Fig. S6 g,h,i).

20 To quantify the two major spatial trends for maximum melt occurrence, i.e. (1) PMW in the center-east of
 21 the Larsen C ice shelf and (2) QuikSCAT ft3 and MAR in the northwest of the NE basin, we (a) explicitly calculate
 22 concurrent melt occurrence in all PMW algorithms (PMWAll) for the first region and (b) define the latter
 23 geographically in order to include most of the NE basin, but deliberately exclude center-east of the Larsen C ice shelf
 24 region where PMW melt is highest. The first region “CL” (Center Larsen, as the entire region is restricted to the Larsen
 25 C ice shelf), where all PMW algorithms agree on high melt occurrence, is defined where PMWAll reports average
 26 yearly total melt days exceeding one standard deviation from the mean for the NE basin. Mean elevation for the CL
 27 region is $42.70 \pm 17.70\sigma$ m (where σ is one standard deviation). PMWAll reports a mean annual 36 days of melt
 28 occurrence (vs 21 days derived from $MF_{0.4}$) and the mean annual MAR meltwater production calculated only where
 29 PMWAll reports melt occurrence is 96 mm w.e./100km² (vs 143 mm w.e./100km² when $MF_{0.4}$ reports melt)(Table
 30 S1, row 11,12).

31 The “NL” (Northern Larsen) mask is defined by finding the mean latitude of the CL region and including all
 32 portions of the NE basin above this latitude, but excluding the CL region (Fig. 2, inset). In the NL region, elevation is
 33 highly-variable, with a mean value ~600m and MAR and QS detect melt both earlier and more often than for PMW
 34 algorithms. The NL region includes the eastern spine of the AP and most inlets (including Cabinet Inlet and SCAR
 35 Inlet), a small portion of the northern Larsen C ice shelf and all regions surrounding the former Larsen A and Larsen
 36 B ice shelves.

Deleted:

Deleted: zwa

Deleted: Supplemental Material

Deleted: 5

Deleted: Supplemental

Deleted: 5

Deleted: zwa

Deleted: Supplemental

Deleted: 5

Deleted: Supplemental

Deleted: 5

Deleted: N

Formatted: Indent: First line: 0.5"

Deleted: in high

Deleted: regions

Deleted: meters

Deleted: Supplemental

Deleted: zwa

Deleted: 5

Deleted: a

Deleted: b

Deleted: Northern

Deleted:

Deleted: a

Deleted: PMWAll-coincident

Deleted: of

Deleted: Supplemental

Deleted: 4c

Deleted:

Deleted: Both masks are shown in the inset in Fig. 3a and Fig. 4c and are used for subsequent analysis of inter-annual meltwater production in MAR.

1 **3.3 Climatology and inter-annual trends for melt extent at the sub-basin scale**

2 We compare the seasonal cycle and interannual variability of melt as modeled by MAR vs observations for both the
3 CL and NL regions by computing regional melt extent over the 2000-2009 period (total melt extent area for each day
4 in NDJF), for each year as well as the climatological average. The PMWAll algorithm is typically treated as the most
5 restrictive condition while the PMW zwa and QuikSCAT ft3 are the most sensitive. Melt extent is defined as the total
6 area reporting melt daily between Nov 1st and February 28th (austral summer, including November to show early
7 melt)(Fig. 6).

8 The melt extent climatology for PMWAll in the CL region shows the initial increase in sustained melt
9 occurring around December 15th with melt extent peaking in January, followed by a series of increasingly smaller melt
10 pulses ending with refreezing at the end of February. While MAR shows peak melt extent at the same point in the
11 season, the progression from melt onset is more gradual, average peak melt extent is generally smaller and interannual
12 variability (indicated by the grey envelope) during peak melt extent is larger (Fig. 6c vs Fig. 6a). In the CL region, the
13 PMWAll metric is generally restricted by the low sensitivity of the 240 algorithm. Interannual variability for melt
14 extent is substantial, with PMWAll reporting a larger melt extent than MAR towards the middle of the melt season in
15 most years (Fig. 6b,d), but not necessarily during melt onset or its ending. In the CL region, PMWAll reports a larger
16 melt extent throughout the melt season during 2000-2001 and 2001-2002 (Fig. 6d). During three periods, MAR reports
17 a larger melt extent than PMWAll, including 1999-2000, the latter half of the 2002-2003 season and the 2003-2004
18 season. While the highly-sensitive PMW ZWA algorithm (Fig. 6e,f) reports sporadic periods where MAR melt extent
19 is larger (during the 1999-2000 and 2003-2004 melt seasons, for example), ZWA generally reports either a larger melt
20 extent or general agreement with MAR. Similarly, melt extent derived from the QuikSCAT ft3 algorithm consistently
21 shows a larger melt extent than MAR, except for a few short periods towards the end of the season in 1999-2000 and
22 2003-2004 (Fig. 6g,h). We note that for several years, both QuikSCAT ft3 and PMW ZWA report substantial melt
23 occurrence early in the season (~Nov 15th) and that the QuikSCAT ft3 climatology frequently reports melt occurrence
24 in the CL region well after February (Fig. 6g).

25 The NL region includes areas which reported low melt occurrence in all PMW algorithms, variable meltwater
26 percolation depth in MAR was variable, and a large range of elevations was observed (Section 3.2), implying that the
27 mask defined by the combined PMWAll algorithm is less clearly linked to consistent modeled physical properties in
28 this region. Here, the MAR melt extent climatology (Fig. 7a,b) is consistently larger than PMWAll throughout the
29 season (Fig. 7c,d). In comparison to the ZWA (Fig. 6c) and QuikSCAT ft3 (Fig. 7g) algorithms, MAR reports less
30 melt extent in the middle of the season (with peak melt extent in January), but larger melt extent at the beginning and
31 end of the melt season. As compared with the CL region, the MAR climatological melt extent shows less inter-annual
32 variability (grey envelope, Fig. 7a). During the 2000-2001 and 2001-2002 melt seasons, MAR shows a larger melt
33 extent than PMWAll (Fig. 7d), but less than the PMW ZWA (Fig. 7f) or QuikSCAT ft3 (Fig. 7h) algorithms. We find
34 that during the 2005-2006 season, MAR shows greater melt extent than PMWAll, consistently less than QuikSCAT
35 ft3, but reports a greater melt extent than ZWA only towards the end of the season. We consider the condition where
36 only QuikSCAT ft3 or PMW ZWA show a greater melt extent than MAR to be potentially indicative of sporadic
37 surface melt.

- Deleted: 2
- Deleted: both yearly
- Deleted: and
- Deleted: as a
- Deleted: 3
- Deleted: an early pulse of
- Deleted: e
- Deleted:
- Deleted: 3
- Deleted: 3
- Deleted: 3
- Deleted: 3
- Deleted: zwa
- Deleted: 3
- Deleted: zwa
- Deleted: 3
- Deleted: zwa
- Deleted: 3
- Deleted: Note that the
- Deleted: Sect
- Deleted: 1
- Deleted: specific
- Deleted: 4
- Deleted: 4
- Deleted: zwa
- Deleted: 4
- Deleted: 4
- Deleted:
- Deleted: 4
- Deleted: 4
- Deleted: zwa
- Deleted: 4
- Deleted: 4
- Deleted: 4
- Deleted: zwa
- Deleted: zwa
- Deleted: likely

1 In summary, we conclude that in the CL region, MAR reports a larger melt extent, ~~from 2009-2009~~ than
2 PMWAll (which is highly-restrictive), but a smaller melt extent than either the PMW ~~ZWA~~ or QuikSCAT ft3
3 algorithms, which are more sensitive. Notably, MAR melt occurrence is comparatively low during the peak melt
4 period. By contrast, in the NL region, MAR reports greater melt occurrence than the most restrictive measure
5 (PMWAll) during peak melt, but far less than the highly-sensitive QuikSCAT ft3 algorithm. The interannual
6 comparison suggests that MAR shows substantially less melt occurrence than observations during the 2000-2001 and
7 2001-2002 seasons in the CL region, but not the NL region.

Deleted:
Deleted: during that period
Deleted: zwa

8 4. Results: Wind and Temperature Biases at the Larsen Ice Shelf station

9 The ~~eastern~~ AP is ~~generally~~ substantially colder than the ~~western~~ AP, and temperature-driven melt primarily results
10 from either ~~large-scale advection~~ from lower latitudes or from westerly föhn flow over the spine of the AP (~~Marshall~~
11 ~~et al., 2006~~). Here, we assess the bias in temperature and melt occurrence associated with wind direction at three AWS
12 ~~locations~~ on the Larsen C Ice Shelf (shown in Fig. 1). We first discuss wind direction and wind speed biases during
13 the summer season at all three locations (without regard to melt occurrence) (Section 4.1). ~~For prominent wind~~
14 ~~direction biases, we quantify the associated temperature and melt occurrence biases in order to capture atmospheric~~
15 ~~conditions where MAR reports less melt occurrence than observations (Section 4.2)~~. All MAR and satellite data used
16 are co-located to the grid cell associated with the AWS (Fig. 1), and we remind the reader that all three stations, at the
17 eastern edge of the CL region (Fig. 2 inset), are located where MAR reported substantially less melt occurrence than
18 PMW algorithms, ~~QuikSCAT ft3 or AWS temperature-based criteria~~.

Deleted: East
Deleted: West
Deleted: warm northerly flow

Deleted: stations located

Deleted: .

Deleted: between MAR and AWS data concurrent with melt occurrence biases between MAR and satellite sources

Deleted: We then find temperature/wind direction biases specifically associated with melt occurrence in MAR, PMWAll and QuikSCAT ft3, in order to capture which wind direction/temperature biases lead to a disproportionate amount of observed melt which is not captured by MAR (Sect. 4.2).

Deleted: station

Deleted: or

Deleted: .

19 4.1 Aggregate wind direction biases

20 Fig. 8 shows wind frequency distributions during the summer season, color-coded for wind direction as represented
21 by the pie graph at the right. We note that AWS data are 3-hourly averages and ERA-Interim are 6-hourly averages
22 for wind speed and direction, while MAR produces daily-averaged outputs. For this reason, a direct comparison
23 between Weibull parameters derived from MAR vs AWS data is not fully justified. The Larsen Ice Shelf AWS has
24 full temporal coverage during the QuikSCAT period while AWS14 and AWS15 were installed after termination of
25 the QuikSCAT mission. These last two stations are used in this study to demonstrate that (a) similar wind biases
26 persisted after the QuikSCAT period at multiple locations, as AWS 14 the Larsen Ice Shelf AWSs are co-located to
27 the same MAR grid cell and that (b) wind biases vary slightly by latitude, AWS15 being located slightly to the south.

Formatted: Font color: Text 1

28 Both MAR and AWSs at all stations show a larger proportion of northerly winds at lower windspeeds (Fig. 8, in
29 yellow and blue), although AWSs report a greater frequency of southwesterly and northwesterly flow (Table 2 col.
30 4,5 rows 4-9). At the Larsen Ice Shelf AWS location, both AWS and MAR report dominant northeasterly flow (Table
31 2, rows 4,8, col2). However, the Larsen Ice Shelf AWS reports slightly more flow which is either southwesterly
32 (28.9% for AWS vs. 23.2% in MAR) or northwesterly (19.3% for AWS vs. 14.1% in MAR) while MAR reports more
33 southeasterly flow overall (23.5% in MAR vs. 17.4% in AWS). These biases are more pronounced at the southern
34 AWS15, where modelled temperature correlates with a larger portion of the southern Larsen C Ice Shelf than for
35 AWS14 (Fig. S7, Fig. 8i,j). ERA-Interim reports substantially more northwesterly flow than either AWS or MAR and

Formatted: Font color: Text 1

Deleted: data at all stations show

Formatted: Font color: Text 1

Deleted: winds as well as more

Formatted: Font color: Text 1

Deleted: Specifically, at

Formatted: Font color: Text 1

Formatted: Font color: Text 1

1 a smaller proportion of southwesterly flow in the 180°- 225° range (especially at the southernmost AWS15 location),
2 although easterly flow is equivalent to AWS-reported estimates. We note that although ERA-Interim has been shown
3 to reproduce the basic structure of föhn flow (Grosvenor et al., 2014), the horizontal spatial resolution may be too
4 coarse to adequately capture southwesterly gap flow here. As discussed further in Section 5, westerly flow towards
5 the stations used in this study may be strongly affected by the fine-scale representation of topography (which is coarse
6 in ERA-Interim) and the lowered orographic barrier due to the smoothing of topography in the northwest in ERA-
7 Interim may contribute to the enhanced northwesterly flow reported by ERA-Interim.

8 4.2 Wind and temperature biases concurrent with observed melt occurrence

9 When daily-averaged temperature (AvgT2m) values are high, it is more likely that melt is sustained, while high
10 maximum daily temperatures (MaxT2m) can also occur during sporadic melt. Melt occurrence is strongly influenced
11 by the temperature of the snow column as well as at the surface; internal melting can occur even when the surface is
12 frozen due to net outgoing longwave radiation (Holmgren, 1971; Hock, 2005). It is therefore possible for melt to occur
13 despite a cold bias. In general, we find a small, but consistent warm MAR bias for AvgT2m, and a consistent cold
14 MaxT2m bias (Table 2, rows 12,13). However, when we restrict the dataset to days when AWS-recorded temperatures
15 exceed 0°C, a condition where melt is most likely, MAR indicates a cold bias for AvgT2m and an enhanced cold bias
16 for MaxT2m (Table 2, rows 15,16). This implies that MAR is colder than observations at the temperature ranges
17 where melt is likely, although melt is still possible due to other components of the energy balance.

18 The cold MaxT2m temperature bias is strongest during northerly flow in general (Table 2, row 13,16, col 2,5),
19 but strongest during easterly flow on the days when MAR reports melt (Table 2, row 23,26, col 2,3). Satellite-based
20 melt is detected primarily when AWS-recorded flow is northeasterly (0°-90°) or southwesterly (180°-270°), with
21 PMW(QS) reporting 42%(36%) northeasterly flow and 29%(26%) southwesterly flow. On days when MAR reports
22 melt (Table 2, rows 19,20), southeasterly flow in MAR is more prominent (while AWS values decline) while the
23 proportion of northwesterly flow declines (but increases at the AWS). We find that the major flow biases account for
24 a relatively small proportion of melt which is captured by observations but not by MAR. The easterly flow bias
25 accounts for 8%(9%) of days where PMWAll(QS) melt occurrence is not also captured by MAR (Table S9) while the
26 southerly flow bias accounts for 6%(6%) of days when PMW(QS) melt occurrence is not also reported by MAR (Table
27 S8). For these wind direction biases, Fig. 9 presents temperature values when observed sources, either PMW All or
28 QuikSCAT ft3, report melt, but MAR does not. We refer to the condition where PMWAll reports melt (but MAR does
29 not) as “PMWex” (i.e. PMW exclusive-or), with the equivalent condition for QuikSCAT ft3 called “QSEx”. We limit
30 the melt days shown in each figure panel to a specific wind bias, thus showing how the wind bias directly influences
31 temperature-driven melt in both satellite-based observations as well as MAR. Tables S8-S12 contain relative
32 proportions of each case (flow bias) divided for each restriction (i.e. MAR, QSEx or PMWEx), as well as the timeseries
33 mean and biases for AvgT2m, AvgT2m>0°C (excluding days when AvgT2m values from AWS are below 0°C),
34 MaxT2m and MaxT2m >0°C.

35 For the main biases, i.e. when MAR either reports northerly winds as southerly (Fig. 9a,b) or westerly winds
36 as easterly (Fig. 9 c,d), modelled temperature values are clustered around 0°C, whereas AWS-observed temperatures,

Formatted: Font color: Text 1

Formatted: Font color: Text 1

Deleted: Fig. 8 shows wind frequency distributions during the summer season, color-coded for wind direction as represented by the pie graph at the right. We note that AWS data are 3-hourly averages and ERA-Interim are 6-hourly averages for wind speed and direction, while MAR produced daily-averaged outputs. For this reason, a direct comparison between Weibull parameters derived from MAR vs AWS data is not fully justified. The Larsen Ice Shelf AWS has full temporal coverage during the QuikSCAT period while AWS14 and AWS15 were installed after termination of the QuikSCAT mission. These last two stations are used in this study to demonstrate that (a) similar wind biases persisted after the QuikSCAT period at multiple locations, as AWS 14 the Larsen Ice Shelf AWSs are co-located to the same MAR grid cell and that (b) wind biases vary slightly by latitude, AWS15 being located slightly to the south. (... [4])

Deleted: Fig. 5 shows wind frequency distributions during the summer season (AWS, MAR-R, MAR from left to right columns, Larsen IS station, AWS 14 and AWS 15 from top to bottom), color-coded for wind direction as represented by the pie graph at the top. We note that AWS data uses 3-hourly data for wind speed and direction without daily-averaging, while MAR produced daily-averaged outputs. For this reason, a direct comparison between Weibull parameters derived from MAR vs AWS data is not meaningful, although we show comparisons between different stations (for the same data source). The Larsen IS station has full temporal coverage during the QuikSCAT period while AWS14 and AWS15 were installed after termination of the QuikSCAT mission. These last two stations are used in this study to demonstrate the consistency of wind biases at multiple locations, as well as how wind biases vary by latitude (AWS15 being located slightly to the south). Whereas MAR is dominated northerly winds at it's lower range of windspeeds (in yellow and blue), AWS data shows a greater frequency of southwesterly winds at the higher range of windspeeds (> 8 m/s). In general, even at lower wind speeds (2-5 m/s), AWS data shows more southwesterly winds than either MAR-R or MAR. This is especially relevant at the southern AWS15 station, where modeled temperature correlates with a larger region of the Larsen IS than temperatures modeled by MAR for the AWS14 station (Supplemental Fig. 6). Observed wind direction (without consideration for wind speed) at AWS15 shows more southwesterly flow (Fig. 5g) than either MAR-R or MAR (Fig. 5 h,i), which show a substantially higher percentage of southeasterly and northerly flow instead. (... [5])

Deleted: AWS T2m

Deleted: estimates

Formatted: Font color: Text 1

Formatted: Font color: Text 1

Deleted: Together, these findings suggest that the bias towards easterly in MAR, as compared to AWS estimates, may account for reduced melt at the Larsen Ice Shelf AWS location.

Formatted: Font color: Text 1

Deleted: Tables S2-S7 include R², RMSE and mean bias values for both surface pressure and daily AvgT2m at all three stations.

Formatted: Font color: Text 1

Formatted: Font color: Text 1

Formatted: Font color: Text 1

1 especially when only satellite-observed melt occurs, are higher. When MAR reports melt, MAR AvgT2m values
2 cluster near 0°C, with a small overall warm bias (Tables S8,S9, row 4, col 8). Under omission conditions (PMWEx
3 and QSEx), AvgT2m values are lower, and the MAR bias is slightly negative, although the standard deviation is high
4 (Tables S8, S9, row 5,6, col 7). With all flow cases, only QuikSCAT fit3 shows melt at very low observed AvgT2m
5 values. By contrast, AWS MaxT2m values are substantially higher than MAR values (the latter clustering around 0°C)
6 (Fig. 9b,d). Temperature biases associated with southwesterly flow are similar to those shown by the overall bias
7 towards easterly flow in MAR, and are shown in Table S10,S11.

- Deleted: (
- Deleted:)
- Formatted: Font color: Text 1
- Formatted: Font color: Text 1
- Formatted: Font color: Text 1

8 Northwestery winds are most likely to produce föhn-induced melt and we find that on days when MAR
9 reports melt, only 13.2% of winds are northwesterly while AWS reports 25.2% of flow as northwesterly (Table 2,
10 rows 9,10, col 5). Northwestery winds show the highest expected windspeeds as well as the highest standard deviation
11 for both MAR and AWS (Table 2, rows 19,20, col 5). While the temperature bias when wind directions are in
12 agreement is relatively minimal, the temperature bias when northwesterly winds are misrepresented is substantial.
13 When MAR reports melt but misrepresents northwesterly winds (this condition accounts for 3% of all MAR melt
14 days), the cool bias for MaxT2m > 0°C is above 4°C (Table S12, row 4, col 10). For the PMWEx condition (when
15 PMW reports melt but MAR does not), AWS MaxT2m values exceed MAR values by more than 5°C (Table S12, row
16 5, col 10). Despite the strength of the temperature bias, this wind direction bias accounts for only 3% of melt in MAR
17 and only 3%(4%) of melt occurrence reported by PMWEx(QSEx). By contrast, when westerly flow is modelled
18 accurately, MAR captures higher AvgT2m values, which frequently exceed 0°C, with a slight cool MAR bias when
19 AvgT2m > 0°C (Fig. 9e). The PMWEx and QSEx conditions still report melt at lower temperature values, and the
20 MAR bias remains positive. Although a cold MAR bias persists, MaxT2m values are generally in better agreement at
21 the Larsen IS AWS location during this condition (Fig 9f, Table S12).

- Formatted: Font color: Text 1

22 5. Discussion and Conclusions

- Deleted: ... [6]

23 We conclude that MAR captures melt which occurs just east of the AP (which is normally the product of westerly
24 föhn flow) with acceptable accuracy according to satellite estimates, but that that melt is underestimated with respect
25 to both AWS and satellite estimates in the eastern part of the Larsen C Ice Shelf. This is partially the result of limited
26 westerly flow in MAR towards the eastern part of the Larsen C ice shelf, as compared to AWS estimates. Specifically,
27 MAR shows lower melt occurrence than satellite estimates in the center and east of the Larsen C Ice Shelf (i.e. the
28 CL region, where eastward flow is likely limited in MAR), while in the north and west of the NE basin (i.e. the NL
29 region which is most immediately affected by westerly flow), MAR reports melt occurrence largely concurrent with
30 satellite estimates. The NL region fits a spatial pattern of föhn-induced melt just lee of the AP and extending eastward
31 from inlets which has been shown in previous studies (Grosvenor et al., 2014) and particularly in the northernmost
32 portion of the NE basin surrounding the Larsen B ice shelf, where the correlation between föhn winds and satellite-
33 based melt occurrence has been shown to be as high as 0.5 between 1999-2002 (Cape et al., 2015, Fig. 12). For
34 example, within the CL region, there are periods during the 2001-2002 season when MAR reports no meltwater
35 production, but raw QuikSCAT backscatter values report periods where over 300 km² of surface area show backscatter
36 values dipping below -15 dB (Fig. S9e).

- Deleted: on
- Deleted: in comparison
- Deleted: values, which may follow from the limited eastward propagation of föhn flow in MAR
- Deleted: föhn
- Deleted: föhn
- Formatted: Font color: Text 1

1 MAR reports warmer temperature compared to AWS observations recorded on the east of the Larsen C ice shelf
2 at temperatures below 0°C, when melt is less likely to occur, but which may still impact the refreezing process.
3 However, when maximum daily temperatures (MaxT2m) and average daily temperatures (AvgT2m) exceed 0°C,
4 MAR shows a substantial cold bias. This is particularly evident when MAR misrepresents westerly winds or northerly
5 winds, and the temperature bias is most extreme when northwesterly flow is misrepresented, i.e. the condition when
6 the most intense föhn flow would be likely. However, this represents only a small proportion of the melt occurrence
7 bias, i.e. melt occurrence reported by satellite estimates, but not by MAR.

8 We demonstrate the impact of westerly winds on melt during a single season, specifically during both mid-
9 December and the beginning of January of the 2001-2002 season. During both of these periods, satellite-based melt
10 extent in the CL region increases substantially, while MAR melt extent declines after an initial pulse (Fig. S9a). In
11 December, MAR shows an increase in northwesterly flow, both at the station and throughout the region while AWS
12 reports northwesterly winds at slightly higher speeds. Beginning approximately on January 1st, the NL region reports
13 substantial northwesterly flow, followed by southwesterly flow, although neither is reported at the Larsen Ice Shelf
14 AWS station east of the NL region. Over January, while both AWS and MAR report northeasterly flow, the AWS
15 station also reports substantial high-speed southwesterly flow not captured by MAR. After this period (beginning on
16 approximately Jan. 1st), AWS AvgT2m temperatures consistently exceed MAR AvgT2m values until the end of the
17 season (Fig. S11), suggesting that because MAR did not accurately model the initial intrusion of westerly winds,
18 subsequent temperature-induced melt was limited over the eastern Larsen C ice shelf, where this AWS is located.
19 Presuming that the flow characteristics are largely similar in this relatively flat region, we conclude that the
20 underestimation of melt in the CL region is partially due to the absence of westerly flow, but that this flow is adequately
21 captured directly east of the AP (comprising the NL region).

22 Previous work has suggested that southwesterly föhn winds can result from gap flow (Elvidge et al. 2015),
23 although we note that the southwesterly jets studied in this single campaign were typically cooler and moister than
24 surrounding air, i.e. föhn flow produced from isentropic drawdown. While a version with a higher spatial resolution
25 may potentially resolve topography sufficiently to include the initial intrusion of southwesterly gap flow, as well as
26 northwesterly föhn flow, it may also further inhibit subsequent eastward flow when the hydrostatic assumption is
27 retained. While a higher resolution of MAR v3.5.2 (used throughout this study) was not run due to computational
28 constraints, the enhanced computational efficiency of a newer version of the MAR model (MAR v3.9, Section 2.1)
29 could enable higher resolution runs over extended periods in the future.

30 To assess both the potential future application of MAR v3.9 over the AP as well as the effects of both vertical
31 and horizontal resolution on modelled melt estimates, we compare melt occurrence and flow characteristics from Nov
32 1, 2004 to March 31, 2005 between multiple versions of the MAR model. This included three versions of v3.9 (Section
33 2.1), with two 5km and 10km resolution versions run with 24 vertical layers as well as an additional 10km resolution
34 version with 32 vertical layers (10km V). The effect of the enhanced horizontal resolution on topography is substantial;
35 the maximum height of the AP in the 5km version of the model is 2567m, but only 2340m in the 10km version. We
36 find that the effect of increasing horizontal resolution to 5km is to limit the consistent strong melt production just
37 leeward of the AP and that an increase in either horizontal resolution or vertical discretization limits eastward flow

1 (Fig. S12). As compared to AWS data at the Larsen IS AWS, all MAR configurations largely replicated the dominant
2 southwesterly and northeasterly flow, although we found an enhanced bias for southeasterly flow with the enhanced-
3 resolution versions of the model (Fig. S13). The effects of local topography on wind speed should be relatively limited
4 as the region surrounding the Larsen ice shelf AWS station is relatively flat. Bedmap2 (Fretwell et al., 2013) reports
5 mean (standard deviation) elevation values of 37.38m (0.53m) in the 5km surrounding the station and 37.37m (0.78m)
6 in the 10km surrounding the station. The mean (standard deviation) values for slope are 0.015°(0.018°) at both
7 resolutions. We conclude that a further increase in vertical discretization or horizontal resolution may potentially
8 reduce flow towards the eastern edge of the Larsen C ice shelf, although the effect of better-resolved topography may
9 allow more westerly flow in MAR to cross the AP.

Deleted: We also note that slightly more southeasterly flow was estimated in the newer version of the model with the same horizontal resolution as v3.5.2.

10 As has been suggested by previous studies (Van Wessem et al., 2015a), the implementation of a non-hydrostatic
11 model may improve the representation of westerly föhn flow over the eastern Larsen Ice Shelf (Hubert Gallée, personal
12 communication). We note that previous work has suggested that a 5km non-hydrostatic model was still unable to
13 capture föhn flow on the eastern portion of the Larsen C ice shelf (according to the AWS records), partially due to the
14 inability to simulate southwesterly föhn jets, and that resolutions as high as 1.5km are required to simulate föhn flow
15 accurately (Turton et al., 2017). However, recent work found that spatial resolutions as high as 2km in the non-
16 hydrostatic WRF model were still unable to fully-resolve the steep surface temperature increases associated with the
17 beginning of föhn flow (Bozkurt et al., 2018), suggesting that neither increased spatial resolution nor a non-hydrostatic
18 model may be sufficient to fully capture the effects of föhn flow. We conclude from the main analysis that reduced
19 eastward propagation of westerly winds may contribute to a lack of MAR melt in the CL region as compared to
20 satellite estimates but that melt just east of the AP (the NL) region is represented with relative accuracy. This is further
21 confirmed by the similarity between the spatial trends for melt occurrence as compared to QuikSCAT estimates. We
22 remind the reader that previous work has suggested that föhn flow occurred only 20% of the time during a single melt
23 season, and that substantial melt occurred in conditions where föhn winds are not present (King et al., 2017),
24 suggesting that other factors contributing to surface melt energy may be equally, if not more, important for developing
25 accurate melt estimates in RCMs. Because the current class of RCMs which employ the hydrostatic assumption, such
26 as MAR, can be run for relatively long periods and contain relatively realistic representations of the snowpack, they
27 can provide additional insights into the cumulative effects of surface melt over multiple seasons, with the
28 understanding that the surface melt produced by föhn flow will likely be under-represented in the eastern regions of
29 the Larsen C ice shelf.

Deleted: MAR to more accurately capture melt just east of the AP

Formatted: Font color: Text 1

30 Previous literature has pointed to several limitations in the remote sensing data sources used here which are either
31 intrinsic to the satellite data itself or a product of the algorithm selected for melt detection (Ashcraft and Long, 2006).
32 Products derived from QuikSCAT are limited in temporal resolution because the satellite passes daily, and may
33 therefore ignore sporadic melt occurring at other times of the day. However, previous studies have compared total
34 melt days from the QuikSCAT ft3 algorithm with a measure derived from surface temperature at seven automatic
35 weather stations and shown a positive QuikSCAT ft3 bias compared to AWS (Steiner and Tedesco, 2014). Similarly,
36 all PMW algorithms are limited by a relatively low resolution (25km) and twice-daily passes. Periods of melt
37 occurrence have also been shown to be sensitive to the choice of algorithm (Tedesco 2009).

Formatted: Font color: Text 1

Deleted: Because of the high topographic variability of the NL region (especially near the spine of the AP), it is possible that PMW algorithms are under-reporting melt occurrence due to low horizontal spatial resolution. A higher-resolution passive microwave product may partly resolve this issue.

1 In future work, we will extend this model run to the 1982-2017 period as well as explore a higher-resolution run
2 of a newer version of MAR, producing hourly outputs for the near-surface atmosphere. These runs will allow us to
3 examine the frequency of föhn winds, the concurrent meltwater production and the effects of föhn-induced melt on
4 the snowpack. We will use this multi-decadal record to examine interannual trends of föhn winds in all seasons as
5 well as the cumulative effect of a changing regional climate on the snowpack of the NE basin.

Deleted: In the aggregate, we conclude that MAR shows lower melt occurrence than satellite estimates in the center and east of the Larsen C ice shelf (i.e. the CL region, where eastward föhn flow is likely limited in MAR), while in the north and west of the NE basin (i.e. the NL region which is most immediately affected by föhn flow), MAR reports melt occurrence largely concurrent with satellite estimates. For example, within the CL region, there are periods during the 2001-2002 season when MAR reports no meltwater production, but raw QuikSCAT backscatter values report periods where over 300 km² of surface area show backscatter values dipping below -15 dB (Supplemental Fig. 8e). We remind the reader that raw backscatter values from QuikSCAT have previously been used to estimate melt flux over the AP (Trusel et al., 2013; Trusel et al., 2012).

Page Break

... [7]

1 **References**

2 [Abdalati, W., and Steffen K.: Passive Microwave-Derived Snow Melt Regions on the Greenland Ice Sheet,](#)
3 [Geophysical Research Letters., 22 \(7\), 787–790, doi:10.1029/95GL00433, 1995.](#)
4
5 [Agosta, C., Amory, C., Kittel, C., Orsi, A., Favier, V., Gallée, H., van den Broeke, M. R., Lenaerts, J. T. M., van](#)
6 [Wessem, J. M., and Fettweis, X.: Estimation of the Antarctic surface mass balance using MAR \(1979–2015\) and](#)
7 [identification of dominant processes, The Cryosphere Discuss., https://doi.org/10.5194/tc-2018-76, in review, 2018.](#)
8
9 [Ahrens, C. Donald.: Meteorology Today : An Introduction to Weather, Climate, and the Environment. Eighth](#)
10 [edition. Thomson/Brooks/Cole, Belmont, CA, 2007.](#)
11
12 [Amory, C., Trouvilliez, A., Gallée, H., Favier, V., Naaim-Bouvet, F., Genthon, C., Agosta, C., Piard, L., and Bellot,](#)
13 [H.: Comparison between Observed and Simulated Aeolian Snow Mass Fluxes in Adélie Land, East Antarctica., The](#)
14 [Cryosphere 9 \(4\), 1373–83, doi:10.5194/tc-9-1373-2015, 2015.](#)
15
16 [Ashcraft, I. S., and Long, D.G.: SeaWinds Views Greenland: In Geoscience and Remote Sensing Symposium, 2000.](#)
17 [Proceedings. IGARSS 2000. IEEE 2000 International, 3,1131–1133, 2000.](#)
18
19 [Ashcraft, I. S., and Long, D.G.: Comparison of Methods for Melt Detection over Greenland Using Active and](#)
20 [Passive Microwave Measurements, International Journal of Remote Sensing, 27 \(12\), 2469–88,](#)
21 [doi:10.1080/01431160500534465, 2006.](#)
22
23 [Barrand, N. E., Vaughan, D. G., Steiner, N., Tedesco, M., Kuipers-Munneke, P. , Van den Broeke, M. R., and](#)
24 [Hosking, J. S.: Trends in Antarctic Peninsula Surface Melting Conditions from Observations and Regional](#)
25 [Climate Modeling, Journal of Geophysical Research: Earth Surface, 118 \(1\), 315–330,](#)
26 [doi:10.1029/2012JF002559, 2013.](#)
27
28 [Bell, R. E., Chu, W. Kingslake, J., Das, I., Tedesco, M., Tinto, K.J., Zappa, C.J., Frezzotti, M., Boghosian, A., and](#)
29 [Lee, W.S.: Antarctic Ice Shelf Potentially Stabilized by Export of Meltwater in Surface River, Nature, 544 \(7650\),](#)
30 [344–348. doi:10.1038/nature22048, 2017.](#)
31
32 [Beran, D.W.: Large Amplitude Lee Waves and Chinook Winds, Journal of Applied Meteorology, 6 \(5\),865–877.](#)
33 [doi:10.1175/1520-0450\(1967\)006<0865:LALWAC>2.0.CO;2., 1967.](#)
34
35 [Bozkurt, D., Rondanelli, R., Marin, J.C. and Garreaud, R.: Foehn Event Triggered by an Atmospheric River Underlies](#)
36 [Record-Setting Temperature Along Continental Antarctica, Journal of Geophysical Research: Atmospheres, 123\(8\),](#)
37 [3871-92, http://doi.org/10.1002/2017JD027796, 2018.](#)

Deleted: [8]

Formatted: Normal

Formatted: Normal

1 [Braithwaite, R. J.: On Glacier Energy Balance, Ablation, and Air Temperature, *Journal of Glaciology*, 27, 381–91,](#)
2 [1981](#)
3
4 [Brandt, R. E., and Warren, S.G.: Solar-Heating Rates and Temperature Profiles in Antarctic Snow and Ice, *Journal*](#)
5 [of Glaciology](#), 39, 99–110. doi:10.1017/S0022143000015756, 1993.
6
7 [Brun, E, David, P., Sudul, M. and G Brunot, G.: A Numerical Model to Simulate Snow-Cover Stratigraphy for](#)
8 [Operational Avalanche Forecasting, *Journal of Glaciology*, 38,13–22, 1992.](#)
9
10 [Cape, M. R., Vernet, M., Skvarca, P., Marinsek, S., Scambos, T. and Domack, E.: Foehn Winds Link Climate-](#)
11 [Driven Warming to Ice Shelf Evolution in Antarctica. *Journal of Geophysical Research: Atmospheres*, 120 \(21\) 11,](#)
12 [37-11, doi:10.1002/2015JD023465, 2015.](#)
13
14 [De Ridder, K., and Gallée, H.: Land Surface-Induced Regional Climate Change in Southern Israel, *Journal of*](#)
15 [Applied Meteorology](#), 37 (11), 1470–1485, 1998.
16
17 [Dee, D. P., Uppala, S. M., Simmons, A. J., Berrisford, P., Poli, P., Kobayashi, S., Andrae, U. et al., The ERA-](#)
18 [Interim Reanalysis: Configuration and Performance of the Data Assimilation System, *Quarterly Journal of*](#)
19 [the Royal Meteorological Society](#), 137 (656), 553–597, doi:10.1002/qj.828, 2011.
20
21 [Drinkwater, M.R., and Liu, X.: Seasonal to Interannual Variability in Antarctic Sea-Ice Surface Melt, *IEEE*](#)
22 [Transactions on Geoscience and Remote Sensing](#), 38(4), 1827–1842, doi:10.1109/36.851767, 2000.
23
24 [Dutra, E., Sandu, I., Balsamo, G., Beljaars, A., Freville, H., Vignon, E., and Brun. E.: Understanding the ECMWF](#)
25 [Winter Surface Temperature Biases over Antarctica, *Technical Memorandum*, 762, 2015.](#)
26
27 [Elvidge, A. D., Renfrew, I.A., King, J.C., Orr, A., Lachlan-Cope, T.A., Weeks, M. and Gray, S.L.: Foehn Jets over](#)
28 [the Larsen C Ice Shelf, Antarctica, *Quarterly Journal of the Royal Meteorological Society*, 141\(688\), 698–](#)
29 [713. doi:10.1002/qj.2382., 2015.](#)
30
31 [Fettweis, X., Box, Jason E., Agosta, C., Amory, C., Kittel, C. and Gallée, H.: Reconstructions of the 1900-2015](#)
32 [Greenland Ice Sheet Surface Mass Balance Using the Regional Climate MAR Model, *The Cryosphere Discussions*,](#)
33 [November, 1–32. https://doi.org/10.5194/tc-2016-268., 2016](#)
34
35 [Fettweis, X., Franco, B., Tedesco, M., van Angelen, J.H., Lenaerts, J. T. M., Van den Broeke, M. R. and Gallée, H.:](#)
36 [Estimating the Greenland Ice Sheet Surface Mass Balance Contribution to Future Sea Level Rise Using the](#)
37 [Regional Atmospheric Climate Model MAR, *The Cryosphere* 7 \(2\), 469–489, doi:10.5194/tc-7-469-2013,](#)

1 [2013.](#)

2

3 [Fettweis, X, Gallée, H., Lefebvre, F., and Van Ypersele, J., Greenland Surface Mass Balance Simulated by a](#)

4 [Regional Climate Model and Comparison with Satellite-Derived Data in 1990–1991, Climate Dynamics](#)

5 [24 \(6\), 623–640, 2005.](#)

6

7 [Franco, B., Fettweis, X., Lang, C., and Ericum, M.: Impact of Spatial Resolution on the Modelling of the](#)

8 [Greenland Ice Sheet Surface Mass Balance between 1990–2010, Using the Regional Climate Model MAR,](#)

9 [The Cryosphere 6 \(3\), 695–711. doi:10.5194/tc-6-695-2012, 2012.](#)

10

11 [Fretwell, P., Pritchard, H. D., Vaughan, D. G., Bamber, J. L., Barrand, N. E., Bell, R., Bianchi, C. et al.: Bedmap2:](#)

12 [Improved Ice Bed, Surface and Thickness Datasets for Antarctica, The Cryosphere, 7 \(1\), 375–393,](#)

13 [doi:10.5194/tc-7-375-2013, 2013.](#)

14

15 [Gallée, H., and Schayes, G.: Development of a Three-Dimensional Meso-Gamma Primitive Equation Model:](#)

16 [Katabatic Winds Simulation in the Area of Terra Nova Bay, Antarctica, Belgian Science Policy Office, 1994.](#)

17

18 [Gallée, H., Trouvilliez, A., Agosta, C., Genthon, C., Favier, V., and Naaim-Bouvet, F.: Transport of Snow by the](#)

19 [Wind: A Comparison Between Observations in Adélie Land, Antarctica, and Simulations Made with the Regional](#)

20 [Climate Model MAR, Boundary-Layer Meteor., 146 \(1\), 133–47, doi:10.1007/s10546-012-9764-z, 2013.](#)

21

22 [Gilbert, R. O.: Statistical Methods for Environmental Pollution Monitoring, Van Nostrand Reinhold Co., New York,](#)

23 [NY, 1987.](#)

24

25 [Glasser, N. F., and Ted A. Scambos.: A Structural Glaciological Analysis of the 2002 Larsen B Ice-Shelf Collapse.,](#)

26 [J. of Glaciology 54 \(184\):3–16, 2008](#)

27

28 [Greene, C. A., Gwyther, D. E., & Blankenship, D. D.: Antarctic Mapping Tools for Matlab. Computers &](#)

29 [Geosciences. <http://dx.doi.org/10.1016/j.cageo.2016.08.003>, 2016.](#)

30

31 [Grosvenor, D. P., King, J.C., Choularton, T. W., and Lachlan-Cope, T.: Downslope Föhn Winds over the Antarctic](#)

32 [Peninsula and Their Effect on the Larsen Ice Shelves. Atmos. Chem. and Phys., 14 \(18\), 9481–9509.,](#)

33 <https://doi.org/10.5194/acp-14-9481-2014>, 2014.

34

35 [Hock, R.: Glacier Melt: A Review of Processes and Their Modelling, Progress in Phys .Geog., 29 \(3\), 362–91,](#)

36 [doi:10.1191/0309133305pp453ra., 2005.](#)

37

- 1 [Hogg, A.E. and Gudmundsson, G.H.: Impacts of the Larsen-C Ice Shelf Calving Event., Nature Climage Change 7, August, 540, 2017.](#)
- 2
- 3
- 4 [Holland, P.R., Hugh F. J. Corr, H. D. Pritchard, Vaughan, D.G., Arthern, R.J., Jenkins, A., and Tedesco, M.: The Air Content of Larsen Ice Shelf, Geoph. Res. Let., 38 \(10\), doi:10.1029/2011GL047245, 2011.](#)
- 5
- 6
- 7 [Holmgren, B.: Climate and Energy Exchange on a Sub-Polar Ice Cap in Summer: Arctic Institute of North America Devon Island Expedition 1961-1963. Acta Univ. Upsal. Abstracts of Uppsala Diss. from the Faculty of Science, pt. 3. Meteorologiska Institutionen Uppsala Universitet., 1971.](#)
- 8
- 9
- 10
- 11 [Holton, J.: The General Circulation, in: An Introduction to Dynamic Meteorology, 4th ed., Elsevier Inc., 329–337, 2004.](#)
- 12
- 13
- 14 [Hubbard, B., Luckman, A., Ashmore, D.W., Bevan, S., Kulessa, B., Kuipers-Munneke, P., Philippe, M. et al.: Massive Subsurface Ice Formed by Refreezing of Ice-Shelf Melt Ponds, Nat. Comm., 7 \(June\), 11897., doi:10.1038/ncomms11897, 2016.](#)
- 15
- 16
- 17
- 18 [Jansen, D., Kulessa, B., Sammonds, P. R., Luckman, A., King, E. C. and Glasser, N.F.: Present Stability of the Larsen C Ice Shelf, Antarctic Peninsula, J. of Glac., 56 \(198\), 593–600, 2010.](#)
- 19
- 20
- 21 [Kingslake, J., Ely, J.C., Das, I., and Bell, R.E.: Widespread Movement of Meltwater onto and across Antarctic Ice Shelves, Nature, 544 \(7650\), 349–352, doi:10.1038/nature22049, 2017.](#)
- 22
- 23
- 24 [Koh, G., and Jordan, R.: Sub-Surface Melting in a Seasonal Snow Cover. J. of Glaciology, 41 \(139\): 474–482. doi:10.3189/S002214300003481X, 1995.](#)
- 25
- 26
- 27 [Kuipers-Munneke, P., van den Broeke, M. R., King, J. C., Gray, T., and Reijmer, C. H.: Near-Surface Climate and Surface Energy Budget of Larsen C Ice Shelf, Antarctic Peninsula, The Cryosphere, 6 \(2\), 353–363, doi:10.5194/tc-6-353-2012, 2012.](#)
- 28
- 29
- 30
- 31 [Kuipers Munneke, P., Picard, G., van den Broeke, M. R., Lenaerts, J. T. M., and van Meijgaard, E.: Insignificant Change in Antarctic Snowmelt Volume since 1979: Antarctic Snowmelt Volume, Geoph. Res. Lett., 39\(1\), doi:10.1029/2011GL050207, 2012](#)
- 32
- 33
- 34
- 35 [Kuipers-Munneke, P., Ligtenberg, S.R.M., Van Den Broeke, M.R., and Vaughan, D.G.: Firn Air Depletion as a Precursor of Antarctic Ice-Shelf Collapse, J. of Glaciology 60 \(220\), 205–14, doi:10.3189/2014JoG13J183, 2014.](#)
- 36
- 37

1 [Kunz, L.B., and Long, D.G.: Melt Detection in Antarctic Ice Shelves Using Scatterometers and Microwave](#)
2 [Radiometers. IEEE Transactions on Geoscience and Remote Sensing, 44 \(9\), 2461–](#)
3 [69. https://doi.org/10.1109/TGRS.2006.874138.2006.](#)

4

5 [Lenaerts, J. T. M., Lhermitte, S., Drews, R., Ligtenberg, S. R. M., Berger, S., Helm, V., Smeets, C. J. P. P. et al.:](#)
6 [Meltwater Produced by Wind–albedo Interaction Stored in an East Antarctic Ice Shelf, Nat. Clim. Change, 7 \(1\), 58–](#)
7 [62, doi:10.1038/nclimate3180, 2016.](#)

8

9 [Liston, G.E., Bruland, O., Winther, J., Elvehøy, H. and Sand, K.: Meltwater Production in Antarctic Blue-Ice Areas:](#)
10 [Sensitivity to Changes in Atmospheric Forcing, Polar Research, 18 \(2\), 283–290, doi:10.3402/polar.v18i2.6586,](#)
11 [1999a.](#)

12

13 [Liston, G. E., Winther, J., Bruland, O., Elvehøy, H. and Sand, K.: Below-Surface Ice Melt on the Coastal Antarctic](#)
14 [Ice Sheet, J. of Glaciology 45 \(150\): 273–85. doi:10.3189/S002214300001775, 1999b.](#)

15

16 [Liu, H., Wang, L., and Jezek, K.C.: Spatiotemporal Variations of Snowmelt in Antarctica Derived from Satellite](#)
17 [ScanningMultichannel Microwave Radiometer and Special Sensor Microwave Imager Data \(1978–2004\), J. of](#)
18 [Geoph. Res.: Earth Surface, 111 \(F1\), doi:10.1029/2005JF000318, 2006.](#)

19

20 [Long, D.G., and Hicks, B.R.: Standard BYU QuikSCAT/SeaWinds Land/Ice Image Products, QuikScat Image](#)
21 [Product Documentation, Brigham Young Univ., Provo, UT, 2000.](#)

22

23 [Luckman, A., Elvidge, A., Jansen, D., Kulesa, B., Kuipers-Munneke, P., King, J., and Barrand, N.E., Surface Melt](#)
24 [and Ponding on Larsen C Ice Shelf and the Impact of Föhn Winds, Antarctic Science, 26 \(6\), 625–635,](#)
25 [doi:10.1017/S0954102014000339, 2014.](#)

26

27 [MacAyeal, D.R., and Sergienko O.V.: The Flexural Dynamics of Melting Ice Shelves, Annals of Glaciology, 54 \(63\),](#)
28 [1–10, doi:doi:10.3189/2013AoG63A256, 2013.](#)

29

30 [Mann, H. B.: Nonparametric Tests Against Trend, Econometrica, 13 \(3\), 245–259, doi:10.2307/1907187, 1945.](#)

31 [Marshall, G. J.: Half-Century Seasonal Relationships between the Southern Annular Mode and Antarctic](#)
32 [Temperatures, Intl. Jour. of Clim., 27 \(3\), 373–83, doi:10.1002/joc.1407, 2007.](#)

33

34 [Marshall, G. J., Orr, A., Van Lipzig, N.P.M., and King, J.C.: The Impact of a Changing Southern Hemisphere Annular](#)
35 [Mode on Antarctic Peninsula Summer Temperatures, J. of Climate, 19 \(20\), 5388–5404, 2006.](#)

36

Formatted: Justified, Line spacing: 1.5 lines

Formatted: Font:(Default) +Theme Body (Times New Roman), 10 pt

Formatted: Font:(Default) +Theme Body (Times New Roman), 10 pt

Formatted: Font:(Default) +Theme Body (Times New Roman), 10 pt, Not Italic

Formatted: Font:(Default) +Theme Body (Times New Roman), 10 pt

Formatted: Font:(Default) +Theme Body (Times New Roman), 10 pt

Formatted: Font:(Default) +Theme Body (Times New Roman)

Formatted: Font:(Default) +Theme Body (Times New Roman)

Formatted: Normal

1 [Mercer, J. H.: West Antarctic Ice Sheet and CO₂ Greenhouse Effect: A Threat of Disaster, Nature ,271 \(January\),](#)
2 [321–325, doi:10.1038/271321a0, 1978.](#)
3
4 [Morris, E. M., and Vaughan, D.G.: Spatial and Temporal Variation of Surface Temperature on the Antarctic Peninsula](#)
5 [And The Limit of Viability of Ice Shelves, In: Antarctic Peninsula Climate Variability: Historical and](#)
6 [Paleoenvironmental Perspectives, American Geophysical Union, 61–68, doi:10.1029/AR079p0061, 2013.](#)
7
8 [Mote, T., Anderson, M.R. , Kuivinen, K.C., and Rowe, M.C.: Passive Microwave-Derived Spatial and Temporal](#)
9 [Variations of Summer Melt On the Greenland Ice Sheet, International Symposium On Remote Sensing of Snow and](#)
10 [Ice, 17: 233–38, 1993.](#)
11
12 [Ridley, J.: Surface Melting on Antarctic Peninsula Ice Shelves Detected by Passive Microwave Sensors, Geoph.](#)
13 [Res. Let., 20 \(23\), 2639–2642, doi:10.1029/93GL02611, 1993.](#)
14
15 [Rott, H., Rack, W., Nagler, T., and Skvarca, P.: Climatically Induced Retreat and Collapse of Northern Larsen Ice](#)
16 [Shelf, Antarctic Peninsula, Annals of Glaciology 27, 86–92, doi:10.1017/S0260305500017262, 1998.](#)
17
18 [Rott, H., Rack, W., Skvarca, P., and De Angelis, H.: Northern Larsen Ice Shelf, Antarctica: Further Retreat after](#)
19 [Collapse, Annals of Glaciology 34 \(1\), 277–82., doi: 10.3189/172756402781817716, 2002.](#)
20
21 [Scambos, T. A.: Glacier Acceleration and Thinning after Ice Shelf Collapse in the Larsen B Embayment, Antarctica,](#)
22 [Geoph. Res. Let., 31 \(18\), doi:10.1029/2004GL020670, 2004.](#)
23
24 [Scambos, T.A., Hulbe, C., Fahnestock, M., and Bohlander, J.: The Link between Climate Warming and Break-up of](#)
25 [Ice Shelves in the Antarctic Peninsula, J. Glaciology 46 \(154\), 516–530,doi:10.3189/172756500781833043, 2000.](#)
26
27 [Smith, L. C.: Melting of Small Arctic Ice Caps Observed from ERS Scatterometer Time Series, Geoph. Res.](#)
28 [Let., 30 \(20\), doi:10.1029/2003GL017641, 2003.](#)
29
30 [Steiner, N., and Tedesco, M.: A Wavelet Melt Detection Algorithm Applied to Enhanced-Resolution Scatterometer](#)
31 [Data over Antarctica \(2000–2009\),The Cryosphere, 8 \(1\), 25–40, doi:10.5194/tc-8-25-2014, 2014.](#)
32
33 [Tedesco, M.: Assessment and Development of Snowmelt Retrieval Algorithms over Antarctica from K-Band](#)
34 [Spaceborne Brightness Temperature \(1979–2008\), Rem. Sen.of Env. ,113 \(5\), 979–997,](#)
35 [doi:10.1016/j.rse.2009.01.009, 2009.](#)
36

Formatted: Normal

1 [Tedesco, M., and Monaghan, A.J.: An Updated Antarctic Melt Record through 2009 and Its Linkages to High-Latitude](#)
2 [and Tropical Climate Variability, *Geophysical Research Letters*, 36 \(18\), doi:10.1029/2009GL039186, 2009.](#)
3
4 [Tedesco, M., Abdalati, W., and Zwally, H. J.: Persistent Surface Snowmelt over Antarctica \(1987–2006\) from 19.35](#)
5 [GHz Brightness Temperatures, *Geoph. Res. Let.*, 34 \(18\), doi:10.1029/2007GL031199, 2007.](#)
6
7 [Tedesco, M.: Snowmelt Detection over the Greenland Ice Sheet from SSM/I Brightness Temperature Daily Variations,](#)
8 [Geoph. Res. Let., 34 \(2\), doi:10.1029/2006gl028466, 2007.](#)
9
10 [Torinesi, O., Fily, M., and Genthon, C.: Variability and Trends of the Summer Melt Period of Antarctic Ice Margins](#)
11 [since 1980 from Microwave Sensors, *J. of Climate*, 16 \(7\), 1047–1060, 2003.](#)
12
13 [Trusel, L. D., Frey, K. E., and Das, S. B.: Antarctic Surface Melting Dynamics: Enhanced Perspectives from Radar](#)
14 [Scatterometer Data, *J. of Geoph. Res.*, 117 \(F2\), doi:10.1029/2011JF002126, 2012.](#)
15
16 [Trusel, L.D., Frey, K.D., Das, S.B., Kuipers-Munneke, P., and Van den Broeke, M.R.: Satellite-Based Estimates of](#)
17 [Antarctic Surface Meltwater Fluxes, *Geoph. Res. Let.*, 40 \(23\): 6148–6153. doi:10.1002/2013GL058138, 2013.](#)
18
19 [Turner, J., Lu, H., White, I., King, J.C., Phillips, T., Hosking, J.S., Bracegirdle, T.J., Marshall, G.J., Mulvaney, R., and](#)
20 [Deb, P.: Absence of 21st Century Warming on Antarctic Peninsula Consistent with Natural Variability, *Nature*, 535](#)
21 [\(7612\), 411–415, doi:10.1038/nature18645, 2016.](#)
22
23 [Turner, J., Colwell, S.R., Marshall, G.J., Lachlan-Cope, T.A., Carleton, A.M., Jones, P.D., Lagun, V., Reid, P.A., and](#)
24 [Iagovkina, S.: Antarctic Climate Change during the Last 50 Years, *Int. Journ. of Clim.*, 25 \(3\), 279–294,](#)
25 [doi:10.1002/joc.1130, 2005.](#)
26
27 [Turton, J. V., Kirchaessner, A., Ross, A. N., and King, J. C.: Does High-Resolution Modelling Improve the Spatial](#)
28 [Analysis of Föhn Flow over the Larsen C Ice Shelf?, *Weather* 72 \(7\), 192–96. <https://doi.org/10.1002/wea.3028>, 2017.](#)
29
30 [Ulaby, F.T., and Stiles, W.H.: The Active and Passive Microwave Response to Snow Parameters: 2. Water Equivalent](#)
31 [of Dry Snow, *J. of Geoph. Res.: Oceans*, 85 \(C2\), 1045–1049, doi:10.1029/JC085iC02p01045, 1980.](#)
32
33 [Van Den Broeke, M. R., and Van Lipzig, N.P.M.: Response of Wintertime Antarctic Temperatures to the Antarctic](#)
34 [Oscillation: Results of a Regional Climate Model, in: *Antarctic Peninsula Climate Variability: Historical and*](#)
35 [Paleoenvironmental Perspectives, *American Geophysical Union*, 43–58, 2003.](#)
36
37 [Van Den Broeke, M. R.: Strong Surface Melting Preceded Collapse of Antarctic Peninsula Ice Shelf, *Geoph. Res.*](#)

1 [Let., 32 \(12\), doi:10.1029/2005GL023247, 2005.](#)

2

3 [van der Veen, C.J.: Fracture Mechanics Approach to Penetration of Surface Crevasses on Glaciers, Cold Regions](#)

4 [Science and Technology 27 \(1\): 31–47. doi:10.1016/S0165-232X\(97\)00022-0, 1998.](#)

5

6 [Van Lipzig, N. P. M.: Precipitation, Sublimation, and Snow Drift in the Antarctic Peninsula Region from a Regional](#)

7 [Atmospheric Model, J. of Geoph. Res., 109 \(D24\), doi:10.1029/2004JD004701, 2004.](#)

8

9 [Van Meijgaard, E., Van Ulf, L. H., Van de Berg, W. J., Bosveld, F. C., Van den Hurk, B., Lenderink, G., and](#)

10 [Siebesma, A.P.: The KNMI Regional Atmospheric Climate Model RACMO Version 2.1., Koninklijk Nederlands](#)

11 [Meteorologisch Instituut., <http://a.knmi2.nl/knmi-library/knmipubTR/TR302.pdf>, 2008.](#)

12

13 [Van Wessem, J. M., Ligtenberg, S. R. M., Reijmer, C. H., van de Berg, W. J., van den Broeke, M. R., Barrand, N.](#)

14 [E., Thomas, E. R.: The Modelled Surface Mass Balance of the Antarctic Peninsula at 5.5 Km Horizontal](#)

15 [Resolution, The Cryosphere Discussions, 9 \(5\), 5097–5136, doi:10.5194/tcd-9-5097-2015, 2015a.](#)

16

17 [Van Wessem, J.M., Reijmer, C.H., van de Berg, W.J., van den Broeke, M.R., Cook, A.J., van Ulf, L.H., and van](#)

18 [Meijgaard, E.: Temperature and Wind Climate of the Antarctic Peninsula as Simulated by a High-Resolution Regional](#)

19 [Atmospheric Climate Model, Journal of Climate 28 \(18\), 7306–26. <https://doi.org/10.1175/JCLI-D-15-0060.1>, 2015b.](#)

20

21 [Van Wessem, J.M., van de Berg, W.J., Noël, B. P. Y., van Meijgaard, E., Amory, C., Birnbaum, G., Jakobs, C.L.:](#)

22 [Modelling the Climate and Surface Mass Balance of Polar Ice Sheets Using RACMO2 – Part 2: Antarctica \(1979–](#)

23 [2016\).” The Cryosphere 12 \(4\), 1479–98, <https://doi.org/10.5194/tc-12-1479-2018>, 2018.](#)

24

25 [Vaughan, D. G., and Doake, C. S. M.: Recent Atmospheric Warming and Retreat of Ice Shelves on the Antarctic](#)

26 [Peninsula, Nature, 379 \(6563\), 328–31, doi:10.1038/379328a0, 1996.](#)

27

28 [Vaughan, D. G.: Recent Trends in Melting Conditions on the Antarctic Peninsula and Their Implications for Ice-Sheet](#)

29 [Mass Balance and Sea Level, Arctic, Antarctic, and Alpine Research, 38 \(1\), 147–152, 2006.](#)

30

31 [Vaughan, D. G.: West Antarctic Ice Sheet Collapse—the Fall and Rise of a Paradigm, Climatic Change, 91 \(1–2\), 65–](#)

32 [79, 2008.](#)

33

34 [Wallace, J. M., and Hobbs, P.V.: Hypsometric Equation, in: Atmospheric Science: An Introductory Survey,](#)

35 [Academic Press, Cambridge, MA, 55–57, 1977.](#)

36

37 [Weertman, J.: Can a Water-Filled Crevasse Reach the Bottom Surface of a Glacier., IASH Publ 95, 139–145., 1973](#)

38

Formatted: Font:(Default) +Theme Body (Times New Roman), 10 pt

Formatted: Line spacing: 1.5 lines

Formatted: Font:(Default) +Theme Body (Times New Roman), 10 pt

Formatted: Font:(Default) +Theme Body (Times New Roman), 10 pt

Formatted: Font:(Default) +Theme Body (Times New Roman)

Formatted: Normal

1 [Wiesenekker, J., Kuipers Munneke, P., van den Broeke, M., and Smeets, C.: A Multidecadal Analysis of Föhn](#)
2 [Winds over Larsen C Ice Shelf from a Combination of Observations and Modeling: Atmosphere 9 \(5\): 172.](#)
3 <https://doi.org/10.3390/atmos9050172>, 2018.

4 ▲

5 [Wilks, D.S.: Statistical Methods in the Atmospheric Sciences: An Introduction. International Geophysics. Elsevier](#)
6 [Science, Amsterdam, Netherlands,1995.](#)

7

8 [Wismann, V.: Monitoring of Seasonal Snowmelt on Greenland with ERS Scatterometer Data, IEEE Transactions on](#)
9 [Geoscience and Remote Sensing, 38 \(4\), 1821–1826, doi:10.1109/36.851766, 2000.](#)

10

11 [Zwally, H. J., Giovinetto, M. B., Beckley, M. A., and Saba, J. L.: Antarctic and Greenland Drainage Systems, GSFC](#)
12 [Cryospheric Sciences Laboratory, 2012.](#)

13

14 [Zwally, H. Jay, Abdalati, W., Herring T., Larson, K., Saba, J., and Steffen, K.: Surface Melt-Induced Acceleration of](#)
15 [Greenland Ice-Sheet Flow, Science ,297 \(5579\), 218–222., 2002.](#)

16

17 [Zwally, H. J., and Fiegles, S.: Extent and Duration of Antarctic Surface Melting, J. of Glaciology, 40, 463–476, 1994.](#)
18

Formatted: Font:(Default) +Theme Body (Times New Roman), 10 pt

Formatted: Line spacing: 1.5 lines

Formatted: Font:(Default) +Theme Body (Times New Roman), 10 pt

Formatted: Font:(Default) +Theme Body (Times New Roman), 10 pt

Formatted: Font:(Default) +Theme Body (Times New Roman), 10 pt

Formatted: Font:(Default) +Theme Body (Times New Roman)

1
3
4
5
6
7
8
9
10
11
12

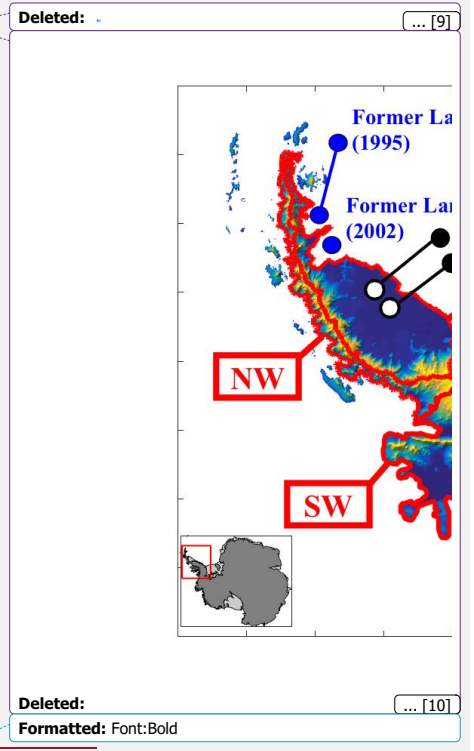
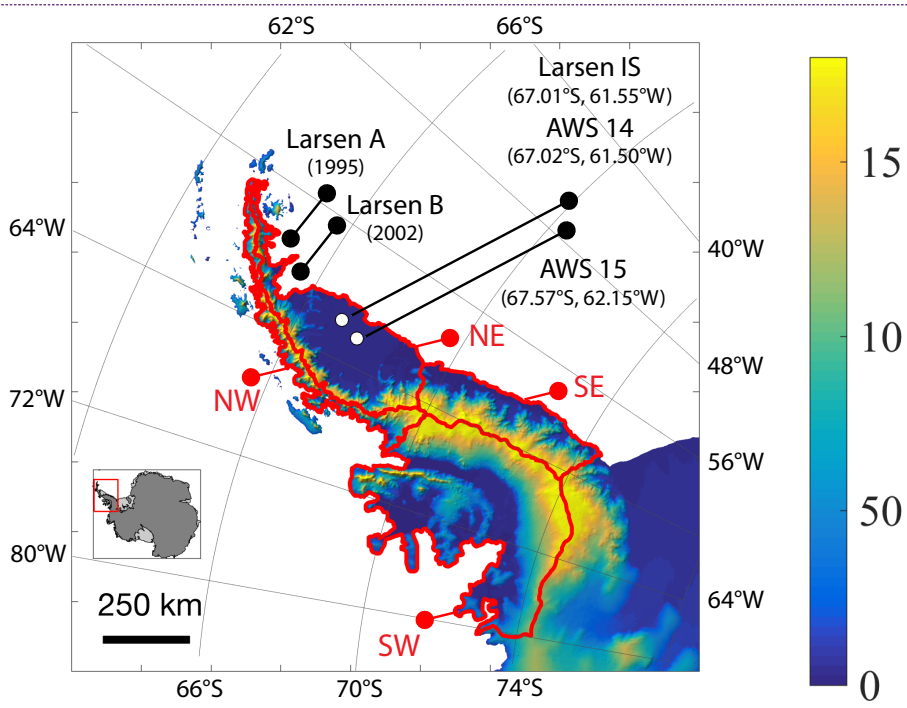
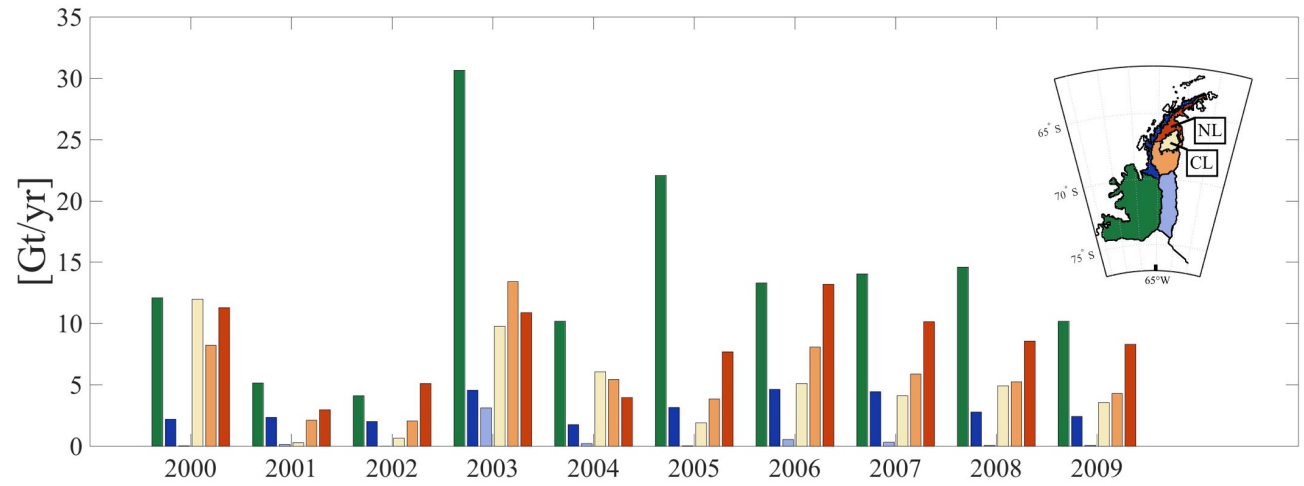


Figure 1: Full MAR domain showing topographic relief from bedmap2 (<https://www.bas.ac.uk/project/bedmap-2>) at 1km, former ice shelves with dates of collapse, locations of automatic weather stations (Larsen IS and AWS 14 stations are located within the same MAR gridcell) and basins corresponding to SW (basin 24) NW (basin 25) NE (basin 26), SE (basin 27) from Zwally, et. al. 2012

<u>Abbreviation</u>	<u>Definition</u>
<u>MAR model : criteria for melt occurrence (Section 2.1)</u>	
<u>LWC_{0.4}</u>	<u>liquid water content in the first meter is greater than 0.4 mm we (water equivalent)</u>
<u>MF_{0.4}</u>	<u>total meltwater production over the day exceeds 0.4 mmwe</u>
<u>Passive microwave : criteria for melt occurrence (Section 2.2.2)</u>	
<u>zwa</u>	<u>threshold based on winter mean temperature brightness, Zwally and Fiegles, 1994</u>
<u>ALA</u>	<u>threshold based on winter mean temperature brightness, Ashcroft and Long, 2006</u>
<u>240</u>	<u>fixed threshold method (Tedesco, 2007)</u>
<u>PMWAll</u>	<u>Condition when zwa, ALA, 240 all report melt occurrence</u>
<u>Active microwave (QuikSCAT) : criteria for melt occurrence (Section 2.2.1)</u>	
<u>QuikSCAT ft3</u>	<u>threshold based on winter mean backscatter (Steiner and Tedesco, 2014)</u>
<u>Observation-based regions of high melt occurrence (Section 3.2)</u>	
<u>CL region</u>	<u>high melt at the center-east of the Larsen C ice shelf, melt days exceeding 1 std dev of PMWAll mean melt occurrence</u>
<u>NL region</u>	<u>high melt in the north and west of the NE basin, consisting of the NE basin above the mean latitude of CL region which excludes the CL region</u>
<u>Conditions for melt occurrence (Section 4.2)</u>	
<u>PMWEx</u>	<u>PMWAll reports melt occurrence but MAR does not</u>
<u>QSEx</u>	<u>QuikSCAT ft3 reports melt occurrence but MAR does not</u>
<u>MAR-R</u>	<u>criteria when MAR data is used only when AWS data is available</u>

Table 1: Abbreviations used throughout text

1
2



3
4
5
6
7
8

Figure 2 Annual meltwater production from MAR [Gt/yr] shown for masks shown in inset ('2001' corresponds to meltwater production from July 2000- June 2001. NW, SW, SE basins are shown as in Fig. 1. NE basin is divided into the NL mask, the CL mask and the remaining portion of the NE basin (NE - (CL+NL)). The CL and NL masks are described in text.

1
2
3
4
5
6
7
8
9
10
11
12
13
14
15
16
17
18
19
20
21
22

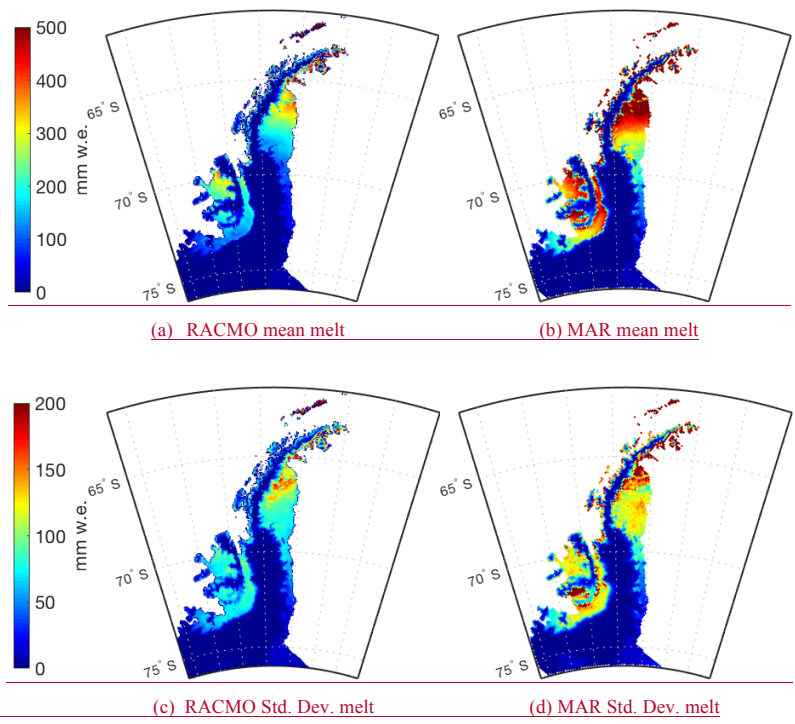
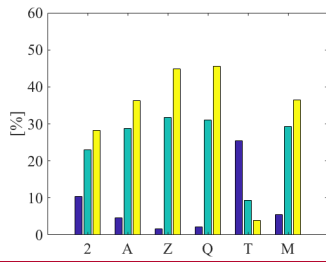
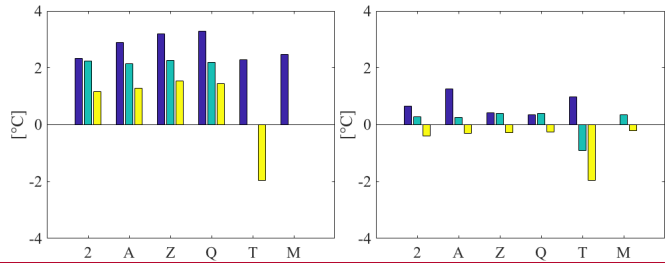


Figure 3 Meltwater production (2000-2009). RACMO2.3p2 at 5.5 km resolution, mean annual meltwater production (a) and standard deviation (c) and MAR v. 3.5.2 at a 10km resolution, mean annual meltwater production (b) and standard deviation (d)

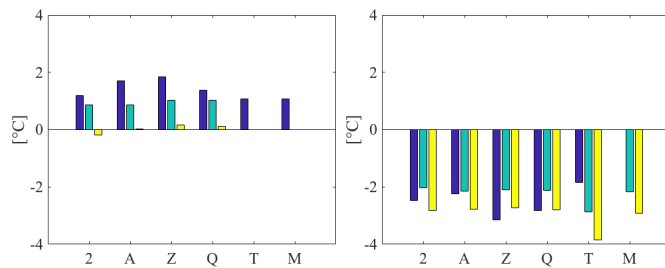


(a) Melt Occurrence at the Larsen Ice Shelf AWS Threshold = 0.4 mm w.e.

MAXT2m(AWS) < 0°C **MAXT2m(AWS) ≥ 0°C**



(b) AvgT2m bias (c) AvgT2m bias



(d) MaxT2m bias (e) MaxT2m bias

Data Sources:

Satellite

- 2 PMW 240
- A PMW ALA
- Z PMW zwa
- Q QuikSCAT

AWS-based

- T AvgT2m > 0°C
- M MaxT2m > 0°C

Melt Occurrence:

- MAR Only
- MAR & Obs
- Obs. Only

Formatted: Keep with next

Formatted: Keep with next

Formatted: Caption, Left, Indent: Left: 0"

Figure 4 Melt Occurrence and Temperature Biases at the Larsen Ice Shelf AWS Station. Percentage of total days (DJF, 2001-2010) showing melt occurrence from observational sources as compared to MAR v3.5.3 melt occurrence using the $MF_{0.4}$ metric (a) Temperature biases (MAR-AWS) for AvgT2m (b,c) and MaxT2m (d,e) when Max T2m is less than 0°C (b,d) or greater than 0°C (c,e)

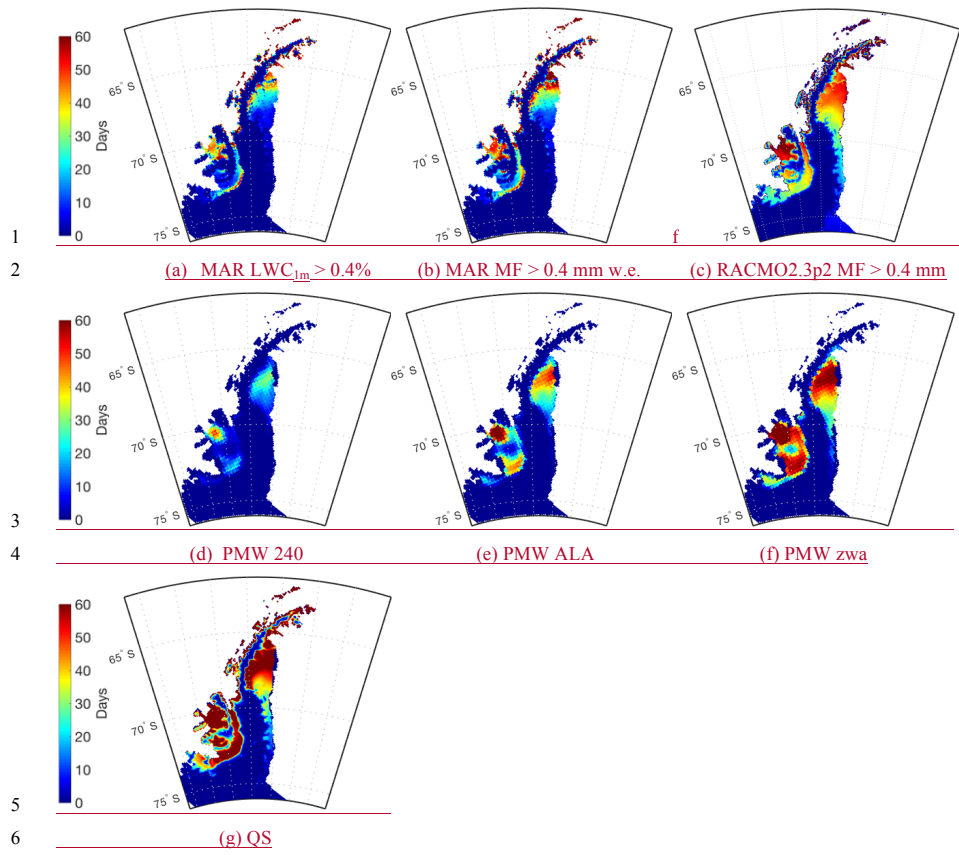


Figure 5 Average number of melt days (2000-2009) from multiple sources (a) MAR, Liquid Water Content > 0.4% for three consecutive days. (b) MAR Total Melt Flux > 0.4 mm w.e. for 1 day or more (c) RACMO2.3p2, Melt Flux > 0.4 mm w.e. Satellite-based metrics include (d) PMW 240 algorithm (e) PMW ALA (f) PMW Zwa (g) QuikSCAT. All satellite-based estimates include a melt day only when part of a sustained three-day period of melt.

Formatted: Caption, Don't keep with next

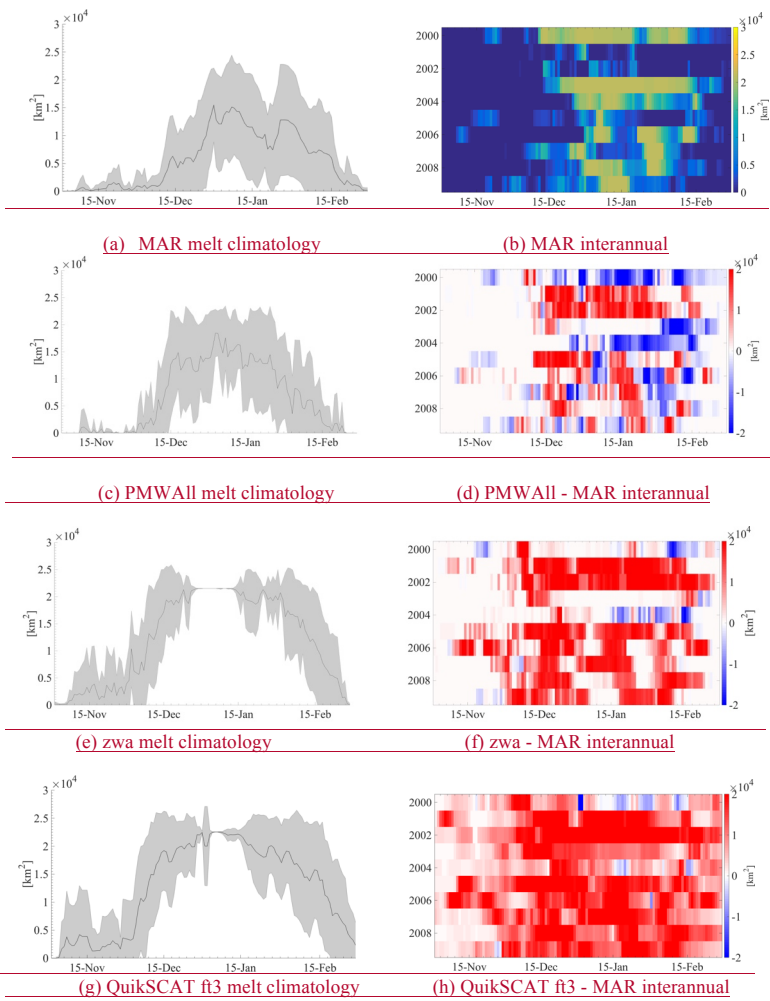
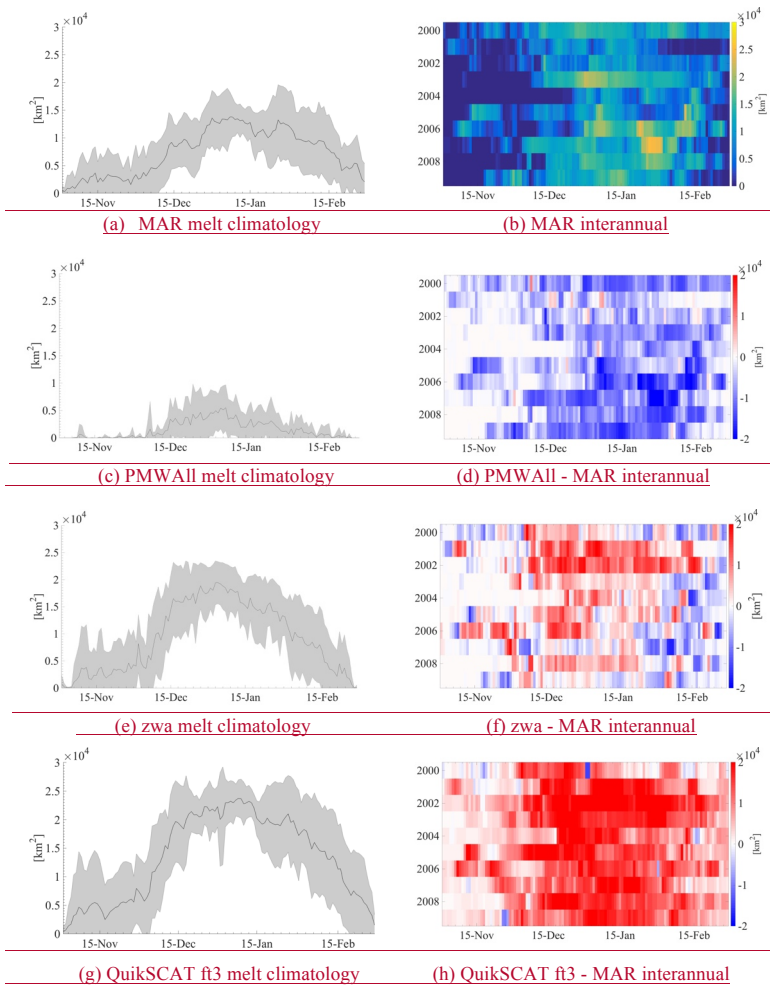


Figure 6 CL-region, described in text and shown in inset in for (a), average and inter-annual melt occurrence in MAR, PMW and QuikSCAT data. (a) MF0.4 melt extent climatology with one standard deviation shown in grey envelope (b) melt extent for MF0.4 from 1999-2009 (c) melt climatology PMW All (d) interannual difference melt extent PMWAll - MAR (e) melt climatology PMW zwa (f) interannual difference in melt extent PMWzwal - MAR (g) melt climatology QuikSCAT ft3 (h) interannual difference in melt extent QuikSCAT ft3 - MAR

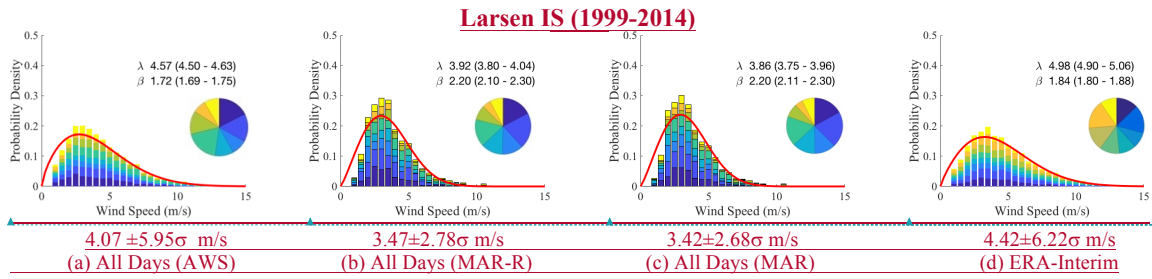
Formatted: Caption, Don't keep with next



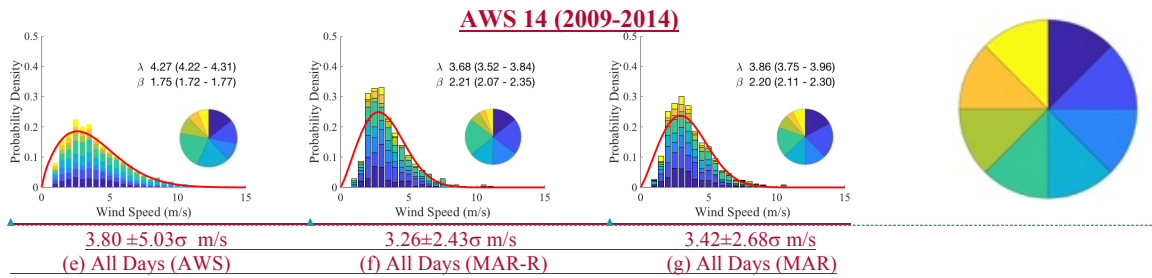
Formatted: Left, Indent: First line: 0.5"

Figure 7 NL-region, described in text and shown inset in (c), average and inter-annual melt occurrence in MAR, PMW and QuikSCAT data. (a) $MF_{0.4}$ melt extent climatology with one standard deviation shown in grey envelope (b) melt extent for $MF_{0.4}$ from 1999-2009 (c) melt climatology PMW All (d) interannual difference melt extent PMWAll - MAR (e) melt climatology PMW zwa (f) interannual difference in melt extent PMWzwal - MAR (g) melt climatology QuikSCAT ft3 (h) interannual difference in melt extent QuikSCAT ft3 - MAR

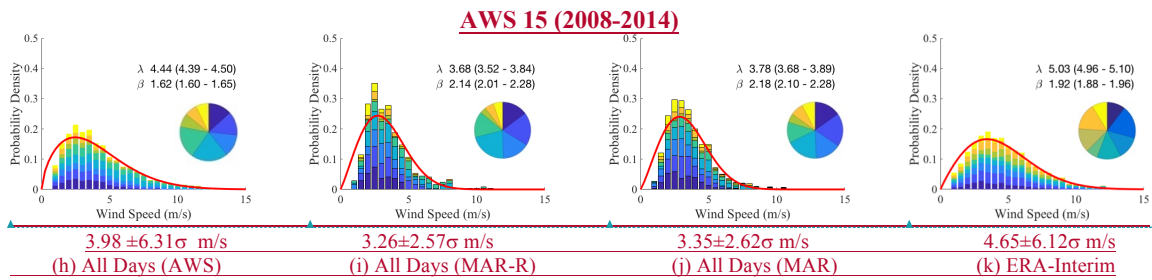
Formatted: Caption, Left, Don't keep with next



Formatted: Indent: Left: 2.5"
 Formatted: Font:12 pt, Bold
 Formatted: Font:12 pt, Bold
 Formatted: Font:12 pt, Bold
 Formatted: Font:12 pt, Bold



Formatted: Indent: Left: 2.5"
 Formatted: Font:12 pt, Bold
 Formatted: Font:12 pt, Bold
 Formatted: Font:12 pt, Bold



Formatted: Indent: Left: 2.5"
 Formatted: Keep with next
 Formatted: Font:12 pt, Bold
 Formatted: Font:12 pt, Bold
 Formatted: Font:12 pt, Bold

Figure 8 Probability distribution (y-axis) of summer (DJF) wind speeds (x-axis) and direction proportions inset. Wind directions corresponding to colors in 45° increments shown right of (g). Curve shows Weibull curve shape (β) and scale (λ , m/s). Datasets for AWS (col 1), MAR-R (col 2), MAR from 1999-2014 period (col 3) and ERA-Interim for the AWS-restricted period (col 4). Shown for station Larsen IS (row 1, a,b,c,d), AWS 14 (row 2, e,f,g), AWS 15 (row 3, h,i,j,k) Values below figures are expected values.

Formatted: Keep with next

Formatted: Font:12 pt, Not Bold

	NE (0°-90°)	SE (90°-180°)	SW (180°-270°)	NW (270°-360°)
DJF All Days				
MAR shows wind direction				
MAR percentage	39.0%	23.5%	23.2%	14.1%
MAR expected wind speed [m/s]	3.48(±2.46)	3.47(±2.62)	4.46(±4.44)	3.66(±4.69)
AWS expected wind speed [m/s]	3.79(±4.35)	4.19(±6.01)	5.35(±9.16)	4.00(±7.63)
AWS shows wind direction				
AWS percentage	34.3%	17.4%	28.9%	19.3%
MAR expected wind speed [m/s]	3.47(±2.49)	3.49(±2.14)	3.86(±3.54)	6.40(±10.14)
AWS expected wind speed [m/s]	3.96(±4.65)	3.77(±4.97)	4.77(±7.89)	6.70(±16.94)
Temp. biases (MAR-AWS)				
Avg T2m	0.68°C	0.65°C	0.94°C	0.72°C
Max T2m	-2.16°C	-1.40°C	-1.19°C	-2.35°C
Temp. bias where T2m > 0°C (MAR-AWS)				
Avg T2m	-1.36°C	-1.50°C	-1.06°C	-1.06°C
Max T2m	-2.96°C	-3.05°C	-2.33°C	-2.75°C
DJF, MAR reports melt				
MAR wind direction percentage	34.7%	27.6%	24.5%	13.2%
AWS wind direction percentage	35.2%	13.9%	25.6%	25.2%
Temp. biases (MAR-AWS)				
Avg T2m	0.77°C	0.56°C	1.05°C	0.52°C
Max T2m	-2.11°C	-2.20°C	-0.95°C	-1.43°C
Temp. bias where T2m > 0°C (MAR-AWS)				
Avg T2m	-0.93°C	-1.13°C	-0.53°C	-0.98°C
Max T2m	-2.57°C	-3.16°C	-1.66°C	-1.61°C

Table 2: Proportions for wind direction and associated temperature biases at the Larsen Ice Shelf AWS station from 2000-2009 restricted to the summer season (DJF)

- Formatted ... [13]
- Deleted: Southerly
- Formatted ... [11]
- Formatted Table ... [12]
- Deleted: Easterly
- Deleted: Westerly
- Formatted ... [14]
- Formatted ... [15]
- Formatted ... [16]
- Deleted: Where
- Formatted ... [17]
- Formatted Table ... [18]
- Formatted ... [19]
- Deleted: wind direction
- Formatted ... [21]
- Deleted: 55.6
- Deleted: 44.4
- Deleted: 63.9
- Deleted: 36.3
- Formatted ... [20]
- Formatted ... [22]
- Formatted ... [23]
- Deleted: 3.49...±2.463.12
- Deleted: 4.21...±24...6283
- Deleted: 3...4675...±4.443.09
- Deleted: 4...6604...±5...6969
- Formatted ... [28]
- Formatted ... [29]
- Deleted: 3.82...±45...3523
- Deleted: 5.10...±69...0114
- Deleted: 4.41...35(±9.166.87
- Deleted: 4.44...±7.638.73
- Deleted: Where
- Formatted ... [34]
- Formatted ... [35]
- Formatted ... [36]
- Deleted: wind direction
- Formatted ... [37]
- Deleted: 51.2
- Deleted: 48.8
- Deleted: 54.5
- Deleted: 45.5
- Formatted ... [38]
- Formatted ... [39]
- Deleted: 4.04...±2.495.31
- Deleted: 72...±2.143.07
- Deleted: 3.48...86(±2.37
- Deleted: 4.4...403...±10.146.26
- Formatted ... [44]
- Formatted ... [45]
- Deleted: 4...9652...±48...6533
- Deleted: 4...7739...±4.976.98
- Deleted: 3.90...±7.894.77
- Deleted: 5...70.22...±11...6.9403
- Formatted ... [49]
- Deleted: eratur...e
- Formatted ... [52]
- Formatted ... [53]
- Formatted ... [54]
- Formatted ... [55]
- Formatted ... [56]
- Formatted ... [57]

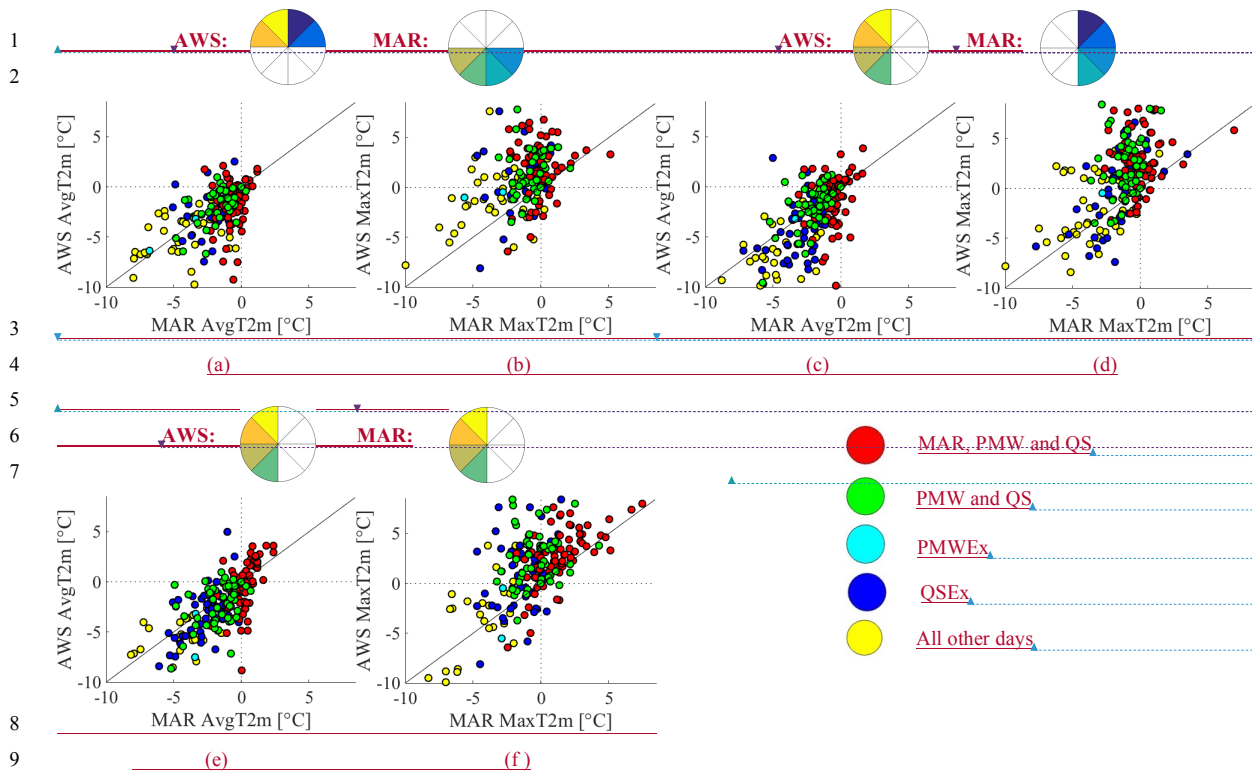


Figure 9 MAR vs AWS temperatures at the Larsen Ice Shelf AWS station for DJF from 2001-2009 for melt occurrence criteria as shown bottom-right and described in text. Wind direction biases are shown for when northerly AWS flow is reported as southerly in MAR (a) AvgT2m (b) MaxT2m, when westerly AWS flow is reported as easterly in MAR (c) AvgT2m (d) MaxT2 and when AWS and MAR both report westerly flow (e) AvgT2m (f) MaxT2m.

Deleted: Missing Northerlyflow . Missing Westerly flow ... [87]

Formatted: Font:Bold

Deleted:

Deleted:

Formatted: Justified, Indent: First line: 0"

Formatted: Justified, Indent: First line: 0"

Deleted: MAR: 3.37(±1.89) m/s AWS: 3.86 (±3.35) m/s MAR: 3.51 (±2.99) AWS: 3.88(±4.76) m/s

Deleted: <sp><sp><sp><sp>

Deleted: Westerly ... [88]

Formatted: Font:Bold

Formatted: Left

Formatted: Left, Indent: Left: 0", First line: 0"

Deleted:

Formatted: English (US)

Formatted: Font:Bold

Formatted: English (US)

Formatted: Keep with next

Formatted: English (US)

Formatted: English (US)

Formatted: English (US)

Formatted: English (US)

Formatted: English (US)

Formatted: Keep with next

Formatted: Caption, Left

Deleted: MAR: 4.31(±4.74) m/s AWS: 4.81 (±7.44) m/s ... [89]

Deleted:

- 1
- 2
- 3

← **Formatted:** Centered, Space After: 0 pt, Line spacing: 1.5 lines, Keep with next

1 **Page 1: [1] Deleted** **Rajashree Datta** **5/7/18 7:30:00 AM**

2 The underestimation of föhn flow in the east of the Larsen C may potentially be resolved by removing the hydrostatic
3 assumption in MAR or increasing spatial resolution. The underestimation of southwesterly flow in particular may be
4 reduced by using higher-resolution topography.

5
6
7 **Page 3: [2] Deleted** **Rajashree Datta** **5/7/18 7:34:00 AM**

8 This is primarily caused by more exposure to open water in combination with prevailing westerly winds on the west AP and
9 southerly winds on the east AP. Moreover, when strong westerly winds cross the bisecting mountain range of the AP (Fig.
10 1), the resulting föhn winds can produce pulses of warming on the East Antarctic Peninsula's ice shelves (Marshall,
11 2007). Föhn winds are a warm, dry air flow on the lee slopes of a mountain range (Beran 1967). This resultant warming
12 can be produced by four main mechanisms. Elvidge (2016) uses a modeling approach to trace four physical processes
13 that occur during föhn flow in the East AP, namely *isentropic drawdown* (sourcing of föhn air from higher altitudes),
14 *latent heating* and *precipitation* (where cooling during uplift on the windward side promotes precipitation),
15 *mechanical mixing* (turbulent sensible heating and drying of low-level flow) and *radiative heating* (where cloudless
16 conditions on the lee side increase the availability of shortwave radiation for heating). The relative importance of each
17 of these mechanisms for surface melt has been shown to be related to the source of föhn flow in the East AP (Elvidge
18 et al., 2015; Grosvenor et al., 2014). For example, southwesterly föhn jets descending from gap flow (from lower-
19 elevation passages in the mountain range) have been shown to be cooler and moister than surrounding föhn flow
20 descending from higher elevations (Elvidge et al., 2015). Recent warming in the East AP has been linked to an increase
21 in föhn winds during recent warming (Cape et al., 2015), which were possibly related to an increase in the speed of
22 warm northwesterly winds which have been associated with positive phases of the Southern Annular Mode (SAM),
23 (Van den Broeke and Van Lipzig, 2003). Because melt in the East AP is as vulnerable to wind dynamics as it is to
24 regional temperature changes, an accurate depiction of föhn flow is crucial for accurate estimates of meltwater
25 production.

26
27 **Page 3: [3] Moved to page 3 (Move #1)** **Rajashree Datta** **5/7/18 7:53:00 AM**

28 Observation-based studies on the formation of melt ponds in the Cabinet Inlet portion of the Larsen C Ice
29 Shelf have focused on the response to föhn winds (Luckman et al., 2014) and the formation of subsurface ice (Hubbard
30 et al., 2016). These last studies taken together discuss both the atmospheric drivers for melt as well as the effects on
31 the ice shelf within our region of interest, but are necessarily limited to a small region where observations are available.
32 By contrast, spaceborne satellites allow us to estimate surface melt occurrence and meltwater production over the
33 entire AP, complementing *in-situ* data. The combination of satellite-based and *in situ* data provide an excellent toolset
34 for model validation.

35
36 **Page 15: [4] Deleted** **Microsoft Office User** **6/13/18 12:12:00 AM**

37 Fig. 8 shows wind frequency distributions during the summer season, color-coded for wind direction as
38 represented by the pie graph at the right. We note that AWS data are 3-hourly averages and ERA-Interim are 6-hourly
39 averages for wind speed and direction, while MAR produced daily-averaged outputs. For this reason, a direct
40 comparison between Weibull parameters derived from MAR vs AWS data is not fully justified. The Larsen Ice Shelf

1 AWS has full temporal coverage during the QuikSCAT period while AWS14 and AWS15 were installed after
2 termination of the QuikSCAT mission. These last two stations are used in this study to demonstrate that (a) similar
3 wind biases persisted after the QuikSCAT period at multiple locations, as AWS 14 the Larsen Ice Shelf AWSs are co-
4 located to the same MAR grid cell and that (b) wind biases vary slightly by latitude, AWS15 being located slightly to
5 the south.

6 Both MAR and AWS are dominated by northerly winds at lower windspeeds (in yellow and blue) although AWS
7 data shows a greater frequency of southwesterly winds when windspeeds are higher (> 8 m/s). This is especially
8 relevant at the southern AWS15, where modeled temperature correlates with a larger portion of the southern Larsen
9 C Ice Shelf than for AWS14 (Supplemental Fig. S7). All AWSs show more southwesterly flow and slightly more
10 northwesterly flow than either MAR-R or MAR, which show a substantially higher percentage of easterly flow instead,
11 a trend which is more pronounced at the southernmost AWS15 (Fig. 7i,j). ERA-Interim reports substantially more
12 northwesterly flow than either AWS or MAR and a smaller proportion of southwesterly flow in the 180° - 225° range
13 (especially at the southernmost AWS15 location), although the proportion of easterly flow is similar to that reported
14 by AWSs. We note that although ERA-Interim has been shown to reproduce the basic structure of föhn flow
15 (Grosvenor et al., 2014), the resolution may be too coarse to adequately capture southwesterly gap flow here. As
16 discussed further in Sect. 5, westerly flow towards the stations used in this study may be strongly affected by the fine-
17 scale representation of topography (which is coarse in ERA-Interim) and the lowered orographic barrier in the
18 northwest in ERA-Interim may contribute to the enhanced northwesterly flow shown here.

19 Specifically, at the Larsen Ice Shelf AWS location, both AWS and MAR reports dominant northeasterly flow
20 (Table 2, rows 4,8, col2). However, the AWS reports slightly more flow which is either southwesterly (28.9% vs.
21 23.2% in MAR) or northwesterly (19.3% vs. 14.1% in MAR) while MAR reports more southeasterly flow overall
22 (23.5% vs. 17.4% in AWS). Melt occurrence (from PMW and QS) is observed primarily when AWS-observed flow
23 is northeasterly (0° - 90°) or southwesterly (180° - 270°), with QS(PMW) reporting that 36%(42%) northeasterly flow
24 and 29%(26%) southwesterly flow. On days when MAR reports melt (Table 2, rows 19,20), southeasterly flow in
25 MAR is even more dominant (but declines at the AWS) while northwesterly flow decreases (while it increases at the
26 AWS). The bias towards easterly flow affects 26% of all days and 10% of melt days in MAR, 21%(18%) of all days
27 where QS(PMW) report melt occurrence, but only 8%(9%) of days where PMW(QS) melt occurrence is not also
28 captured by MAR. Similarly, the bias towards southerly flow captures 26% of all days and 8% of melt days in MAR,
29 13%(15%) of days where QS(PMW) report melt occurrence, but only 6%(6%) of days when PMW(QS) melt
30 occurrence is not also reported by MAR. Most notably, for 4% of all melt days in MAR, AWS reports southwesterly
31 winds while MAR reports southeasterly winds and this bias accounts for 3%(4%) of days when PMW(QS) report melt
32 but MAR does not. In summary, despite biases in wind directions reported by MAR, the overall impact on melt
33 occurrence is fairly limited according to comparisons with satellite estimates. Within the next section we prominent
34 wind direction biases in greater detail.

37 Fig. 5 shows wind frequency distributions during the summer season (AWS, MAR-R, MAR from left to right columns,
38 Larsen IS station, AWS 14 and AWS 15 from top to bottom), color-coded for wind direction as represented by the pie

1 graph at the top. We note that AWS data uses 3-hourly data for wind speed and direction without daily-averaging,
2 while MAR produced daily-averaged outputs, For this reason, a direct comparison between Weibull parameters
3 derived from MAR vs AWS data is not meaningful, although we show comparisons between different stations (for
4 the same data source) .The Larsen IS station has full temporal coverage during the QuikSCAT period while AWS14
5 and AWS15 were installed after termination of the QuikSCAT mission. These last two stations are used in this study
6 to demonstrate the consistency of wind biases at multiple locations, as well as how wind biases vary by latitude
7 (AWS15 being located slightly to the south). Whereas MAR is dominated northerly winds at it's lower range of
8 windspeeds (in yellow and blue), AWS data shows a greater frequency of southwesterly winds at the higher range of
9 windspeeds (> 8 m/s). In general, even at lower wind speeds (2-5 m/s), AWS data shows more southwesterly winds
10 than either MAR-R or MAR. This is especially relevant at the southern AWS15 station, where modeled temperature
11 correlates with a larger region of the Larsen IS than temperatures modeled by MAR for the AWS14 station
12 (Supplemental Fig. 6). Observed wind direction (without consideration for wind speed) at AWS15 shows more
13 southwesterly flow (Fig. 5g) than either MAR-R or MAR (Fig. 5 h,i), which show a substantially higher percentage
14 of southeasterly and northerly flow instead.

15 Specifically, while both MAR and AWS show a higher proportion of northerly (vs southerly) winds, the
16 proportion of northerly winds in MAR is slightly higher (Table 1). While both MAR and AWS report a larger
17 proportion of easterly (vs westerly) flow, MAR reports 64% of flow to be easterly where AWS reports only 55%
18 easterly flow. We show that MAR melt occurrence at the Larsen Ice Shelf station is concurrent with both increased
19 northerly and westerly flows. On days when MAR reports melt (compared to days with no melt), northerly winds are
20 more frequent (according to both MAR and AWS estimates), and the proportion of westerly winds increases slightly
21 in MAR but decreases slightly in AWS data (Table 1).

22 When daily-averaged temperature (AvgT2m) values are high, it is more likely that melt is sustained, while high
23 maximum daily temperatures (MaxT2m) can also occur during sporadic melt. Melt occurrence is strongly influenced
24 by the temperature of the snow column as well as at the surface; internal melting can occur even when the surface is
25 frozen due to net outgoing longwave radiation (Holmgren 1971)(Hock 2005) In general, we find a small, but consistent
26 warm MAR bias for AvgT2m, and a consistent cold MaxT2m bias. However, when we restrict the dataset to days
27 when AWS 2m-temperature estimates exceed 0°C, (a condition where melt is most likely), MAR indicates a cold bias
28 for AvgT2m and an enhanced cold bias for MaxT2m, i.e. while MAR shows an overall warm bias, this bias is reversed
29 at the temperature ranges where melt is likely (although melt is still possible due to other elements in the energy
30 balance). On days when MAR meltwater production meets the $MF_{0.4}$ criteria, we find that the magnitude of all biases
31 is greatly reduced. In particular, we note that the MaxT2m bias for westerly winds (for the ALL condition) is
32 substantial, showing a -2.42°C cool bias in MAR for all available data and -3.04°C when data is restricted to days
33 when MaxT2m > 0°C.

36
37 Three wind direction biases are dominant on days when observed sources (either PMW All or QuikSCAT ft3) report
38 melt, but MAR does not. We refer to the condition where PMWAll reports melt (but MAR does not) as “PMWEx”

1 (i.e. PMW exclusive-or), with the equivalent condition for QuikSCAT ft3 called “QSEx”. We focus on these specific
2 wind biases and find the associated temperature biases. Supplemental tables 2-7 include R^2 , RMSE and mean bias
3 values for both surface pressure and daily AvgT2m at all three stations.

4 **4.2.1 Observed northeasterly flow**

5 The largest proportion of melt occurrence for either MAR, PMWEx or QSEx is reported when northeasterly winds
6 are dominant, specifically when winds are recorded by the Larsen Ice Shelf AWS station as northeasterly (0° - 90°).
7 Northeasterly AWS flow accounts for a large proportion of general flow and an even larger proportion of flow when
8 either MAR or PMWEx report melt, i.e. 36% of general flow, 39% of days where MAR reports melt, 42% of days
9 where PMWEx reports melt and 36% of days where QSEx reports melt. On days when AWS reports northeasterly
10 winds, MAR primarily reports northeasterly flow (0° - 90° , case 1), but also reports a substantial bias for northwesterly
11 flow (270° - 360° , case 2). In case 2, associated temperature biases may be influenced by the inclusion of warmer
12 westerly winds in MAR. We add that the majority of northeasterly AWS flow is actually captured in a narrower
13 northeasterly band in MAR from 0 - 45° , accounting for 13.4% of ALL days. We examine these two cases separately
14 to quantify how a modeled westerly wind bias affects temperature and melt (in comparison to the case when wind
15 direction matches observed estimates). Supplemental tables 8-10 contain relative proportions of each case (flow bias)
16 divided by the general melt restriction (i.e. MAR, QSEx or PMWEx), as well as the timeseries mean and biases for
17 AvgT2m, AvgT2m $>0^\circ\text{C}$ (excluding days when AvgT2m values from AWS are below 0°C), MaxT2m and MaxT2m
18 $>0^\circ\text{C}$.

19 In the instance where northeasterly flow is modeled accurately (case 1, Fig. 6a), modeled temperature values
20 are clustered around 0°C , whereas AWS-observed temperatures (especially when only satellite-observed melt occurs)
21 are higher. When MAR reports melt, MAR AvgT2m values cluster near 0°C , with a small overall warm bias (0.69°C).
22 Under omission conditions (PMWEx and QSEx), AvgT2m values are lower, and MAR bias is slightly cold, although
23 standard deviation is high. As with all flow cases, only QuikSCAT ft3 shows melt at very low observed AvgT2m
24 values. By contrast, AWS MaxT2m values are substantially higher than MAR values (the latter clustering around 0°C)
25 (Fig. 6b). We find that where QuikSCAT ft3 uniquely reports melt (QSEx), AvgT2m values at the lower range of
26 temperatures report a stronger cool MAR bias for MaxT2m .

27 In case 2, AvgT2m values show a small warm MAR bias in all melt conditions, i.e. for ALL data points
28 (0.79°C), for when MAR shows melt (0.82°C), and finally for both the PMWEx (0.44°C) and QSEx(0.65°C)
29 conditions (Supplemental Table 8). However, when MAR reports melt and AWS AvgT2m values exceed 0°C , there
30 is a substantial cold bias (-1.13°C)(Fig 6c), which may lead to reduced meltwater production. In contrast to case 1,
31 modeled MaxT2m values in case 2 do not cluster around 0°C (Fig. 6b,d) and MAR melt days report larger MaxT2m
32 values.

33 In summary, when MAR reports westerly flow, Avg T_s values are higher (as is melt occurrence). As with
34 the comparison with case 1 and case 2, we find that in all instances when MAR reports northeasterly flow (with all
35 AWS-observed wind directions considered), AvgT2m and MaxT2m temperatures cluster near 0°C (Fig. 6e,f), whereas
36 when MAR reports northwesterly flow (with all AWS wind directions taken into consideration), MaxT2m values are,

1 on average, higher, and the temperature bias is narrowed (Fig. 6 g,h). Expected values for windspeeds for each
2 condition based on a Weibull fit show comparable expected values, but larger standard deviations for AWS-estimated
3 windspeeds when MAR reports northwesterly flow (Fig. 6 c,d g,h).

4 **4.2.2 Observed southwesterly flow**

5 For all days in the summer season (“ALL”, i.e. without regard for melt occurrence), we find that MAR reports 15%
6 of winds to be southwesterly at the Larsen Ice Shelf station location while AWS reports ~ 30% southwesterly flow.
7 We note that the relative proportions of southwesterly/southeasterly flow in AWS is approximately reversed in MAR,
8 with AWS reporting 18.3% of flow to be southwesterly and MAR reporting 29.2% southwesterly flow. We focus
9 specifically on the condition where both MAR and AWS report southwesterly flow (between 180° and 270°), which
10 accounts for 5.7% of total flow and only 4.9% of MAR melt days, but a larger proportion of days where only observed
11 sources report melt, i.e. 5.6% for the PMWEx condition and 8% for the QSEx condition.

12 As with case 2 for northwesterly winds in section 4.2.1, MAR captures higher AvgT2m values which
13 frequently exceed 0°C, with a slight cool MAR bias when AvgT2m > 0°C (Fig 7a). The PMWEx and QSEx conditions
14 report melt at lower temperature values, where the MAR bias is slightly warmer. Although a cold MAR bias persists,
15 MaxT2m values are, in general, higher with AWS and MAR values showing greater agreement (Fig 7b). Expected
16 windspeeds for southwesterly winds are substantially higher (with a greater standard deviation) than the base condition
17 when wind direction is not considered, with AWS reporting an even higher standard deviation (i.e. high-speed sporadic
18 winds).

19
20 **Page 19: [7] Deleted**

Rajashree Datta

5/7/18 1:02:00 PM

21 In the aggregate, we conclude that MAR shows lower melt occurrence than satellite estimates in the center and east
22 of the Larsen C ice shelf (i.e. the CL region, where eastward föhn flow is likely limited in MAR), while in the north
23 and west of the NE basin (i.e. the NL region which is most immediately affected by föhn flow), MAR reports melt
24 occurrence largely concurrent with satellite estimates. For example, within the CL region, there are periods during the
25 2001-2002 season when MAR reports no meltwater production, but raw QuikSCAT backscatter values report periods
26 where over 300 km² of surface area show backscatter values dipping below -15 dB (Supplemental Fig. 8e). We remind
27 the reader that raw backscatter values from QuikSCAT have previously been used to estimate melt flux over the AP
28 (Trusel et al., 2013; Trusel et al., 2012).

29 In comparison to AWS estimates, MAR displays a general warm bias in the East AP at lower temperatures where
30 melt is less likely to occur, but which may still impact the refreeze process. However, when maximum daily
31 temperatures (MaxT2m) and average daily temperatures (AvgT2m) exceed 0°C, MAR shows a substantial cold bias
32 which may limit melting. We note a smaller proportion of westerly winds in MAR compared to observed values at
33 the Larsen Ice Shelf AWS station, especially an absence of southwesterly flow, which tends to have higher observed
34 windspeeds. The general cold bias in MAR is partially closed when observed northeasterly winds are reported by
35 MAR as northwesterly, i.e. MAR reports both higher AvgT2m and MaxT2m values as well as greater melt occurrence.
36 Similar biases are shown for southwesterly flow, which accounts for a disproportionate amount of satellite-observed
37 melt which is not captured by MAR. The importance of westerly winds is demonstrated during mid-December in the

1 2001-2002 season, at which point satellite-based melt extent in the CL region increases substantially, while MAR melt
2 extent declines (Supplemental Fig. 8a). This period is concurrent with an increase in westerly winds at the Larsen IS
3 AWS station which are not modeled MAR (Supplemental Fig 9b vs f). Additionally, we note that shortly after this
4 point, AWS AvgT2m temperatures consistently exceed MAR AvgT2m values until the end of the season
5 (Supplementary Fig. 10).

6 Previous work has suggested that southwesterly föhn winds can result from gap flow (Elvidge et al. 2015),
7 although we note that the southwesterly jets studied in this single campaign were typically cooler and moister than
8 surrounding air (i.e. föhn flow produced from isentropic drawdown). We note that the low windspeed bias in MAR
9 may have a minor impact overall, but could strongly impact melt in the East AP if southwesterly flow is more
10 accurately captured in future versions of MAR. We hypothesize that the underestimation of westerly flow at the eastern
11 reaches of the Larsen C ice shelf is likely due to the hydrostatic assumption (allowing for no vertical acceleration of
12 air mass) preventing eastward, downward flow in the near-surface atmosphere. The implementation of a non-
13 hydrostatic model will likely be required to fully capture föhn flow in the East AP (Hubert Gallée, personal
14 communication). We conclude that the relative absence of fast, warm westerly and southwesterly winds contributes
15 to a lack of MAR melt in the CL region as compared to satellite estimates.

16 Previous literature has pointed to several limitations in the remote sensing data sources used here which are either
17 intrinsic to the satellite data itself or a product of the algorithm selected for melt detection. Products derived from
18 QuikSCAT are limited in temporal resolution because the satellite passes at a twice-daily scale, and may therefore
19 ignore sporadic melt occurring at other times of day. However, previous studies have compared total melt days from
20 the QuikSCAT ft3 algorithm with a measure derived from surface temperature at seven automatic weather stations
21 and shown a positive QuikSCAT ft3 bias compared to AWS (Steiner and Tedesco, 2014). Similarly, all PMW
22 algorithms are limited by a relatively low resolution (25km) and twice-daily passes. Periods of melt occurrence have
23 also been shown to be highly sensitive to the choice of algorithm (Tedesco 2009). Because of the high topographic
24 variability of the NL region (especially near the spine of the AP), it is possible that PMW algorithms are under-
25 reporting melt occurrence due to low horizontal spatial resolution. A higher-resolution passive microwave product
26 may better resolve this issue.

27 In the northernmost portions of the NL region, sporadic MAR-modeled meltwater percolates deeply into the
28 snowpack in November (as deep as 10m early in the season in some years), which is consistent with MAR $MF_{0.4}$,
29 PMW zwa and QuikSCAT ft3 reporting melt occurrence at this point while other algorithms/melt metrics do not. The
30 deep percolation of meltwater is potentially enabled by low density snow early in the season. This early-season melt
31 is frequently followed by a near-complete refreeze. Future work will focus on the interannual variability of early-
32 season melt as this may have a substantial impact on the density of the firn layer in the Larsen C ice shelf.

33 In light of the biases reviewed here, we report MAR meltwater production over the 1999-2009 period (Fig.
34 8) and consider the potential implications of the wind/temperature biases found in this analysis on regional meltwater
35 production. Over the full study domain, the total annual meltwater production estimated by MAR shows substantial
36 inter-annual variation with the NE basin accounting for the highest aggregate meltwater production, closely followed
37 by the SW basin (in green). The NE basin is divided into three regions: the NL and CL masks and the remainder of

1 the basin. We note that the SW basin does not covary with the NE basin (with all subregions taken together) and the
2 subregions of the NE basin do not consistently covary with one another. The meltwater production shown here does
3 not account for refreeze and we note that the effects of refrozen melt on the snowpack will vary regionally depending
4 on local properties. The NL region dominates meltwater production in the NE basin in most years except for 1999-
5 2000, 2002-2003 and 2003-2004. The 2001-2002 melt season shows the second lowest overall melt production during
6 the study period (only the preceding year is lower). Declining aggregate meltwater production across the AP does not
7 necessarily correspond to declining meltwater production in the most vulnerable regions of the northeastern AP
8 (including the Larsen C ice shelf). Because melt in the NL region is particularly sensitive to föhn-induced melt, we
9 note that changes in circulation patterns may affect the northwest regions differently than the southern regions. The
10 strong relationship between wind direction and temperature bias points to the need for isolating dominant inter-annual
11 patterns of melt in the Northern Larsen C Ice Shelf and associating them with large-scale atmospheric drivers.

12
13 **Page 20: [8] Deleted**

Rajashree Datta

6/12/18 9:19:00 PM

14
15
16
17 **Page 29: [9] Deleted**

Rajashree Datta

5/7/18 1:41:00 PM

18 19 **References**

20 Abdalati, W., and Steffen K.: Passive Microwave-Derived Snow Melt Regions on the Greenland Ice Sheet,
21 *Geophysical Research Letters.*, 22 (7), 787–790, doi:10.1029/95GL00433, 1995.

22
23 Ahrens, C. Donald.: *Meteorology Today : An Introduction to Weather, Climate, and the Environment.* Eighth
24 edition. Thomson/Brooks/Cole, Belmont, CA, 2007.

25
26 Amory, C., Trouvilliez, A., Gallée, H., Favier, V., Naaim-Bouvet, F., Genthon, C., Agosta, C., Piard, L., and Bellot.
27 H.: Comparison between Observed and Simulated Aeolian Snow Mass Fluxes in Adélie Land, East Antarctica., *The*
28 *Cryosphere* 9 (4), 1373–83, doi:10.5194/tc-9-1373-2015, 2015.

29
30 Ashcraft, I. S., and Long. D.G.: SeaWinds Views Greenland: In *Geoscience and Remote Sensing Symposium*, 2000.
31 *Proceedings. IGARSS 2000. IEEE 2000 International*, 3,1131–1133, 2000.

32
33 Ashcraft, I. S., and Long. D.G.: Comparison of Methods for Melt Detection over Greenland Using Active and
34 Passive Microwave Measurements, *International Journal of Remote Sensing*, 27 (12), 2469–88,
35 doi:10.1080/01431160500534465, 2006.

36
37 Barrand, N. E., Vaughan, D. G., Steiner, N., Tedesco, M., Kuipers-Munneke, P. , Van den Broeke, M. R., and
38 Hosking, J. S.: Trends in Antarctic Peninsula Surface Melting Conditions from Observations and Regional
39 Climate Modeling, *Journal of Geophysical Research: Earth Surface*, 118 (1), 315–330,
40 doi:10.1029/2012JF002559, 2013.

1
2 Bell, R. E., Chu, W. Kingslake, J., Das, I., Tedesco, M., Tinto, K.J., Zappa, C.J., Frezzotti, M., Boghosian, A., and
3 Lee.W.S.: Antarctic Ice Shelf Potentially Stabilized by Export of Meltwater in Surface River, *Nature*, 544 (7650),
4 344–348. doi:10.1038/nature22048, 2017.
5
6 Beran, D.W.: Large Amplitude Lee Waves and Chinook Winds, *Journal of Applied Meteorology*, 6 (5),865–877.
7 doi:10.1175/1520-0450(1967)006<0865:LALWAC>2.0.CO;2., 1967.
8
9 Braithwaite, R. J.: On Glacier Energy Balance, Ablation, and Air Temperature, *Journal of Glaciology*, 27, 381–91,
10 1981
11
12 Brandt, R. E., and Warren, S.G.: Solar-Heating Rates and Temperature Profiles in Antarctic Snow and Ice, *Journal*
13 *of Glaciology*, 39, 99–110. doi:10.1017/S0022143000015756, 1993.
14
15 Brun, E, David, P., Sudul, M. and G Brunot, G.: A Numerical Model to Simulate Snow-Cover Stratigraphy for
16 Operational Avalanche Forecasting, *Journal of Glaciology*, 38,13–22, 1992.
17
18 Cape, M. R., Vernet, M., Skvarca, P., Marinsek, S., Scambos, T. and Domack, E.: Foehn Winds Link Climate-
19 Driven Warming to Ice Shelf Evolution in Antarctica. *Journal of Geophysical Research: Atmospheres*, 120 (21) 11,
20 37-11, doi:10.1002/2015JD023465, 2015.
21
22 De Ridder, K., and Gallée, H.: Land Surface-Induced Regional Climate Change in Southern Israel, *Journal of*
23 *Applied Meteorology*, 37 (11), 1470–1485, 1998.
24
25 Dee, D. P., Uppala, S. M., Simmons, A. J., Berrisford, P., Poli, P., Kobayashi, S., Andrae, U. et al., The ERA-
26 Interim Reanalysis: Configuration and Performance of the Data Assimilation System, *Quarterly Journal of*
27 *the Royal Meteorological Society*, 137 (656), 553–597, doi:10.1002/qj.828, 2011.
28
29 Drinkwater, M.R., and Liu, X.: Seasonal to Interannual Variability in Antarctic Sea-Ice Surface Melt, *IEEE*
30 *Transactions on Geoscience and Remote Sensing*, 38(4), 1827–1842, doi:10.1109/36.851767, 2000.
31
32 Dutra, E., Sandu, I., Balsamo, G., Beljaars, A., Freville, H., Vignon, E., and Brun. E.: Understanding the ECMWF
33 Winter Surface Temperature Biases over Antarctica, *Technical Memorandum*, 762, 2015.
34
35 Elvidge, A. D., Renfrew, I.A., King, J.C., Orr, A., Lachlan-Cope, T.A., Weeks, M. and Gray, S.L.: Foehn Jets over
36 the Larsen C Ice Shelf, Antarctica, *Quarterly Journal of the Ro/yal Meteorological Society*, 141(688), 698–
37 713. doi:10.1002/qj.2382., 2015.

1
2 Fettweis, X., Franco, B., Tedesco, M., van Angelen, J.H., Lenaerts, J. T. M., Van den Broeke, M. R. and Gallée, H.:
3 Estimating the Greenland Ice Sheet Surface Mass Balance Contribution to Future Sea Level Rise Using the
4 Regional Atmospheric Climate Model MAR, *The Cryosphere* 7 (2), 469–489, doi:10.5194/tc-7-469-2013,
5 2013.
6
7 Fettweis, X, Gallée, H., Lefebvre, F., and Van Ypersele. J., Greenland Surface Mass Balance Simulated by a
8 Regional Climate Model and Comparison with Satellite-Derived Data in 1990–1991, *Climate Dynamics*
9 24 (6), 623–640, 2005.
10
11 Fettweis, X., Box, J.E., Agosta, C., Amory, C., Kittel, C., and Gallée, H.: Reconstructions of the 1900-2015
12 Greenland Ice Sheet Surface Mass Balance Using the Regional Climate MAR Model, *The Cryosphere*
13 *Discussions*, November, 1–32, doi:10.5194/tc-2016-268, 2015.
14
15 Franco, B., Fettweis, X., Lang, C., and Erpicum, M.: Impact of Spatial Resolution on the Modelling of the
16 Greenland Ice Sheet Surface Mass Balance between 1990–2010, Using the Regional Climate Model MAR,
17 *The Cryosphere* 6 (3), 695–711. doi:10.5194/tc-6-695-2012, 2012.
18
19 Fretwell, P., Pritchard, H. D., Vaughan, D. G., Bamber, J. L., Barrand, N. E., Bell, R., Bianchi, C. et al.: Bedmap2:
20 Improved Ice Bed, Surface and Thickness Datasets for Antarctica, *The Cryosphere*, 7 (1), 375–393,
21 doi:10.5194/tc-7-375-2013, 2013.
22
23 Gallée, H., and Schayes, G.: Development of a Three-Dimensional Meso-Gamma Primitive Equation Model:
24 Katabatic Winds Simulation in the Area of Terra Nova Bay, Antarctica, Belgian Science Policy Office, 1994.
25
26 Gallée, H., Trouvilliez, A., Agosta, C., Genthon, C., Favier, V., and Naaim-Bouvet, F.: Transport of Snow by the
27 Wind: A Comparison Between Observations in Adélie Land, Antarctica, and Simulations Made with the Regional
28 Climate Model MAR, *Boundary-Layer Meteorol.*, 146 (1), 133–47, doi:10.1007/s10546-012-9764-z, 2013.
29
30 Gilbert, R. O.: *Statistical Methods for Environmental Pollution Monitoring*, Van Nostrand Reinhold Co., New York,
31 NY, 1987.
32
33 Glasser, N. F., and Ted A. Scambos.: A Structural Glaciological Analysis of the 2002 Larsen B Ice-Shelf Collapse.,
34 *J. of Glaciology* 54 (184):3–16, 2008
35
36 Grosvenor, D. P., King, J.C., Choularton, T. W., and Lachlan-Cope, T.: Downslope Föhn Winds over the Antarctic
37 Peninsula and Their Effect on the Larsen Ice Shelves. *Atmos. Chem. and Phys.*, 14 (18), 9481–9509.,

1 <https://doi.org/10.5194/acp-14-9481-2014>., 2014.

2

3 Hock, R.: Glacier Melt: A Review of Processes and Their Modelling, *Progress in Phys .Geog.*, 29 (3), 362–91,
4 doi:10.1191/0309133305pp453ra., 2005.

5

6 Holland, P.R., Hugh F. J. Corr, H. D. Pritchard, Vaughan, D.G., Arthern, R.J., Jenkins, A., and Tedesco, M.: The Air
7 Content of Larsen Ice Shelf, *Geoph. Res. Let.*, 38 (10), doi:10.1029/2011GL047245, 2011.

8

9 Holmgren, B.: *Climate and Energy Exchange on a Sub-Polar Ice Cap in Summer: Arctic Institute of North America*
10 *Devon Island Expedition 1961-1963. Acta Univ. Upsal. Abstracts of Uppsala Diss. from the Faculty of Science, pt. 3.*
11 *Meteorologiska Institutionen Uppsala Universitet.*, 1971.

12

13 Holton, J.: The General Circulation, in: *An Introduction to Dynamic Meteorology*, 4th ed., Elsevier Inc., 329–337,
14 2004.

15

16 Hubbard, B., Luckman, A., Ashmore, D.W., Bevan, S., Kulesa, B., Kuipers-Munneke, P., Philippe, M. et al.: Massive
17 Subsurface Ice Formed by Refreezing of Ice-Shelf Melt Ponds, *Nat. Comm.*, 7 (June), 11897.,
18 doi:10.1038/ncomms11897, 2016.

19

20 Jansen, D., Kulesa, B., Sammonds, P. R., Luckman, A., King, E. C. and Glasser, N.F.: Present Stability of the Larsen
21 C Ice Shelf, Antarctic Peninsula, *J. of Glac.*, 56 (198), 593–600, 2010.

22

23 Kingslake, J., Ely, J.C., Das, I., and Bell, R.E.: Widespread Movement of Meltwater onto and across Antarctic Ice
24 Shelves, *Nature*, 544 (7650), 349–352, doi:10.1038/nature22049, 2017.

25

26 Koh, G., and Jordan, R.: Sub-Surface Melting in a Seasonal Snow Cover. *J. of Glaciology*, 41 (139): 474–482.
27 doi:10.3189/S002214300003481X, 1995.

28

29 Kuipers-Munneke, P., van den Broeke, M. R., King, J. C., Gray, T., and Reijmer, C. H.: Near-Surface Climate and
30 Surface Energy Budget of Larsen C Ice Shelf, Antarctic Peninsula, *The Cryosphere*, 6 (2), 353–363, doi:10.5194/tc-
31 6-353-2012, 2012.

32

33 Kuipers Munneke, P., Picard, G., van den Broeke, M. R., Lenaerts, J. T. M., and van Meijgaard, E.: Insignificant
34 Change in Antarctic Snowmelt Volume since 1979: Antarctic Snowmelt Volume, *Geoph. Res. Lett.*, 39(1),
35 doi:10.1029/2011GL050207, 2012

36

1 Kuipers-Munneke, P., Ligtenberg, S.R.M., Van Den Broeke, M.R., and Vaughan, D.G.: Firn Air Depletion as a
2 Precursor of Antarctic Ice-Shelf Collapse, *J. of Glaciology* 60 (220), 205–14, doi:10.3189/2014JoG13J183, 2014.
3

4 Lenaerts, J. T. M., Lhermitte, S., Drews, R., Ligtenberg, S. R. M., Berger, S., Helm, V., Smeets, C. J. P. P. et al.:
5 Meltwater Produced by Wind–albedo Interaction Stored in an East Antarctic Ice Shelf, *Nat. Clim. Change*, 7 (1), 58–
6 62, doi:10.1038/nclimate3180, 2016.
7

8 Liston, G.E., Bruland, O., Winther, J., Elvehøy, H. and Sand, K.: Meltwater Production in Antarctic Blue-Ice Areas:
9 Sensitivity to Changes in Atmospheric Forcing, *Polar Research*, 18 (2), 283–290, doi:10.3402/polar.v18i2.6586,
10 1999a.
11

12 Liston, G. E., Winther, J., Bruland, O., Elvehøy, H. and Sand, K.: Below-Surface Ice Melt on the Coastal Antarctic
13 Ice Sheet, *J. of Glaciology* 45 (150): 273–85. doi:10.3189/S0022143000001775, 1999b.
14

15 Liu, H., Wang, L., and Jezek, K.C.: Spatiotemporal Variations of Snowmelt in Antarctica Derived from Satellite
16 Scanning Multichannel Microwave Radiometer and Special Sensor Microwave Imager Data (1978–2004), *J. of*
17 *Geoph. Res.: Earth Surface*, 111 (F1), doi:10.1029/2005JF000318, 2006.
18

19 Long, D.G., and Hicks, B.R.: Standard BYU QuikSCAT/SeaWinds Land/Ice Image Products, QuikScat Image
20 Product Documentation, Brigham Young Univ., Provo, UT, 2000.
21

22 Luckman, A., Elvidge, A., Jansen, D., Kulesa, B., Kuipers-Munneke, P., King, J., and Barrand, N.E., Surface Melt
23 and Ponding on Larsen C Ice Shelf and the Impact of Föhn Winds, *Antarctic Science*, 26 (6), 625–635,
24 doi:10.1017/S0954102014000339, 2014.
25

26 MacAyeal, D.R., and Sergienko O.V.: The Flexural Dynamics of Melting Ice Shelves, *Annals of Glaciology*, 54 (63),
27 1–10, doi:doi:10.3189/2013AoG63A256, 2013.
28

29 Mann, H. B.: Nonparametric Tests Against Trend, *Econometrica*, 13 (3), 245–259, doi:10.2307/1907187, 1945.
30 Marshall, G. J.: Half-Century Seasonal Relationships between the Southern Annular Mode and Antarctic
31 Temperatures, *Intl. Jour. of Clim.*, 27 (3), 373–83, doi:10.1002/joc.1407, 2007.
32

33 Marshall, G. J., Orr, A., Van Lipzig, N.P.M., and King, J.C.: The Impact of a Changing Southern Hemisphere Annular
34 Mode on Antarctic Peninsula Summer Temperatures, *J. of Climate*, 19 (20), 5388–5404, 2006.
35

36 Mercer, J. H.: West Antarctic Ice Sheet and CO₂ Greenhouse Effect: A Threat of Disaster, *Nature* ,271 (January),
37 321–325, doi:10.1038/271321a0, 1978.

1
2 Morris, E. M., and Vaughan, D.G.: Spatial and Temporal Variation of Surface Temperature on the Antarctic Peninsula
3 And The Limit of Viability of Ice Shelves, In: Antarctic Peninsula Climate Variability: Historical and
4 Paleoenvironmental Perspectives, American Geophysical Union, 61–68, doi:10.1029/AR079p0061, 2013.
5
6 Mote, T., Anderson, M.R. , Kuivinen, K.C., and Rowe, M.C.: Passive Microwave-Derived Spatial and Temporal
7 Variations of Summer Melt On the Greenland Ice Sheet, International Symposium On Remote Sensing of Snow and
8 Ice, 17: 233–38, 1993.
9
10 Ridley, J.: Surface Melting on Antarctic Peninsula Ice Shelves Detected by Passive Microwave Sensors, Geoph.
11 Res. Let., 20 (23), 2639–2642, doi:10.1029/93GL02611, 1993.
12
13 Rott, H., Rack, W., Nagler, T., and Skvarca, P.: Climatically Induced Retreat and Collapse of Northern Larsen Ice
14 Shelf, Antarctic Peninsula, Annals of Glaciology 27, 86–92, doi:10.1017/S0260305500017262, 1998.
15
16 Rott, H., Rack, W., Skvarca, P., and De Angelis, H.: Northern Larsen Ice Shelf, Antarctica: Further Retreat after
17 Collapse, Annals of Glaciology 34 (1), 277–82., doi: 10.3189/172756402781817716, 2002.
18
19 Scambos, T. A.: Glacier Acceleration and Thinning after Ice Shelf Collapse in the Larsen B Embayment, Antarctica,
20 Geoph. Res. Let., 31 (18), doi:10.1029/2004GL020670, 2004.
21
22 Scambos, T.A., Hulbe, C., Fahnestock, M., and Bohlander, J.: The Link between Climate Warming and Break-up of
23 Ice Shelves in the Antarctic Peninsula, J. Glaciology 46 (154), 516–530,doi:10.3189/172756500781833043, 2000.
24
25 Smith, L. C.: Melting of Small Arctic Ice Caps Observed from ERS Scatterometer Time Series, Geoph. Res.
26 Let., 30 (20), doi:10.1029/2003GL017641, 2003.
27
28 Steiner, N., and Tedesco, M.: A Wavelet Melt Detection Algorithm Applied to Enhanced-Resolution Scatterometer
29 Data over Antarctica (2000–2009),The Cryosphere, 8 (1), 25–40, doi:10.5194/tc-8-25-2014, 2014.
30 Tedesco, M.: Assessment and Development of Snowmelt Retrieval Algorithms over Antarctica from K-Band
31 Spaceborne Brightness Temperature (1979–2008), Rem. Sen.of Env. ,113 (5), 979–997,
32 doi:10.1016/j.rse.2009.01.009, 2009.
33
34 Tedesco, M., and Monaghan, A.J.: An Updated Antarctic Melt Record through 2009 and Its Linkages to High-Latitude
35 and Tropical Climate Variability, Geophysical Research Letters, 36 (18), doi:10.1029/2009GL039186, 2009.
36

1 Tedesco, M., Abdalati, W., and Zwally, H. J.: Persistent Surface Snowmelt over Antarctica (1987–2006) from 19.35
2 GHz Brightness Temperatures, *Geoph. Res. Let.*, 34 (18), doi:10.1029/2007GL031199, 2007.
3

4 Tedesco, M.: Snowmelt Detection over the Greenland Ice Sheet from SSM/I Brightness Temperature Daily Variations,
5 *Geoph. Res. Let.*, 34 (2), doi:10.1029/2006gl028466, 2007.
6

7 Torinesi, O., Fily, M., and Genthon, C.: Variability and Trends of the Summer Melt Period of Antarctic Ice Margins
8 since 1980 from Microwave Sensors, *J. of Climate*, 16 (7), 1047–1060, 2003.
9

10 Trusel, L. D., Frey, K. E., and Das, S. B.: Antarctic Surface Melting Dynamics: Enhanced Perspectives from Radar
11 Scatterometer Data, *J. of Geoph. Res.*, 117 (F2), doi:10.1029/2011JF002126, 2012.
12

13 Trusel, L.D., Frey, K.D., Das, S.B., Kuipers-Munneke, P., and Van den Broeke, M.R.: Satellite-Based Estimates of
14 Antarctic Surface Meltwater Fluxes, *Geoph. Res. Let.*, 40 (23): 6148–6153. doi:10.1002/2013GL058138, 2013.
15

16 Turner, J., Colwell, S.R., Marshall, G.J., Lachlan-Cope, T.A., Carleton, A.M., Jones, P.D., Lagun, V., Reid, P.A., and
17 Iagovkina, S.: Antarctic Climate Change during the Last 50 Years, *Int. Journ. of Clim*, 25 (3), 279–294,
18 doi:10.1002/joc.1130, 2005.
19

20 Turner, J., Lu, H., White, I., King, J.C., Phillips, T., Hosking, J.S., Bracegirdle, T.J., Marshall, G.J., Mulvaney, R., and
21 Deb, P.: Absence of 21st Century Warming on Antarctic Peninsula Consistent with Natural Variability, *Nature*, 535
22 (7612), 411–415, doi:10.1038/nature18645, 2016.
23

24 Ulaby, F.T., and Stiles, W.H.: The Active and Passive Microwave Response to Snow Parameters: 2. Water Equivalent
25 of Dry Snow, *J. of Geoph. Res.: Oceans*, 85 (C2), 1045–1049, doi:10.1029/JC085iC02p01045, 1980.
26

27 Van Den Broeke, M. R., and Van Lipzig, N.P.M.: Response of Wintertime Antarctic Temperatures to the Antarctic
28 Oscillation: Results of a Regional Climate Model, in: *Antarctic Peninsula Climate Variability: Historical and*
29 *Paleoenvironmental Perspectives*, American Geophysical Union, 43–58, 2003.
30

31 Van Den Broeke, M. R.: Strong Surface Melting Preceded Collapse of Antarctic Peninsula Ice Shelf, *Geoph. Res.*
32 *Let.*, 32 (12), doi:10.1029/2005GL023247, 2005.
33

34 van der Veen, C.J.: Fracture Mechanics Approach to Penetration of Surface Crevasses on Glaciers, *Cold Regions*
35 *Science and Technology* 27 (1): 31–47. doi:10.1016/S0165-232X(97)00022-0, 1998.
36

37 Van Lipzig, N. P. M.: Precipitation, Sublimation, and Snow Drift in the Antarctic Peninsula Region from a Regional

1 Atmospheric Model, *J. of Geoph. Res.*, 109 (D24), doi:10.1029/2004JD004701, 2004.

2

3 Van Meijgaard, E., Van Ulft, L. H., Van de Berg, W. J., Bosveld, F. C., Van den Hurk, B., Lenderink, G., and
4 Siebesma, A.P.: The KNMI Regional Atmospheric Climate Model RACMO Version 2.1., Koninklijk Nederlands
5 Meteorologisch Instituut., <http://a.knmi2.nl/knmi-library/knmipubTR/TR302.pdf>, 2008.

6

7 Van Wessem, J. M., Ligtenberg, S. R. M., Reijmer, C. H., van de Berg, W. J., van den Broeke, M. R., Barrand, N.
8 E., Thomas, E. R. et al.: The Modelled Surface Mass Balance of the Antarctic Peninsula at 5.5 Km Horizontal
9 Resolution, *The Cryosphere Discussions*, 9 (5), 5097–5136, doi:10.5194/tcd-9-5097-2015, 2015.

10

11 Vaughan, D. G., and Doake, C. S. M.: Recent Atmospheric Warming and Retreat of Ice Shelves on the Antarctic
12 Peninsula, *Nature*, 379 (6563), 328–31, doi:10.1038/379328a0, 1996.

13

14 Vaughan, D. G.: Recent Trends in Melting Conditions on the Antarctic Peninsula and Their Implications for Ice-Sheet
15 Mass Balance and Sea Level, *Arctic, Antarctic, and Alpine Research*, 38 (1), 147–152, 2006.

16

17 Vaughan, D. G.: West Antarctic Ice Sheet Collapse—the Fall and Rise of a Paradigm, *Climatic Change*, 91 (1–2), 65–
18 79, 2008.

19

20 Wallace, J. M., and Hobbs, P.V.: Hypsometric Equation, in: *Atmospheric Science: An Introductory Survey*,
21 Academic Press, Cambridge, MA, 55–57, 1977.

22

23 Weertman, J.: Can a Water-Filled Crevasse Reach the Bottom Surface of a Glacier., *IASH Publ 95*, 139–145., 1973

24

25 Wilks, D.S.: *Statistical Methods in the Atmospheric Sciences: An Introduction*. International Geophysics, Elsevier
26 Science, Amsterdam, Netherlands, 1995.

27

28 Wismann, V.: Monitoring of Seasonal Snowmelt on Greenland with ERS Scatterometer Data, *IEEE Transactions on*
29 *Geoscience and Remote Sensing*, 38 (4), 1821–1826, doi:10.1109/36.851766, 2000.

30 Zwally, H. J., Giovinetto, M. B., Beckley, M. A., and Saba, J. L.: *Antarctic and Greenland Drainage Systems*, GSFC
31 Cryospheric Sciences Laboratory, 2012.

32

33 Zwally, H. Jay, Abdalati, W., Herring T., Larson, K., Saba, J., and Steffen, K.: Surface Melt-Induced Acceleration
34 of Greenland Ice-Sheet Flow, *Science*, 297 (5579), 218–222., 2002.

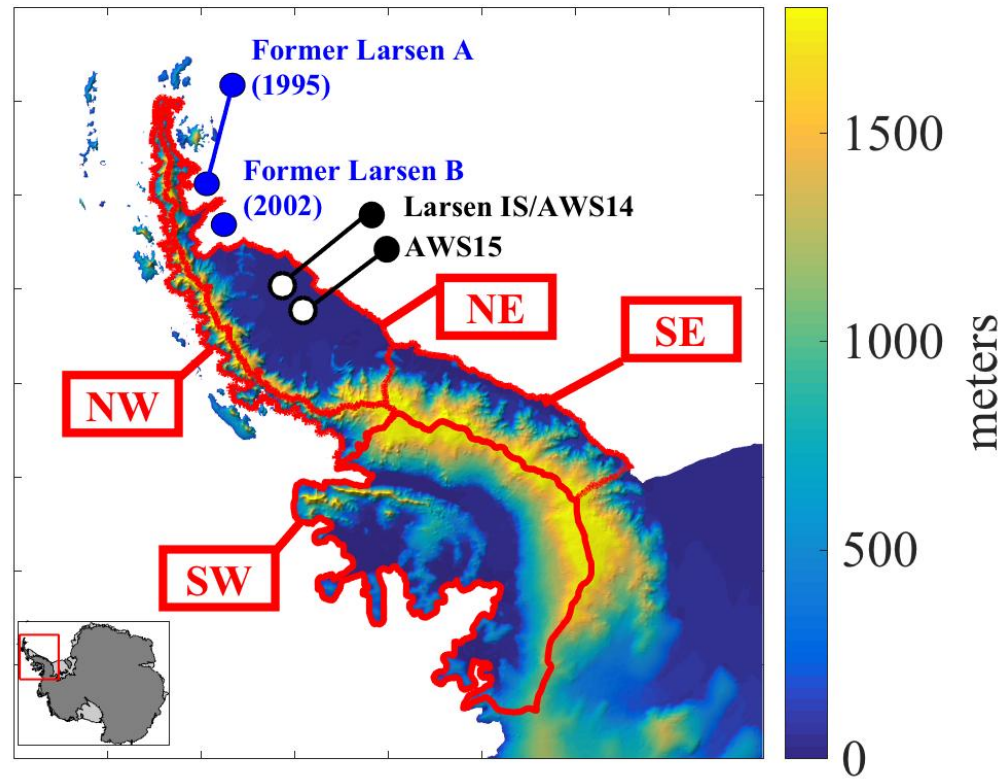
35

36 Zwally, H. J., and Fiegles, S.: Extent and Duration of Antarctic Surface Melting, *J. of Glaciology*, 40, 463–476, 1994.

37

38

1
2



1
2
3
4
5
6
7

Figure 1: Full MAR domain showing topographic relief, former ice shelves with dates of collapse, locations of automatic weather stations and basins corresponding to SW (basin 24) NW (basin 25) NE (basin 26), SE (basin 27) from Zwally, et. al. 2012

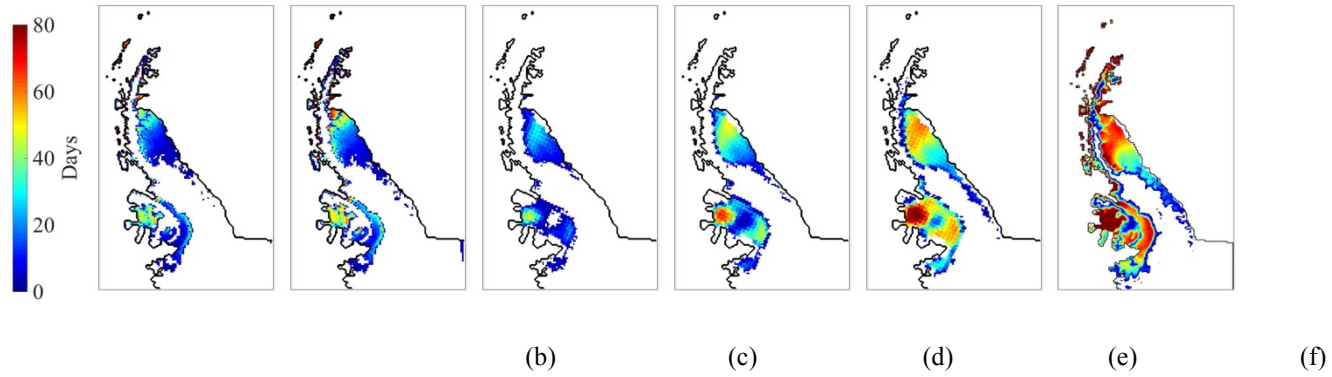
Page Break

MAR

PMW

QS

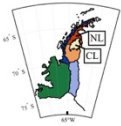
MF > 0.4 LWC_{1m} 240 ALA zwa
> 0.4%



1
2
3
4
5
6
7

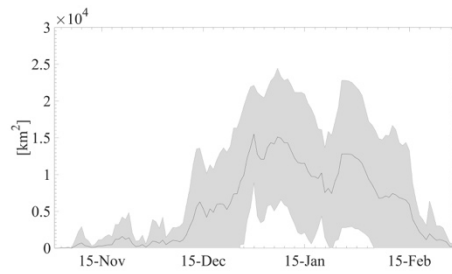
Figure 2: Average number of melt days from multiple sources (a) MAR, Liquid Water Content > 0.4% for three consecutive days. (b) MAR Total Melt Flux > 0.4 mmwe for 1 day or more. Satellite-based: (c) PMW 240 algorithm (d) PMW ALA (e) PMW Zwa (f) QuikSCAT. All satellite-based estimates include a melt day only when part of a sustained three-day period of melt. All averages are taken from the 2000-2009 period to retain consistency with the availability of QuikSCAT data

1

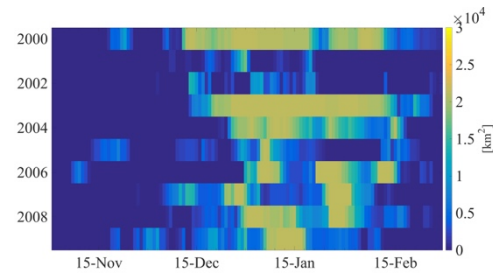


2

3



MAR melt climatology

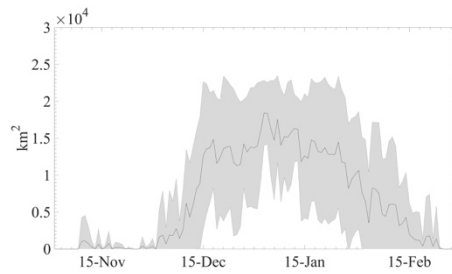


(b) MAR interannual

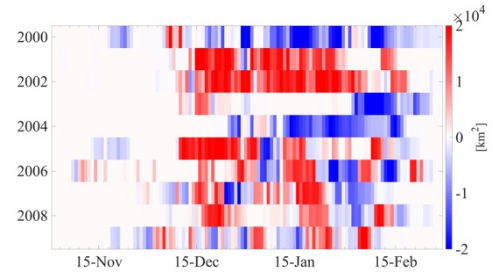
4

5

6



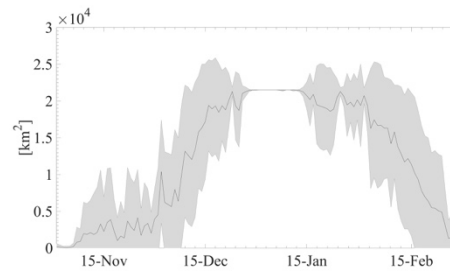
(c) PMWAll melt climatology



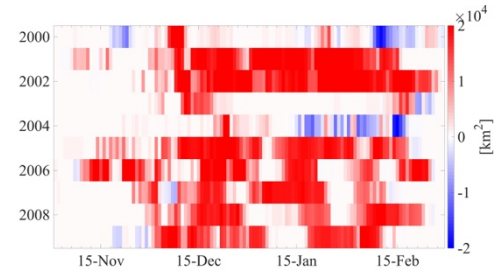
(d) PMWAll - MAR interannual

7

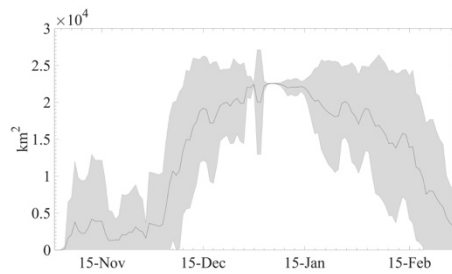
8



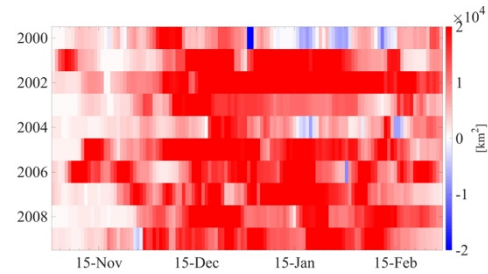
(e) zwa melt climatology



(f) zwa - MAR interannual



(g) QuikSCAT ft3 melt climatology

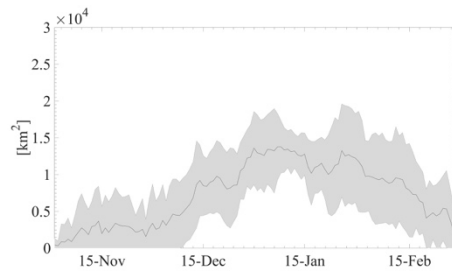


(h) QuikSCAT ft3 - MAR interannual

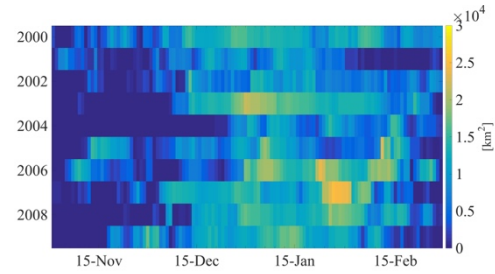
1
2
3
4
5
6

Figure 3: CL-region, described in text and shown in inset in for (a), average and inter-annual melt occurrence in MAR, PMW and QuikSCAT data. (a) MF_{0.4} melt extent climatology with one standard deviation shown in grey envelope (b) melt extent for MF_{0.4} from 1999-2009 (c) melt climatology PMW

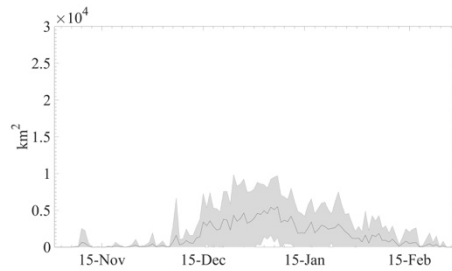
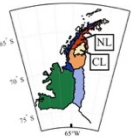
1 All (d) interannual difference melt extent PMWall - MAR (e) melt climatology PMW zwa (f) interannual difference in melt extent PMWzwal - MAR
2 (g) melt climatology QuikSCAT ft3 (h) interannual difference in melt extent QuikSCAT ft3 - MAR
3



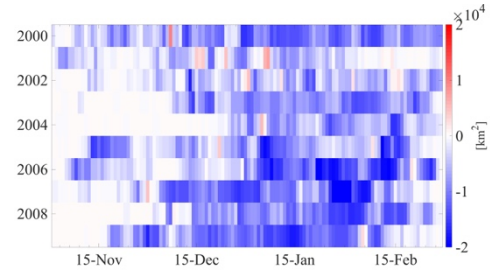
MAR melt climatology



(b) MAR interannual

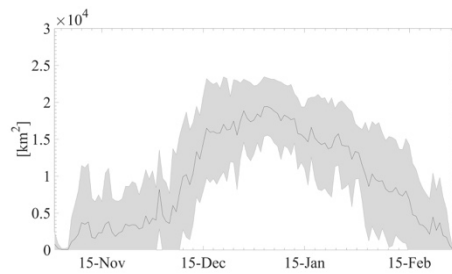


(c) PMWAll melt climatology

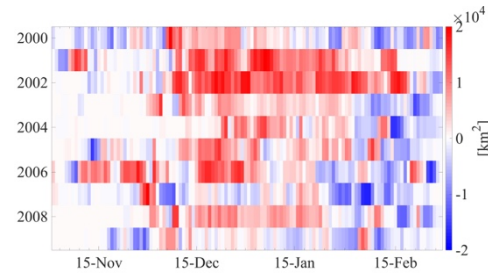


(d) PMWAll - MAR interannual

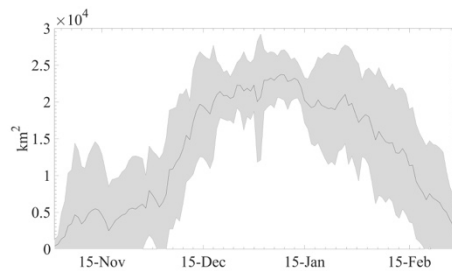
4
5
6
7
8
9



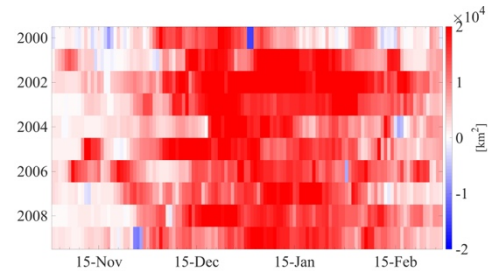
(e) zwa melt climatology



(f) zwa - MAR interannual



(g) QuikSCAT ft3 melt climatology

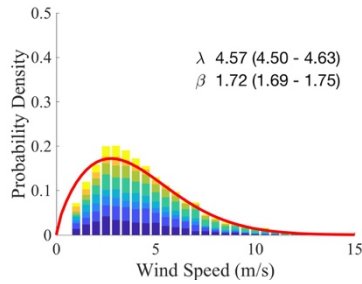
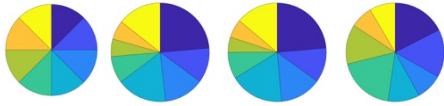


(h) QuikSCAT ft3 - MAR interannual

Figure 4: NL-region, described in text and shown inset in (c), average and inter-annual melt occurrence in MAR, PMW and QuikSCAT data. (a) MF_{0.4} melt extent climatology with one standard deviation shown in grey envelope (b) melt extent for MF_{0.4} from 1999-2009 (c) melt climatology PMW All (d) interannual difference melt extent PMWAll - MAR (e) melt climatology PMW zwa (f) interannual difference in melt extent PMWzwal – MAR (g) melt climatology QuikSCAT ft3 (h) interannual difference in melt extent QuikSCAT ft3 - MAR

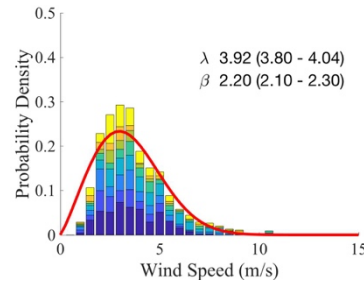
1

Larsen IS (1999-2014)



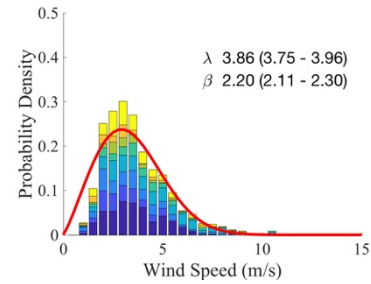
$4.07 \pm 5.95\sigma$ m/s

(a) All Days (AWS)



$3.47 \pm 2.78\sigma$ m/s

(b) All Days (MAR-R)



$3.42 \pm 2.68\sigma$ m/s

(c) All Days (MAR)

2

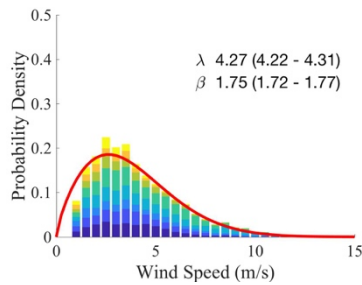
3

4

5

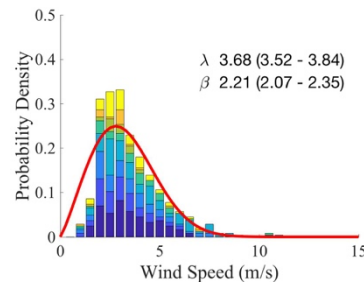
6

AWS 14 (2009-2014)



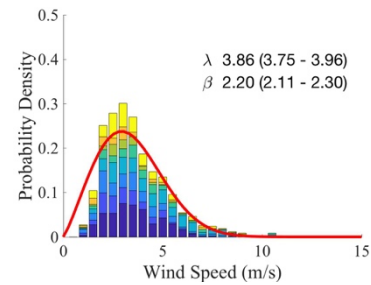
$3.80 \pm 5.03\sigma$ m/s

(d) All Days (AWS)



$3.26 \pm 2.43\sigma$ m/s

(e) All Days (MAR-R)



$3.42 \pm 2.68\sigma$ m/s

(f) All Days (MAR)

7

8

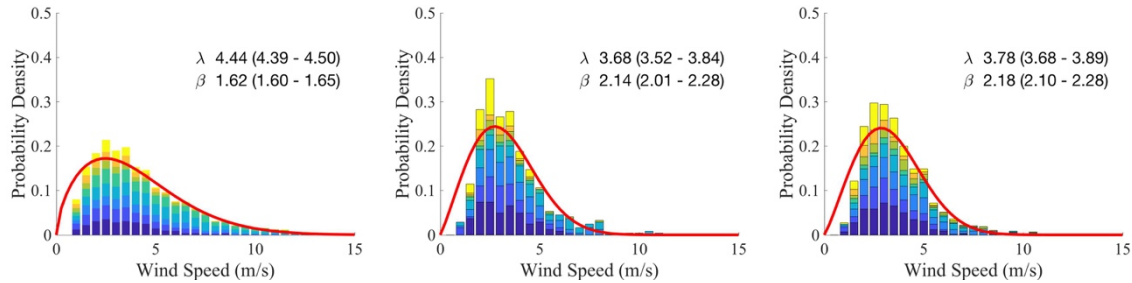
9

10

1

2

AWS 15 (2008-2014)



3.98 ± 6.31σ m/s

3.26 ± 2.57σ m/s

3.35 ± 2.62σ m/s

(g) All Days (AWS)

(h) All Days (MAR-R)

(i) All Days (MAR)

3

4

5

6

7

8

9

10

11

12

13

Figure 5: Probability distribution (y-axis) of summer (DJF) wind speeds (x-axis) with wind speed direction proportions shown in each inset. Wind directions corresponding to instet colors shown in 45° increments in inset left of (a). Curve shows best-fit Weibull curve with parameters for shape (β) and scale (λ , m/s). Datasets are for AWS data (left column), MAR outputs restricted to AWS availability (middle column) and MAR data for the 2001-2014 period (right column). Shown for (a) Larsen, AWS (b) Larsen, MAR at AWS availability (c) Larsen, MAR full period (d) AWS 14, (e) AWS 14, MAR at AWS availability (f) AWS 14, MAR full period (g) AWS 15, AWS (h) AWS 15, MAR at AWS availability (i) AWS 15, MAR full period. Values shown below figures are expected values from the Weibull distribution

	Northerly	Southerly	Easterly	Westerly
DJF All Days				
Where MAR shows wind direction				
MAR wind direction percentage	55.6%	44.4%	63.9%	36.3%
MAR expected wind speed [m/s]	3.49(±3.12)	4.21(±4.83)	3.75(±3.09)	4.04(±5.69)
AWS expected wind speed [m/s]	3.82(±5.23)	5.10(±9.14)	4.41(±6.87)	4.44(±8.73)
Where AWS shows wind direction				
AWS wind direction percentage	51.2%	48.8%	54.5%	45.5%
MAR expected wind speed [m/s]	4.04(±5.31)	3.72(±3.07)	3.48(±2.37)	4.43(±6.26)
AWS expected wind speed [m/s]	4.52(±8.33)	4.39(±6.98)	3.90(±4.77)	5.22(±11.03)
Temperature biases				
Avg T2m Bias (MAR - AWS)	0.58°C	0.77°C	0.43°C	0.76°C
Max T2m Bias (MAR - AWS)	-2.21°C	-1.11°C	-1.75°C	-2.42°C
Temperature bias where Ts > 0°C				
Avg T2m Bias (MAR - AWS)	-1.25°C	-1.42°C	-1.32°C	-1.29°C
Max T2m Bias (MAR - AWS)	-2.80°C	-2.40°C	-2.84°C	-3.04°C
DJF, MAR reports melt				
MAR wind direction	59.5%	40.5%	62.8%	37.2%
AWS wind direction	55%	45%	56.7%	43.3%
Temperature biases				
Avg T2m Bias (MAR - AWS)	0.28°C	0.18°C	0.25°C	0.24°C
Max T2m Bias (MAR - AWS)	-0.78°C	-0.41°C	-0.73°C	-0.43°C
Temperature bias where Ts > 0°C				
Avg T2m Bias (MAR - AWS)	-0.69°C	-0.76°C	-0.47°C	-0.63°C
Max T2m Bias (MAR - AWS)	-1.06°C	-0.92°C	-1.31°C	-0.64°C

1
2
3
4

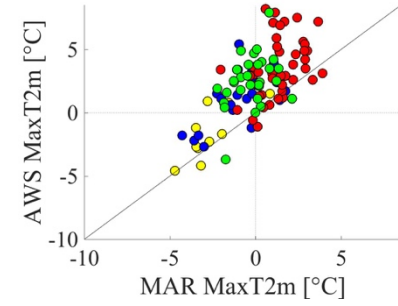
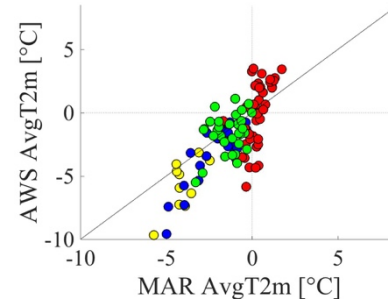
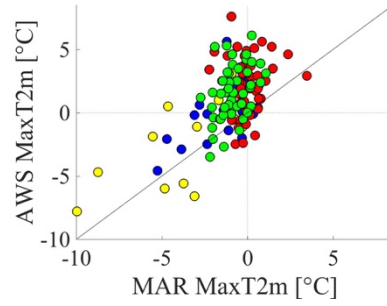
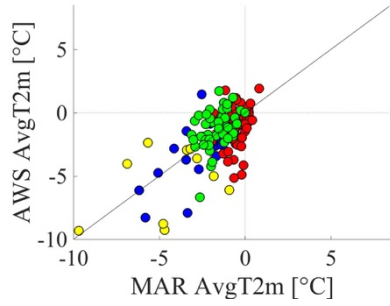
Table 1: Proportions for wind direction and associated temperature biases at the Larsen Ice Shelf AWS station from 2000-2009 restricted to the summer season (DJF)

Section Break (Next Page)

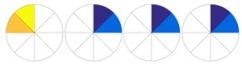
1

MAR: 3.37(±1.89) m/s AWS: 3.86 (±3.35) m/s

MAR: 3.51 (±2.99) AWS: 3.88(±4.76) m/s



2



3

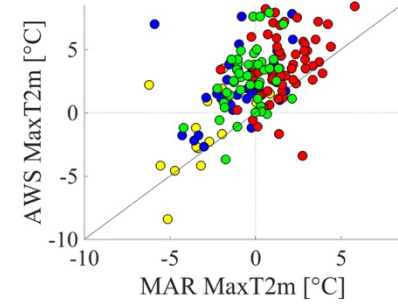
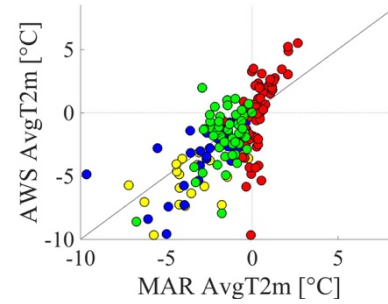
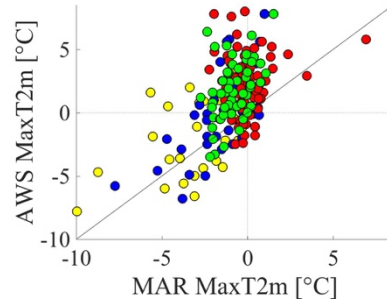
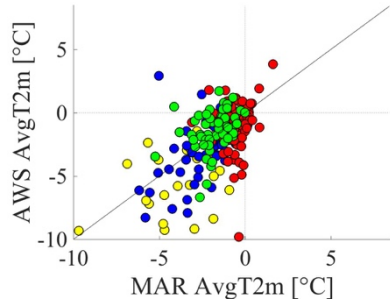
4

5

6

MAR: 3.42(±2.17) m/s AWS: 3.71 (±3.93) m/s

MAR: 3.47 (±2.49) AWS: 3.96(±4.65) m/s



7



8

9

10

11

12

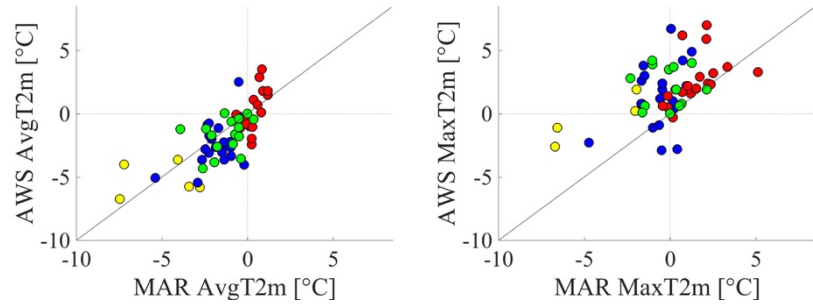
Figure 6: MAR vs AWS temperatures at the Larsen Ice Shelf AWS station for DJF from 2001-2009 for wind biases AWS -> MAR shown by pie charts (when AWS data is available). Red shows days where MAR shows melt. Blue shows “QSEx” days, i.e. when QuikSCAT reports melt (and MAR does

- 1 not), Cyan indicates “PMWEx” when PMWAll shows melt and MAR does not. Green indicates when PMWEx and QSEx both report melt (and MAR
- 2 does not). Yellow (only shown for g,h) indicates all other days for completeness. Northeasterly agreement (case 1) (a) AvgTs (b) MaxTs, Northeasterly

1 AWS winds reported as northwesterly in MAR (case 2) (c) AvgTs (d)MaxTs, All wind directions in AWS reported as northeasterly in MAR (e) AvgTs
 2 (f) MaxTs

3
 4

MAR: 4.31(±4.74) m/s AWS: 4.81 (±7.44) m/s



5



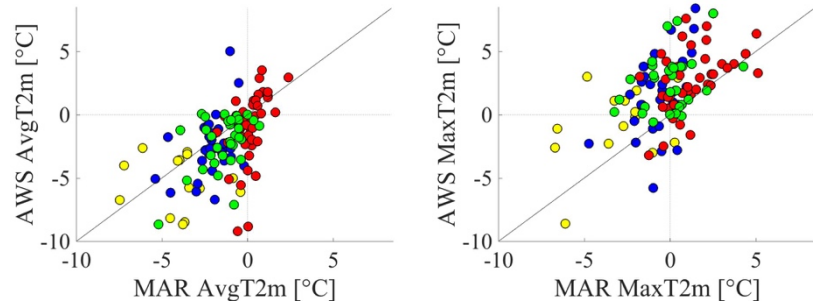
6

7 (b)

8

9

MAR: 3.83(±3.53) m/s AWS: 4.36 (±6.26) m/s



10

11

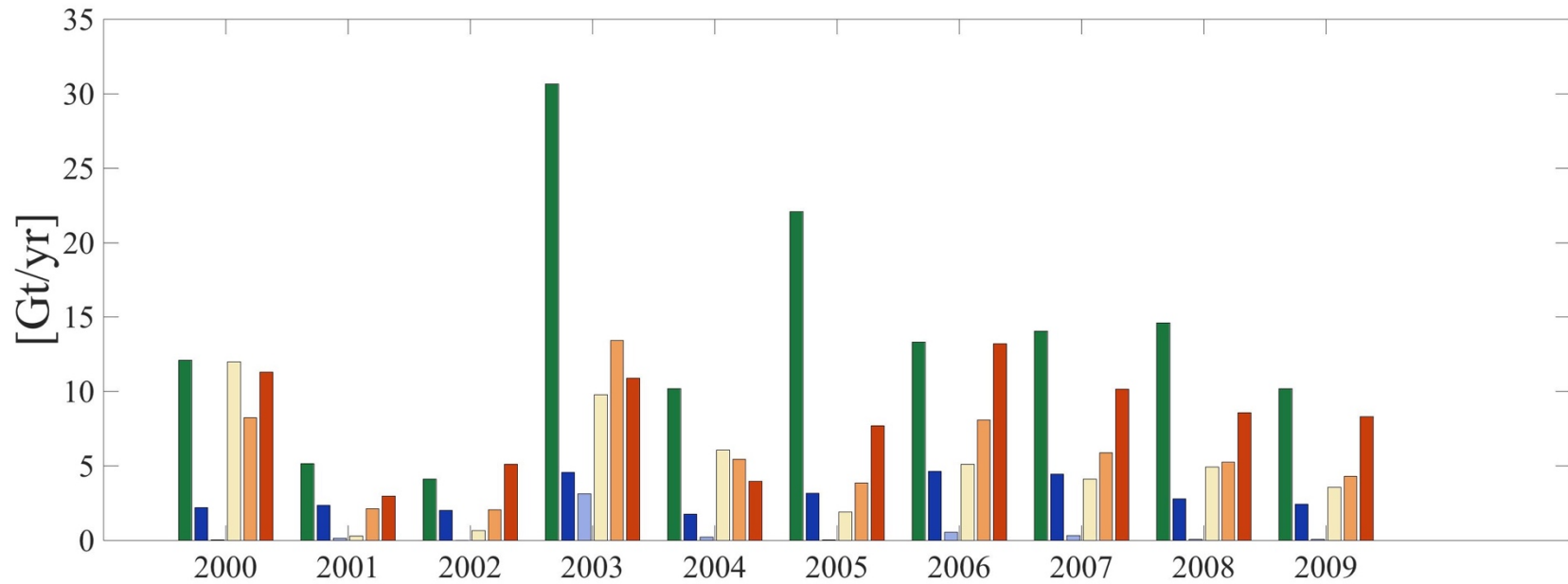
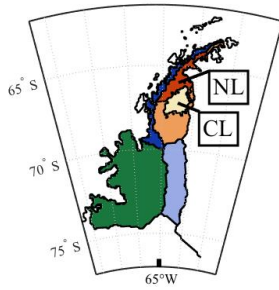
(c) (d)

12

1 **Figure 7: MAR vs AWS temperatures at the Larsen Ice Shelf AWS station for DJF from 2001-2009 for wind biases AWS -> MAR shown by pie charts**
2 **(when AWS data is available). Red shows days where MAR shows melt. Blue shows “QSEx” days, i.e. when QuikSCAT reports melt (and MAR does**
3 **not), Cyan indicates “PMWEx” when PMWAll shows melt and MAR does not. Green indicates when PMWEx an QSEx both report melt (and MAR**
4 **does not). Yellow (only shown for g,h) indicates all other days for completeness. Southwesterly wind direction agreement (a) AvgTs (b) MaxTs, All wind**
5 **directions in AWS which are reported as southwesterly in MAR (c) AvgTs (d)MaxTs,**

6

[Section Break \(Next Page\)](#)



1
2
3
4
5

Figure 8: Annual meltwater production from MAR [Gt/yr] shown for masks shown in inset ('2001' corresponds to the meltwater from July,2000-June,2001). NW, SW, SE basins are kept intact as in Fig. 1. NE basin is divided into the NL mask, the CL mask and the remaining portion of the NE basin (NE - (CL+NL)). The CL and NL masks are described in text

Section Break (Next Page)

Page 38: [11] Formatted	Microsoft Office User	5/19/18 10:55:00 AM
Left, Line spacing: single		
Page 38: [12] Formatted Table	Microsoft Office User	5/19/18 10:57:00 AM
Formatted Table		
Page 38: [13] Formatted	Microsoft Office User	5/20/18 9:59:00 AM
Line spacing: single		
Page 38: [14] Formatted	Microsoft Office User	5/20/18 11:26:00 AM
Font color: Text 1		
Page 38: [15] Formatted	Microsoft Office User	5/19/18 10:55:00 AM
Left, Line spacing: single		
Page 38: [16] Formatted	Microsoft Office User	5/19/18 10:52:00 AM
Line spacing: single		
Page 38: [17] Formatted	Microsoft Office User	5/19/18 10:55:00 AM
Left, Line spacing: single		
Page 38: [18] Formatted Table	Microsoft Office User	5/19/18 10:57:00 AM
Formatted Table		
Page 38: [19] Formatted	Microsoft Office User	5/19/18 10:52:00 AM
Line spacing: single		
Page 38: [20] Formatted	Microsoft Office User	5/19/18 10:55:00 AM
Left, Line spacing: single		
Page 38: [21] Formatted	Microsoft Office User	5/19/18 10:52:00 AM
Line spacing: single		
Page 38: [22] Formatted	Microsoft Office User	5/19/18 10:55:00 AM
Left, Line spacing: single		
Page 38: [23] Formatted	Microsoft Office User	5/19/18 10:52:00 AM
Line spacing: single		
Page 38: [24] Deleted	Microsoft Office User	5/20/18 10:49:00 AM
3.49		
Page 38: [24] Deleted	Microsoft Office User	5/20/18 10:49:00 AM
3.49		
Page 38: [25] Deleted	Microsoft Office User	5/20/18 10:56:00 AM
4.21		

Page 38: [25] Deleted	Microsoft Office User	5/20/18 10:56:00 AM
	4.21	
Page 38: [25] Deleted	Microsoft Office User	5/20/18 10:56:00 AM
	4.21	
Page 38: [26] Deleted	Microsoft Office User	5/20/18 11:00:00 AM
	3.	
Page 38: [26] Deleted	Microsoft Office User	5/20/18 11:00:00 AM
	3.	
Page 38: [26] Deleted	Microsoft Office User	5/20/18 11:00:00 AM
	3.	
Page 38: [27] Deleted	Microsoft Office User	5/20/18 11:03:00 AM
	4.	
Page 38: [27] Deleted	Microsoft Office User	5/20/18 11:03:00 AM
	4.	
Page 38: [27] Deleted	Microsoft Office User	5/20/18 11:03:00 AM
	4.	
Page 38: [27] Deleted	Microsoft Office User	5/20/18 11:03:00 AM
	4.	
Page 38: [28] Formatted	Microsoft Office User	5/19/18 10:55:00 AM
	Left, Line spacing: single	
Page 38: [29] Formatted	Microsoft Office User	5/19/18 10:52:00 AM
	Line spacing: single	
Page 38: [30] Deleted	Microsoft Office User	5/20/18 10:49:00 AM
	3.82	
Page 38: [30] Deleted	Microsoft Office User	5/20/18 10:49:00 AM
	3.82	
Page 38: [30] Deleted	Microsoft Office User	5/20/18 10:49:00 AM
	3.82	
Page 38: [31] Deleted	Microsoft Office User	5/19/18 10:46:00 AM
	5.10	
Page 38: [31] Deleted	Microsoft Office User	5/19/18 10:46:00 AM
	5.10	
Page 38: [31] Deleted	Microsoft Office User	5/19/18 10:46:00 AM
	5.10	
Page 38: [32] Deleted	Microsoft Office User	5/20/18 11:00:00 AM
	4.41	
Page 38: [32] Deleted	Microsoft Office User	5/20/18 11:00:00 AM
	4.41	
Page 38: [33] Deleted	Microsoft Office User	5/19/18 10:49:00 AM
	4.44	

Page 38: [33] Deleted	Microsoft Office User	5/19/18 10:49:00 AM
4.44		
Page 38: [34] Formatted	Microsoft Office User	5/19/18 10:55:00 AM
Left, Line spacing: single		
Page 38: [35] Formatted	Microsoft Office User	5/19/18 10:52:00 AM
Line spacing: single		
Page 38: [36] Formatted	Microsoft Office User	5/19/18 10:55:00 AM
Left, Line spacing: single		
Page 38: [37] Formatted	Microsoft Office User	5/19/18 10:52:00 AM
Line spacing: single		
Page 38: [38] Formatted	Microsoft Office User	5/19/18 10:55:00 AM
Left, Line spacing: single		
Page 38: [39] Formatted	Microsoft Office User	5/19/18 10:52:00 AM
Line spacing: single		
Page 38: [40] Deleted	Microsoft Office User	5/20/18 10:52:00 AM
4.04		
Page 38: [40] Deleted	Microsoft Office User	5/20/18 10:52:00 AM
4.04		
Page 38: [41] Deleted	Microsoft Office User	5/20/18 10:57:00 AM
72		
Page 38: [41] Deleted	Microsoft Office User	5/20/18 10:57:00 AM
72		
Page 38: [42] Deleted	Microsoft Office User	5/20/18 11:00:00 AM
3.48		
Page 38: [42] Deleted	Microsoft Office User	5/20/18 11:00:00 AM
3.48		
Page 38: [43] Deleted	Microsoft Office User	5/20/18 11:04:00 AM
4.4		
Page 38: [43] Deleted	Microsoft Office User	5/20/18 11:04:00 AM
4.4		
Page 38: [43] Deleted	Microsoft Office User	5/20/18 11:04:00 AM
4.4		
Page 38: [44] Formatted	Microsoft Office User	5/19/18 10:55:00 AM
Left, Line spacing: single		
Page 38: [45] Formatted	Microsoft Office User	5/19/18 10:52:00 AM
Line spacing: single		

Page 38: [46] Deleted	Microsoft Office User	5/20/18 10:54:00 AM
	4	
Page 38: [46] Deleted	Microsoft Office User	5/20/18 10:54:00 AM
	4	
Page 38: [46] Deleted	Microsoft Office User	5/20/18 10:54:00 AM
	4	
Page 38: [46] Deleted	Microsoft Office User	5/20/18 10:54:00 AM
	4	
Page 38: [47] Deleted	Microsoft Office User	5/20/18 10:57:00 AM
	4	
Page 38: [47] Deleted	Microsoft Office User	5/20/18 10:57:00 AM
	4	
Page 38: [47] Deleted	Microsoft Office User	5/20/18 10:57:00 AM
	4	
Page 38: [48] Deleted	Microsoft Office User	5/20/18 11:01:00 AM
	3.90	
Page 38: [48] Deleted	Microsoft Office User	5/20/18 11:01:00 AM
	3.90	
Page 38: [49] Deleted	Microsoft Office User	5/20/18 11:04:00 AM
	5	
Page 38: [49] Deleted	Microsoft Office User	5/20/18 11:04:00 AM
	5	
Page 38: [49] Deleted	Microsoft Office User	5/20/18 11:04:00 AM
	5	
Page 38: [49] Deleted	Microsoft Office User	5/20/18 11:04:00 AM
	5	
Page 38: [50] Formatted	Microsoft Office User	5/19/18 10:55:00 AM
Left, Line spacing: single		
Page 38: [51] Deleted	Microsoft Office User	5/20/18 11:05:00 AM
eratur		
Page 38: [51] Deleted	Microsoft Office User	5/20/18 11:05:00 AM
eratur		
Page 38: [52] Formatted	Microsoft Office User	5/19/18 10:52:00 AM
Line spacing: single		
Page 38: [53] Formatted	Microsoft Office User	5/19/18 10:55:00 AM
Left, Line spacing: single		
Page 38: [54] Formatted	Microsoft Office User	5/19/18 10:52:00 AM
Line spacing: single		
Page 38: [55] Formatted	Microsoft Office User	5/19/18 10:55:00 AM

Left, Line spacing: single

Page 38: [56] Formatted	Microsoft Office User	5/19/18 10:52:00 AM
--------------------------------	------------------------------	----------------------------

Line spacing: single

Page 38: [57] Formatted	Microsoft Office User	5/19/18 10:55:00 AM
--------------------------------	------------------------------	----------------------------

Left, Line spacing: single

Page 38: [58] Formatted	Microsoft Office User	5/19/18 10:52:00 AM
--------------------------------	------------------------------	----------------------------

Line spacing: single

Page 38: [59] Formatted	Microsoft Office User	5/19/18 10:55:00 AM
--------------------------------	------------------------------	----------------------------

Left, Line spacing: single

Page 38: [60] Formatted	Microsoft Office User	5/19/18 10:52:00 AM
--------------------------------	------------------------------	----------------------------

Line spacing: single

Page 38: [61] Formatted	Microsoft Office User	5/19/18 10:55:00 AM
--------------------------------	------------------------------	----------------------------

Left, Line spacing: single

Page 38: [62] Formatted	Microsoft Office User	5/19/18 10:52:00 AM
--------------------------------	------------------------------	----------------------------

Line spacing: single

Page 38: [63] Formatted	Microsoft Office User	5/19/18 10:55:00 AM
--------------------------------	------------------------------	----------------------------

Left, Line spacing: single

Page 38: [64] Formatted	Microsoft Office User	5/19/18 10:52:00 AM
--------------------------------	------------------------------	----------------------------

Line spacing: single

Page 38: [65] Formatted	Microsoft Office User	5/20/18 11:26:00 AM
--------------------------------	------------------------------	----------------------------

Font color: Text 1

Page 38: [66] Formatted	Microsoft Office User	5/19/18 10:55:00 AM
--------------------------------	------------------------------	----------------------------

Left, Line spacing: single

Page 38: [67] Formatted	Microsoft Office User	5/19/18 10:52:00 AM
--------------------------------	------------------------------	----------------------------

Line spacing: single

Page 38: [68] Formatted	Microsoft Office User	5/19/18 10:55:00 AM
--------------------------------	------------------------------	----------------------------

Left, Line spacing: single

Page 38: [69] Formatted Table	Microsoft Office User	5/19/18 10:57:00 AM
--------------------------------------	------------------------------	----------------------------

Formatted Table

Page 38: [70] Formatted	Microsoft Office User	5/19/18 10:52:00 AM
--------------------------------	------------------------------	----------------------------

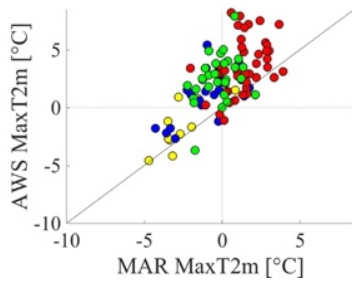
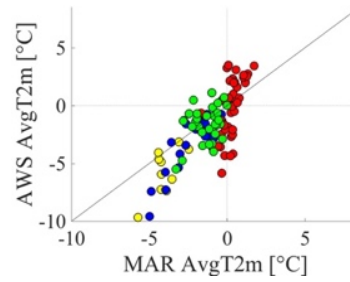
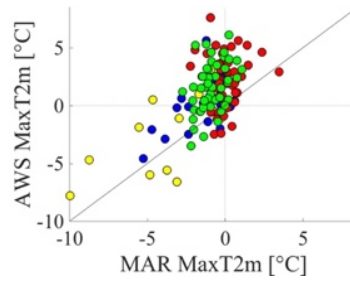
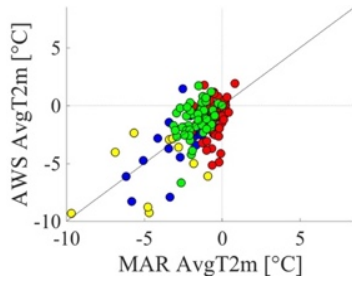
Line spacing: single

Page 38: [71] Formatted	Microsoft Office User	5/19/18 10:55:00 AM
--------------------------------	------------------------------	----------------------------

Left, Line spacing: single

Page 38: [72] Formatted	Microsoft Office User	5/19/18 10:52:00 AM
Line spacing: single		
Page 38: [73] Formatted	Microsoft Office User	5/19/18 10:55:00 AM
Left, Line spacing: single		
Page 38: [74] Formatted	Microsoft Office User	5/19/18 10:52:00 AM
Line spacing: single		
Page 38: [75] Formatted	Microsoft Office User	5/19/18 10:55:00 AM
Left, Line spacing: single		
Page 38: [76] Formatted	Microsoft Office User	5/19/18 10:52:00 AM
Line spacing: single		
Page 38: [77] Formatted	Microsoft Office User	5/19/18 10:55:00 AM
Left, Line spacing: single		
Page 38: [78] Formatted	Microsoft Office User	5/19/18 10:52:00 AM
Line spacing: single		
Page 38: [79] Formatted	Microsoft Office User	5/19/18 10:55:00 AM
Left, Line spacing: single		
Page 38: [80] Formatted	Microsoft Office User	5/19/18 10:52:00 AM
Line spacing: single		
Page 38: [81] Formatted	Microsoft Office User	5/19/18 10:55:00 AM
Left, Line spacing: single		
Page 38: [82] Formatted	Microsoft Office User	5/19/18 10:52:00 AM
Line spacing: single		
Page 38: [83] Formatted	Microsoft Office User	5/19/18 10:55:00 AM
Left, Line spacing: single		
Page 38: [84] Formatted	Microsoft Office User	5/19/18 10:52:00 AM
Line spacing: single		
Page 38: [85] Deleted	Microsoft Office User	5/19/18 12:15:00 PM
1		
Page 38: [85] Deleted	Microsoft Office User	5/19/18 12:15:00 PM
1		
Page 38: [86] Deleted	Microsoft Office User	5/19/18 12:25:00 PM
1.31		
Page 38: [86] Deleted	Microsoft Office User	5/19/18 12:25:00 PM
1.31		

Missing Northerlyflow Missing Westerly flow



MAR: 4.31(±4.74) m/s AWS: 4.81 (±7.44) m/s

